1-1-1999

# Photopolymerization of biomembrane templates : nanometer-scale hydrogels and the photoinduced release of vesicle contents.

Howard K. Bowman
*University of Massachusetts Amherst*

# PHOTOPOLYMERIZATION OF BIOMEMBRANE TEMPLATES: NANOMETER-SCALE HYDROGELS AND THE PHOTOINDUCED RELEASE OF VESICLE CONTENTS

A Dissertation Presented

by

HOWARD K BOWMAN, III

Submitted to the Graduate School of the
University of Massachusetts Amherst in partial fulfillment
of the requirements for the degree of

DOCTOR OF PHILOSOPHY

February 1999

Polymer Science & Engineering

# PHOTOPOLYMERIZATION OF BIOMEMBRANE TEMPLATES: NANOMETER-SCALE HYDROGELS AND THE PHOTOINDUCED RELEASE OF VESICLE CONTENTS

A Dissertation Presented

by

HOWARD K BOWMAN, III

Approved as to style and content by:

David A. Tirrell, Chair

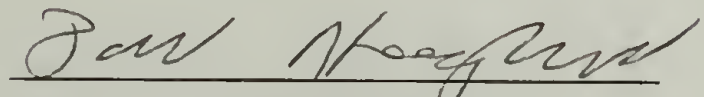

David A. Hoagland, Member

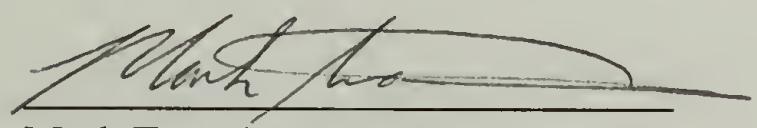

Mark Tuominen, Member

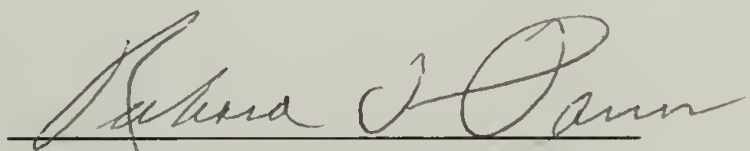

Richard J. Farris, Department Head
Polymer Science & Engineering

# DEDICATION

This thesis is dedicated to the memory of my grandmother, Lelia B. Clark.

# ACKNOWLEDGEMENTS

The cooperation of many individuals has been essential in the completion of this thesis. First and foremost, I wish to express my sincere gratitude to Professor David Tirrell, who provided me the financial means and intellectual support that was necessary to complete this thesis. I especially want to thank Professor Tirrell for his kind words of encouragement and insightful personal advice that he gave me at just the right moments during my sometimes-trying graduate education. Special thanks go to my committee members, Professors David Hoagland and Mark Tuominen for their patience and invaluable technical assistance. I would be remiss in not mentioning my indebtedness to Professor Evan Evans of the University of British Columbia. Specifically, I want to thank Professor Evans for allowing me to conduct research in his laboratories in Vancouver and his limitless enthusiasm he exhibited during my several visits. Without Professor Evans's keen insight into the physics of membranes, I could not have completed this work. I must acknowledge the expert technical assistance of Andrew Leung and Wieslawa Rawicz, as they have taught me well the "art" of vesicle micromanipulation.

Through the years, I have had the opportunity to work with people in the Tirrell group that possessed considerable talents and boundless energy. Among those people to whom I am most indebted are Vince Conticello, Dave Flanagan, Jan van Hest, Jeff Linhardt, Wendy Naimark, Wendy Petka, Jim Thomas and Michael Yu. Special thanks go to Linda Strzegowski, for her patience and extraordinary skills that I put to the test in preparing this document. When the Tirrell group moved to the California Institute of Technology, Carissa, Scott, Mary, Eric and I stayed behind. I cannot think of a better group to finish with. I thank all of these individuals for their friendship.

I extend my thanks and love to my parents, Howard and Sarah as well as my sister Ann for their unflagging support. I could have never undertaken this endeavor without their support. My wife, Cindy, deserves special recognition for enduring the graduate "experience" with me. To say her love and support is appreciated would be an understatement, as I feel her contribution has been much deeper than this. Cindy provided me with that intangible energy to press on, and for that, I consider this thesis to be as much hers as it is mine.

ABSTRACT

PHOTOPOLYMERIZATION OF BIOMEMBRANE TEMPLATES: NANOMETER-SCALE HYDROGELS AND THE PHOTOINDUCED RELEASE OF VESICLE CONTENTS

FEBRUARY 1999

HOWARD K BOWMAN, III, B.S., UNIVERSITY OF ALABAMA AT BIRMINGHAM

PH.D., UNIVERSITY OF MASSACHUSETTS AMHERST

Directed by: Professor David A. Tirrell

Long nanotubes of fluid-bilayers were used to create templates for photochemical polymerization into solid-phase conduits and networks. Micromechanical methods were developed which allowed each nanotube to be pulled from a micropipette-held feeder vesicle by mechanical retraction of the vesicle after molecular bonding to a rigid substrate. The caliber of the tube was controlled precisely in a range from 20 to 200 nanometers by setting the suction pressure in the micropipette. Branched conduits were formed by coalescing separate nanotubes drawn serially from the feeder vesicle surface. Single nanotubes and nanotube junctions could be linked together between bonding sites on a surface to create a functionalized network. After assembly, the templates were stabilized by photoinitiated radical cross-linking of hydrophilic monomer contained in the aqueous solution confined by the lipid bilayer boundary.

Nanometer-sized vesicles that were prepared by extrusion were also used as templates for photopolymerization. Results from dynamic light scattering and electron microscopy experiments suggest that UV initiated, free-radical polymerization of vesicle-encapsulated monomer resulted in the formation of cross-linked polymer networks that

were surrounded by a bilayer lipid membrane. Using fluorescence spectroscopy to monitor the release of an initially entrapped marker, it was determined that lumenal polymerization neither disrupted the semi-permeable membrane, nor did it effect the osmotic release of encapsulated solutes. The addition of detergent to a suspension of polymerized vesicles completely dissolved the bilayer membrane, leaving behind a rigid gel replica of the vesicular template.

Two polymerizable amphiphiles with reactive headgroups were prepared and incorporated into the phospholipid bilayer, so as to provide a means to copolymerize the bilayer sheath with the liposome-encapsulated monomer. By monitoring the release of entrapped solutes, it was discovered that photopolymerization of vesicles constructed with either one of the amphiphilic monomers in combination with encapsulated monomer resulted in membrane destabilization, and the complete release of the entrapped solutes. This represented a new approach to the photoinduced release of vesicle contents. In fact, vesicles that contained the polymerizable lipid but not the entrapped monomer also exhibited contents release upon polymerization. During polymerization, the propagating membrane-bound polymer destabilized the membrane. Two simple models were put forth to explain the photoinduced release from polymerized vesicles. One takes into consideration the mechanical stresses that develop in the membrane in response to asymmetric polymerization; the second suggests that release of contents was caused by formation of a membrane-bound, polymeric surfactant which forms "pores" in the membrane.

TABLE OF CONTENTS

APPENDICES

# LIST OF TABLES

# LIST OF FIGURES

# INTRODUCTION

The first chapter of this thesis describes how synthetic vesicles were used to fabricate lipid tubes with lengths of hundreds of microns and internal radii as small as 15 nanometers. Each nanotube was pulled from a micropipette-held feeder vesicle by mechanical retraction of the vesicle after molecular bonding to a rigid substrate. Micropipette aspiration set the level of tension in the membrane, and in turn, membrane tension controlled the nanotube diameter. The fabrication of such structures was made possible by the fluidity of the biomembrane interface, meaning the nanotubes were intrinsically unstable, and could not survive removal from the aqueous processing medium. Therefore, the challenge was to develop chemical strategies that stabilized the membrane template. Achieving this goal has shown that the lipid nanotube can serve as templates for the production of nanoscale conduits and networks. Because one of the long term goals of this project is to prepare functional electrical devices from arrays of nanotubes, we have developed methods to prepare nanotube junctions that are linked together between bonding sites on a conducting surface.

In the course of the investigation into the chemical stabilization of lipid nanotubes, it was realized that lumenal polymerization might impart unique mechanical properties onto the *membrane template*. Therefore, much of the second chapter will be devoted to those experiments which have been designed to elucidate the effect of polymerization on the bilayer membrane. Specifically, we ascertained if the bilayer template continued to encapsulate the polymer network after polymerization; if it was completely stripped away from the encapsulated hydrogel by detergent and if the polymerization process caused temporary or permanent defects in the membrane.

Knowledge of the condition of the membrane template after polymerization is vital if this technology is to be used to make functionalized, nano-scale networks. For example, lipid nanotubes could potentially serve two purposes: (1) as *templates* to prepare conducting nanowires, and (2) as an *insulating* layer that surrounds a conductive medium. If, in fact, the membrane does remain intact after lumenal polymerization, would the presence of an encapsulated gel increase the vesicle stability towards osmotic stress? Data collected from dynamic light scattering, electron microscopy and fluorescence spectroscopy monitoring the release of entrapped solutes provided the information necessary to answer these and other questions.

In addition to lumenal polymerization, another general approach to stabilize a phospholipid vesicle is to polymerize reactive amphiphiles that are directly incorporated in the bilayer sheath. Interestingly, prior to this investigation, no attempt had been made to purposely anchor phospholipid membrane to an encapsulated polymer network by reacting polymerizable lipids that form the bilayer with entrapped monomer. Covalently linking a fluid membrane to an encapsulated polymer network could have profound effects on the membrane stability. Therefore, in continuing our general investigation into the different strategies to stabilize biomembrane templates, two reactive amphiphiles were synthesized that were specifically designed to copolymerize with vesicle-entrapped monomer. That is, the hydrophilic headgroups of the lipids were methacrylated, thus providing a means to form covalent point attachments between the membrane and a hydrogel in the interior compartment of the lipid capsule. A portion of chapter 2 and all of chapter 3 will be devoted to the interesting effects these polymers had on the bilayer membrane.

The micropipette manipulation of giant vesicles is carried out on an instrument built around an inverted optical microscope. Such an instrument was constructed, and in appendix A its major optical components will be described. Also described in this chapter are the micromanipulation procedures that have been used to create nano-scale biomembrane templates for photopolymerization.

# CHAPTER 1

# BIOMEMBRANE TEMPLATES FOR NANOSCALE CONDUITS AND NETWORKS

## Introduction

The fabrication of nanometer-scale materials has attracted considerable attention because of the potential application of such materials in microelectronics,[1] drug delivery[2] and bioencapsulation.[3] Ultra-small structures often have unique properties, (e.g., electronic, optical, catalytic, etc.), which differ from the analogous properties of a macroscopic sample of the same material.[4-8] Here, we report a method to prepare long nanotubes of fluid-lipid bilayers that can be used to create templates for photopolymerization into solid-phase conduits and networks. The nearly millimeter long hollow tubes have diameters precisely controlled in the 20 to 200 nm range and can be linked on a surface to create a functional network. After assembly, the templates can be stabilized by photoinitiated radical cross-linking of macromonomers contained in the aqueous solution confined by the lipid bilayer boundary.

## Nanofabrication Methods

Submicron-sized components have traditionally been prepared by various lithographic processes, which entail a series of etching steps where the exposed (positive) or unexposed (negative) portions of a resist film are selectively dissolved by an

appropriate solvent (developer).[9] With conventional photolithography, patterns are exposed by illumination through a shadow mask composed of clear and opaque regions. This process can be used to create microdevices with features as small as ~120 nm.[10] Unfortunately, devices that demand smaller features can not be produced by photolithography because of the practical limits of resolution set by diffraction of the exposing radiation. Diffraction causes diminished resolution and a shallow depth of focus limiting the size of the smallest features to approximately the wavelength of the radiation.

The limitations of conventional photolithography have been the catalyst for developing direct imaging alternatives that do not require "masks". These techniques use focused beams of high-energy radiation (e.g., X-rays, laser, and e-beams, etc.) that generate well-defined patterns in substrates. These "scanning" processes are excellent methods to fabricate devices with components that have features in the sub-100 nm range.[11]

For manufacturing purposes, the various forms of lithography have one obvious advantage; they are massively parallel processes and can be used to produce complex devices in a very short time. However, one of the main objectives of nanotechnology is to determine the potential application of nanostructures constructed from a wide variety of materials. This includes those substances that are not easily processed by lithography.[12,13] It must be recognized that many of the emerging new techniques to fabricate nanoscale-materials will not meet the stringent requirements for industrial

application. These new developments do provide the means to study novel systems that can not be synthesized by existing technologies.

The design challenge, then, is to develop a new technique, which addresses the specific limitations of lithography. One major drawback of lithography is the harsh chemical conditions that are used to process substrates. Many materials can not withstand these conditions, new processes must be developed for materials that are not easily manipulated by lithography. Patterned substrates prepared by lithography have flat, two-dimensional features that are restricted to the plane of a surface; it would be interesting to explore innovative ways to prepare three-dimensional nanostructures.

In the last 10 years, numerous strategies have been developed which complement lithography, including processes where atoms and specially designed molecules spontaneously self-assemble into structurally well defined aggregates. Some excellent examples include the self-assembly of carbon and other materials into nanotubes and quantum wires[14-16] and the coalescence of lipid surfactants from solution into submicrometer tubules.[17,18] Because of the bulk nature of the processes used to assemble such aggregates, it is difficult to preset the dimensions (such as tube length and the number of layers in the tube wall), and it is even more difficult to pattern macroscopic arrangements of the tube structures.

New techniques which yield nanoscale structures that have the ability to make macroscopic patterns are the fabrication of sub-10-nanometer metal-oxide devices using an AFM,[19] nanochannel glass arrays that serve as template structures for quantum confined systems,[20] and quantum corrals built from atoms which confine electrons to

length scales approaching the de Broglie wavelength.[21] Martin[22] has developed a "template" method that involves synthesizing the desired material within the pores of a nanoporous membrane. Each core is viewed as a small beaker in which a piece of the desired material is synthesized. Given the cylindrical geometry of each pore, nanocylinders with the dimensions of the pore are produced. This method allows the chemist to control the size and shape of the nanostructures by choosing membranes with the proper pore architecture.

Membrane Tethers

We have developed a new "template" process for the fabrication of polymeric nanowires. A robust crosslinked gel is produced in the lumen of a well-defined nanoconduit by photo-crosslinking monomer that is confined by the template barrier. In our method, the template is a long, hollow tube constructed of fluid lipid bilayers. We have prepared near millimeter length cylinders with diameters precisely set in the 20-200 nm range that are stabilized by photo-crosslinking macromonomers confined by the lipid bilayer boundary.

The formation of bilayer nanotubes has been studied for nearly three decades. Blackshear[23] and Hochmuth[24] were the first to observe that long, hollow membrane cylinders or "tethers" could be extracted from red blood cells. Red blood cells, which are point attached to glass and are subjected to a fluid-shear force detach from the glass and are anchored to it by one or two submicron sized tethers (Figure 1.1). Hochmuth et. al.[25] later demonstrated that fluid-shear forces greater than ~ $10^{-6}$ dyn cause tethers to spontaneously form and steadily elongate because the blood cells are forced to flow away

from the point of attachment. In these tests, the tether structure is modeled as an elastic material because micrographs of tethered cells exposed to different shear reveal the tether radius is inversely proportional to the tether force.

In 1982, Hochmuth and Evans[26] developed a new method to extract tethers from red blood cells, which will be referred to as the "bead" method, where a cell is aspirated by a glass micropipette and adsorbed to a small glass bead at a point that is diametrically opposite to the point of aspiration. Mechanical retraction of the bead causes a tether to form between the cell and bead. The bead, as it is steadily moved away, exerts a force on the membrane (tether force), and causes the membrane material from the cell to flow into a submicron tether that "bridges" the bead to the aspirated cell (Figure 1.2).

Tethers are also readily extracted from giant multi- and unilamellar vesicles composed of synthetic lipids.[27,28] This demonstrates it is possible to pull tethers from bilayer membranes that are not supported by a cytoskeletal structure, and from live neuronal growth cones using a force generated by a laser tweezers trap.[29] Frequently, when vesicles are dehydrated to create large excesses of surface area, or when cytoskeletal structures are destroyed inside cells, spherical blebs appear and remain tethered to the outer membrane by invisible bilayer tubes.[30] The frequent occurrence of tethers in nature shows that the closed spherical topology preferred by lamellar-phase lipids is extremely difficult to disrupt.

To date, tethers have been used extensively to measure the mechanical properties of fluid membranes (e.g., bending rigidity, membrane surface tension, and viscous slip between coupled monolayers); however, prior to initiation of this research program, no

attempt had been made to use them as templates for the production of stable nanostructures. As the results reported herein demonstrate, we have developed a technique that utilizes tethers as templates for photochemical polymerization into solid-phase conduits and networks. Each nanotube is pulled from a micropipette-held feeder vesicle by mechanical retraction of the vesicle after molecular bonding to a rigid substrate (e.g., bead, gold surface, glass, etc.). The suction pressure in the micropipette used to hold the vesicle precisely controls the caliber of each tube. In addition to single tubes, branched conduits can be formed by coalescing separate nanotubes that are drawn serially from the feeder vesicle surface. Single nanotubes and nanotube junctions can be linked together between bonding sites on a surface to create a functionalized network. After assembly, the templates can be stabilized by photoinitiated radical cross-linking of macromonomers contained in the aqueous solution confined by the lipid bilayer boundary.

## Experimental Section

### Materials

All materials were used as received. Stearoyl-oleoyl phosphatidylcholine (SOPC), dioleoyl phosphatidylethanolamine (DOPE), dioleoyl phosphatidylcholine (DOPC) and N-rhodamine egg phosphatidylethanolamine (Rhod PE) were purchased from Avanti Polar Lipids, Inc. (Alabaster, AL). The triethylammonium salt of N-([6-(biotinoyl) amino] hexanoyl)-dipalmitoyl phosphatidylethanolamine (biotin-X-DPPE), in which the biotin moiety is conjugated to the DPPE head group through a hydrocarbon spacer 10 to 15 Å long, was purchased from Molecular Probes (Eugene, OR). Cholesterol, dioctyl

disulfide, sodium chloride, sodium bicarbonate and rose bengal were purchased from Aldrich Chemical Co. (Milwaukee, WI). Sucrose, dextrose, sodium phosphate monobasic (99%, ACS reagent), potassium phosphate, dibasic (99%, ACS reagent), potassium chloride (99%, ACS reagent), chloroform (HPLC grade), and methanol (ACS reagent grade) were purchased from Fisher Scientific (Fair Lawn, NJ). Triethanolamine (free base, TEOA) ,4-(2-hydroxyethyl)-1-piperazineethanesulfonic acid (HEPES), bovine serum albumin and Triton X-100 were purchased from Sigma Chemical Co. (St. Louis, MO). Ethanol (US Industrials Co.) was deoxygenated with bubbling nitrogen just prior to use. Fluorescein conjugated avidin, neutravidin and N-hydroxysulfosuccinimide biotin ester (NHS-LC-biotin) were purchased from Pierce (Rockford, IL). Poly(ethyleneglycol) 1000 dimethacrylate (PEGDMA) was purchased from Polysciences, Inc. (Warrington, PA). A 12"x12"x1/16" Teflon sheet was purchased from McMaster-Carr (New Brunswick, NJ). Biotinylated poly(methacrylic acid-ran-N-ethyl-2-amino-acrylamide) copolymer beads were prepared by Patrick Kiser at the University of Washington, Seattle. The hydrochloride salt of 11-aminoundecanylthiol was a gift from the group of Professor George Whitesides of Harvard University.

Preparation of Giant Vesicles

Lipid compositions were chosen to ensure that the phase transition temperature of the mixture would be well below room temperature. The chemical structures of the lipids used to construct the giant vesicles are shown in Figure 1.3. Using a small glass syringe, a 30 μl drop of a 1 mg/ml lipid solution in chloroform/methanol (2:1) was placed on a roughened Teflon disk, spread over the entire surface using the syringe needle, and placed

in a 50 ml glass beaker. The Teflon disk was prepared by roughening its surface with medium grade sandpaper, cleaned with detergent and thoroughly rinsed with both deionized water and several milliliters of chloroform. The volatile organic solvents were removed from the lipid film by placing it under a high vacuum for a minimum of 2 hours while keeping the lipid in constant darkness. After purging the vacuum with nitrogen, the dried lipid film was prehydrated by a warm, water-saturated argon or nitrogen jet for 15 minutes.

The solution to be encapsulated (200 mM sucrose plus ingredients for polymerization) was passed through a 0.2 or 0.45 μm syringe filter, and gently added to the pre-hydrated lipid. Typically, vesicles formed after the system was left to swell overnight at approximately 40 °C. A 250 μL aliquot of vesicles was harvested from the top of the beaker and resuspended in about 1 ml of an equiosmolar glucose solution.

Generally, vesicles were formed in a solution containing 200 mM sucrose, 100 mM triethanolamine, 0.1 mM rose bengal, and 10 weight % PEGDMA. After resuspension in equiosmolar glucose, the vesicles were injected into a microscope chamber and a single vesicle was aspirated by a pipette and transferred into the adjacent chamber where photopolymerization tests were conducted. The second chamber contained a slightly hyperosmotic glucose solution plus 0.1 mM rose bengal, 100 mM triethanolamine, 25 mM NaCl, 2 weight % PEG 2000 (no methacrylate groups), and 0.2 weight % albumin.

## Photopolymerization of Biomembrane Templates

First, a single vesicle was transferred to the microchamber on the microscope stage that did not contain multifunctional monomer. A suitable pattern was formed with the biomembrane templates, and then stabilized by crosslinking the entrapped PEGDMA by photoinitiated free-radical polymerization. Free radicals were generated by the dye-sensitized photooxidation of TEOA using rose bengal as the photosensitizer. Photopolymerization was initiated by irradiation with a focused, 514-nm laser beam generated from a Coherent Inova 90-4 argon-ion laser set at 1 W.

## Molecular Adhesion System

The molecular attachment system used in all experiments was based on the bacterial adhesion complex formed between biotin and avidin. Biotin binds with biotin-binding proteins such as avidin and neutravidin with exceptionally high affinity ($10^{-15}$ $M^{-1}$).[31] In all experiments, the vesicle bilayer was doped with 1 mol % biotinylated lipid (biotin-X-DPPE) and adsorbed to neutravidin coated substrates.

Preparation of Neutravidin Coated Beads. Neutravidin binds strongly to biotinylated 5 μm copolymer beads. Approximately ~ $10^5$ biotinylated beads were suspended in 1 ml of 50 μg $ml^{-1}$ neutravidin and PBS buffer (2.5 g NaCl, 0.0625 g KCl, 0.359 g $Na_2HPO_4$, 0.075 g $KH_2PO_4$ diluted to 250 mL, pH = 7.3). After the suspension had been incubated for one hour at room temperature, non-adsorbed protein was rinsed away with 150 mM NaCl.

Preparation of Gold Contacts. Micron-sized gold contacts were deposited onto glass coverslips using electron-beam lithography. Patterned substrates were prepared by spin coating 4 % PMMA (MW = 9.5 x $10^5$) in anisole (spin rate 4000 RPM for 45 sec) onto a cleaned glass coverslip, followed by 25 minute vacuum drying at 180 °C to remove the casting solvent. Direct imaging exposures were performed using a NPGS direct writing tool (Nabity Lithography Systems) with a exposure dosage of 400 μC $cm^{-2}$, 12 kV accelerating voltage, and a 19 pA beam current. Selective dissolution of the exposed regions was carried out by a 5 min soak in methylisobutylketone and isopropanol (1:3 V/V), followed by a 1 min rinse in isopropanol. The substrate was placed in a vacuum chamber, then, to facilitate gold adhesion, a 30-Å chromium layer was deposited. Then a 300-Å layer of gold was evaporated onto the substrate. The chromium/gold covered PMMA was dissolved by acetone, resulting in the desired gold pattern. The substrates were stored in glass vials under vacuum until used.

Preparation of Monolayers. Just prior to use, the gold substrates were rinsed with chloroform and ethanol and blown dry with a filtered jet of nitrogen. Self-assembled monolayers (SAMs) were prepared by immersing the substrates into solutions of 11-aminoundecanylthiol and dioctyl disulfide for ~ 2 hours. The thiol/disulfide solutions were freshly prepared in deoxygenated, absolute ethanol. The total concentration of sulfur-terminated chains in the solution was kept constant at 1 mM, where dioctyl disulfide was counted at twice its actual concentration. Following immersion, each grid was washed with 100 mM sodium bicarbonate, pH 8.4.

The amine terminus of the thiols was reacted with succinimidyl-6-(biotinamido) hexanoate (NHS-LC-biotin) in 100 mM sodium bicarbonate buffer (pH 8.4) at room temperature. Immediately prior to biotinylation, 0.6 mg of NHS-LC-biotin was dissolved in 250 µl sodium bicarbonate. Approximately 200 µl of the solution was placed onto the gold substrate and the reaction proceeded at room temperature for 30 minutes. Unreacted biotin and the reaction by-product N-hydroxysulfosuccinimide were washed away with phosphate buffered saline (PBS buffer: 2.5 g NaCl, 0.0625 g KCl, 0.359 g $Na_2HPO_4$, 0.075 g $KH_2PO_4$ diluted to 250 mL, pH 7.3). The avidin derivative was bound to the surface by placing a 200-µL drop of 250 µg $ml^{-1}$ of protein on the coverslip for 1 hour, after which it was washed with PBS to remove unbound protein.

Micromanipulation

A small aliquot of the harvested vesicles that were suspended in an equiosmolar glucose solution was injected into the sample microchamber on the stage of the Hoffman modified inverted videomicroscope. [Note: A detailed discussion of the optical imaging system is given in appendix A]. For each test, a single vesicle was aspirated by a glass micropipette pulled from borosilicate capillary tubing (Kimble capillary tubes 0.7-1 mm o.d.; Narishige PC-10 vertical pipette puller), and transferred into the adjacent test chamber. Depending upon the experiment, the chamber contained neutravidin-coated microspheres or gold contacts.

Transparent vesicles exhibited excellent contrast with the Hoffman optics provided there was an optical gradient across the membrane. Optically invisible bilayer nanotubes could not be viewed in bright field but were visualized by epiilumination,

which excites lissamine rhodamine B labeled lipids doped in the bilayer. The bandpass filter HQ535/50 (Chroma) was used to select the excitation wavelength for lissammine rhodamine B from a 100 W mercury arc lamp (Oriel). A Chroma Q565/LP dichroic mirror and HQ610/75 second barrier filter were used in combination to filter the fluorescence signal.

All experiments were conducted in a dual microchamber on the stage of an inverted Zeiss microscope at room temperature. Images were collected by Dage 72 charge-coupled devices (Micro Video Instruments, Inc.) and recorded on a Panasonic video S-VHS video cassette recorder. A complete description of image collection and micromanipulation techniques is given in appendix 4.

## Results

### Tether Formation Process

Tethers were extracted from giant bilayer vesicles (20 to 40 μm) that were constructed from a mixture of lipids, specifically 64 mol% SOPC, 33 mol% cholesterol, 2 mol% Rhod PE and 1 mol% biotin-X-DPPE. The vesicles were suspended in a glucose solution that was osmotically balanced with the interior sucrose solution. The sucrose/glucose gradient across the membrane ensured that high quality images were obtained with the Hoffman optics, and that the vesicles sank to the bottom of the chamber due to the more dense internal sucrose solution.

Two physical conditions were required for nanotube formation from bilayer vesicles: (i) The bilayer must be bonded to a spot on a rigid surface and (ii) there must be a reservoir of excess bilayer surface beyond that sufficient to enclose the vesicle volume

as a sphere. These two conditions were easily attained and manipulated externally. First, vesicles after preparation were slightly dehydrated by increasing the osmotic strength of the aqueous suspension. After aspiration into a micropipette, the excess surface of the vesicle was drawn into a projection inside the pipette (Figure 1.4 A), which provided the reservoir of bilayer for nanotube production. By incorporating biotin-X-DPPE in the bilayer composition, strong point attachments were made when the vesicle was touched to a avidin coated bead that was held by a second pipette. When the pipette holding the vesicle was withdrawn, a nanotube formed (Figures 1.4 A and B). Both bright-field and fluorescence optical images show the feeder vesicle connected by the invisible nanotube to an immobilized microsphere coated with neutravidin. The nanotube was exposed by excitation of fluorescently labeled lipids doped in the bilayer surface. [Note: The tube appears thick (~ 0.5 μm) in the fluorescence image, though the actual dimension is an order of magnitude smaller (~ 40 nm).]

Tether Mechanics

A unique feature of this technique is the level of control over the diameter of the nanotubes. Rand and Evans et. al.[32,33] have shown the isotropic tension $T_m$ in the vesicle bilayer is controlled by the pipette suction pressure $\Delta P$, that is,

$$T_m \approx \frac{(\Delta P)R_p/2}{1 - R_p/R}$$

where $R_p$ and R are the radii of the pipette lumen and the spherical body of the vesicle, respectively. In turn, the tension controls the nanotube diameter $(2r_t)$,[27,29,34] as established by a mechanical force balance, that is,

$$r_t^2 = k_c / 2T_m$$

where $k_C$ is the bending stiffness of the bilayer (~ $10^{-19}$ N-m) (Figure 1.5). Nanotube diameter is controlled precisely by bilayer tension. Furthermore, the nanotube diameter is independent of the rate of tube extraction, which verifies that the mechanical force balance is dominated by the elastic properties of the bilayer.[27] It is remarkable that with the aid of an optical microscope, nanometer-scale structures can be fabricated with precisely controlled dimensions down to about 20 nm, which is almost an entire order of magnitude smaller than the features obtainable by conventional photolithography.

Measurement of Tether Radius

Insight into the mechanics of tether formation permits the tether radius to be measured as it is formed.[32] The membrane projection inside the pipette serves as the material reservoir, that is, as the tether is extracted from the membrane, the membrane material in the projection is depleted. Due to conservation of material (i.e., lipid exchange with the aqueous buffer is effectively zero), and since the tension in the membrane is held constant, tether extraction occurs at constant surface area and constant cell volume.[32] Using the constraint of fixed surface area alone, the rate of decrease in projection length $L_p$ inside the pipette is approximately equal to the increase in nanotube length $L_t$, that is, $-2\Pi R_p dL_p \approx 2\Pi R_t dL_t$ , where $dL_p$ is the measurable decrease in length of the aspirated projection and $dL_t$ is the increase in the length of the tether, respectively. By plotting $L_p$ versus $L_t$, the tether radius can be calculated from the slope ($R_t \approx -R_p(dL_p/dL_t)_t$) (Figure 1.6). [Note: Hochmuth and Evans[35] have shown that by

imposing both the constant area and volume conditions, the tether radius can be written as an equality, $R_t = (1 - R_p/R)R_p(-dL_p/dL_t)$ where the factor $1 - R_p/R \approx 0.7$ ].

Production of Nanotube Junctions

Because the lipids were selected to form a fluid surface, two or more nanotubes drawn from the same feeder vesicle coalesce to a single junction when the vesicle is pulled away from the attachment sites. Fluorescence microscope images of the process to produce a Y-branched nanotube element are shown in Figure 1.7. Serial repetition of these procedures between points in an array of sites can create a complex network of nanotubes and branched elements.

Nanotubes Drawn Between Metal Contacts

Lipid nanotubes were drawn between metal contacts by adsorbing a biotinylated vesicle serially to neutravidin coated micron sized gold squares. Conventional electron-beam lithography was used to prepare 5 μm gold contacts on a glass coverslip. The gold contacts were made adhesive towards biotin by a three-step chemical process (Figure 1.8). First, a self-assembled monolayer (SAM) was deposited onto the gold by immersion into a solution of 11-aminoundecanylthiol and dioctyl disulfide.[36-38] This resulted in a surface coated with a hydrophobic matrix of methyl groups interspersed with primary amine groups. In the second step, the surface was biotinylated by coupling the amines with NHS-LC-biotin. [Note: The purpose of the disulfide molecules is to dilute the surface concentration of biotin, as the most efficient adhesion is achieved when aggregates of avidin are minimized.[27]] In the final step, neutravidin was added and

allowed to bind to the biotinylated SAM. Figure 1.9 shows a gold TEM grid that was derivatized using this process. Fluorescein-labeled avidin protein is adsorbed to a biotinylated gold TEM grid, and fluorescence illumination reveals the protein layer. Several SAMs were prepared on different gold grids where the amine terminated thiol mol ratio varied from 1 to 0.005. The observed fluorescence decreased substantially as the amine thiol concentration decreased, demonstrating that protein adsorption was due to specific interactions between biotin and avidin as opposed to non-specific adsorption of the protein.

Figures 1.10 A and B show a tube drawn across two gold contacts. In Figure 1.10 A, the feeder vesicle is brought into adhesive contact with one of two gold pads separated by 30 μm; the attached nanowire is too small to be seen in the bright-field image. Figure 1.10 B shows the fluorescence image of the same microscopic field after the feeder vesicle has been removed, and reveals the patterned nanowire through the luminescence of the Rhod PE lipid doped into the nanotube wall.

Polymerization in the Lumen

Nanotubes and networks that were prepared in this way were intrinsically unstable, and could not survive removal from the aqueous processing medium. Photoinitiated radical cross-linking of (PEGDMA) (Figure 1.11) confined to the interior of the lipid assembly was chosen as a prototype chemistry for stabilization of the membrane template. Cross-linked multimethacrylates form elastic networks that are widely used in applications where strength and shape stability are required.[39] PEGDMA is soluble both in water and in organic solvents, but after cross-linking, the polymerized

material forms a resilient and insoluble polyethylene glycol (PEG) gel. The PEG structure is attractive in the present context for several reasons: (i) The capability of swelling in aqueous and organic environments enables post-polymerization processing of patterns and networks in a wide variety of solvents, (ii) PEG does not denature enzymes or other proteins of potential interest in biosensor or biomaterials technology [PEG-modified enzymes are used currently in clinical applications[40]], and (iii) PEG surfaces are relatively inert with respect to biological cells, suggesting that cell viability and function should not be altered in cellular devices based on patterned PEGDMA networks. For stabilization, PEGDMA was present in the aqueous solution confined by the lipid bilayer and was cross-linked through radicals generated by dye-sensitized photooxidation of triethanolamine.[41] Rose bengal was included as a photosensitizer for excitation by the 514-nm line of an argon ion laser.

Stable casts of lipid bilayer templates are shown in Figure 1.12. The images show a variety of microscopic shapes after photopolymerization and removal of the lipid bilayer template by a detergent solution. In Figure 1.12 A, a vesicle (diameter ~ 20 μm) was cross-linked into a rigid replica of its smooth shape while held by micropipette suction. In Figures 1.12 B to D, images are shown of a large tube (~ 0.5 to 1 μm diameter) attached to the feeder vesicle after cross-linking the core and removing the bilayer. The long cylinder could be repeatedly stressed by pulling on it with a small bore micropipette (Figure 1.12 C). After each release, the cylinder merely relaxes into a loosely coiled "rope-like" shape (Figure 1.12 D), demonstrating the robustness and flexibility of the cross-linked polymer structure. By comparison, fluid bilayer tubes prior

to polymerization are simply drawn back into the vesicle body by membrane tension unless restrained by a pulling force.

## Discussion

These techniques provide a basis for fabrication of functional nanoscale conduit patterns and networks of various kinds. The fluid character of the lipid-derived nanotubes is advantageous in that it allows fabrication of flexible nanometer-scale structures and entrapment of molecular and particulate species. In addition to crosslinking the vesicle lumen, stabilization of the fluid membrane could also be achieved by polymerization of the lipids that form the bilayer sheath, using lipids with polymerizable functional groups. It has already been demonstrated that lipid tubules can be used as precursors for formation of submicrometer silica tubes[42] and as templates for deposition of metals[17] and metal oxides.[43] The methods developed in these earlier approaches should be directly applicable to the patterns made as described here, and should produce robust structures with useful mechanical and electronic properties. Potentially more versatile, the cross-linked core of a polymerized nanotube provides unrestricted opportunity for elaboration of network properties. Photo-crosslinking of water-soluble conjugated polymers can lead to networks of organic conductors and impregnation of the core with metal salts can be used to metallize the structure after reduction. Others have reported a similar approach for deposition of metals in carbon nanotubes.[44,45] The cross-linked core of nanotubes can serve to immobilize enzymes or other proteins capable of modulating electron transfer or biochemical recognition processes, and it is conceivable that nanotube arrays might be used to link together

patterns of biological cells immobilized on substrates[13] to create integrated "cellular" biosensors and devices. Finally, polymeric structures prepared in this way might be exploited as novel masks for lithographic fabrication of functional nanostructures.

Nanotubes might also provide an important means to study nanofluidic behavior, i.e. questions about the dynamics of fluids confined to spaces with dimensions that approach the size of the constituent molecules of the fluid. Flow in confined spaces with dimensions that approach the solvent size deviates from the standard fluid mechanics predictions. The fluid particles must diffuse "single file" through the channel, and are restricted from passing each other. There is some experimental evidence for this from NMR experiments in zeolites.[46,47] The diffusion of single fluorescent molecules and fluorescently labeled latex beads could be measured through direct optical imaging as a function of tube diameter.

The nanotubes could have important applications in analytical molecular separation. The nanotubes represent the ultimate capillaries for electrophoresis. By custom tailoring the chemistry of the internal wall structure, nanotubes could be made suitable for use in electrophoretic separation. One of the advantages of using the nanotubes is that they could be used to perform separations on extremely small amounts of sample material- an important criterion when working with precious biological reagents, such as transcription factors or the contents of a single cell or subcellular organelle.

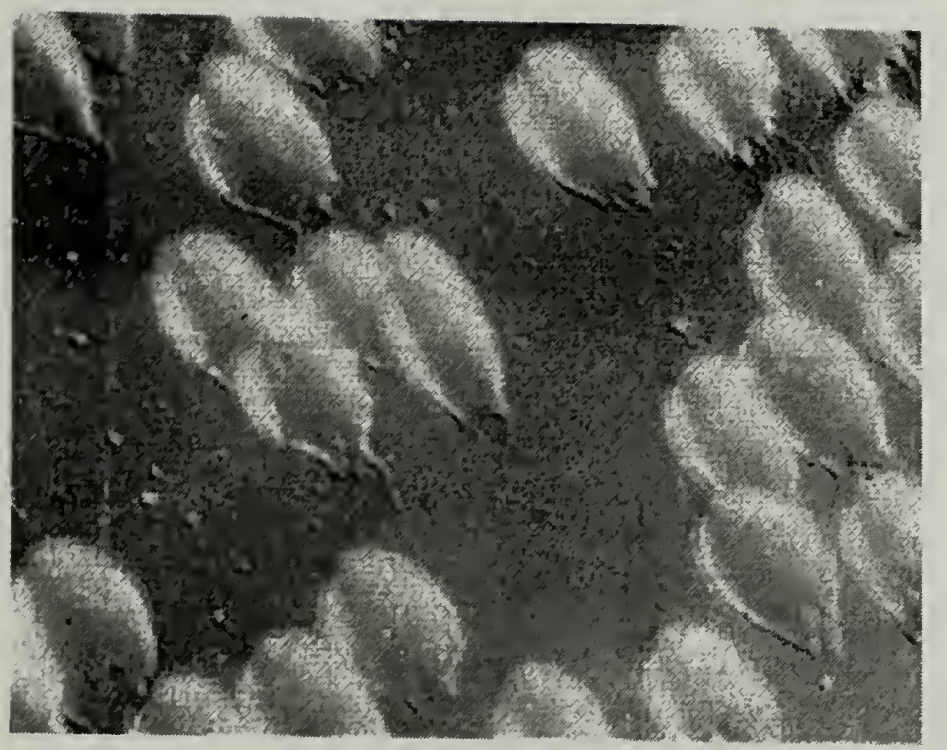

Figure 1.1 Red blood cells that are "tethered" to glass. From Blackshear et. al.[23]

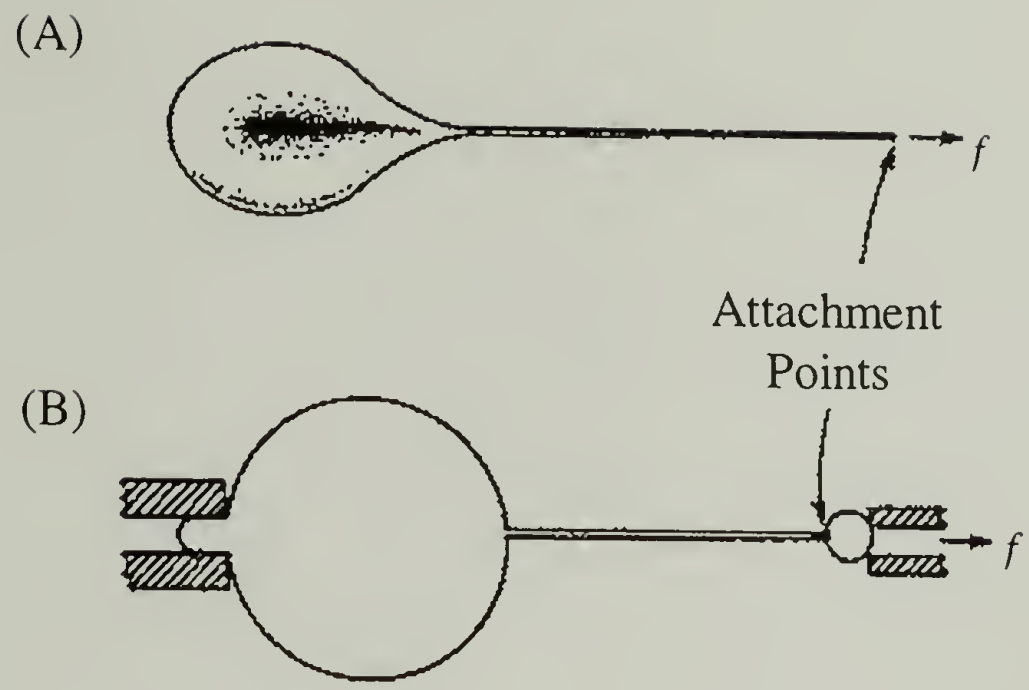


Figure 1.2 Schematic illustration of the "flow" and "bead" techniques used to extract tethers from red blood cells. Each process requires a cell point-adhered to a rigid substrate and excess surface area in the membrane. (A) Illustrates the "flow" method. A flaccid red blood cell is tethered to the glass substrate, and a tether is formed between the cell and the point of attachment when the cell body is exposed to a flow-induced shear of ~ $10^{-6}$ dyn. (B) Illustrates the "bead" method. A red blood cell is aspirated into a pipette until the cell body has a spherical shape, next, a bead is adsorbed to the membrane surface, then it is retracted and a tether is drawn between the cell and bead. From Waugh and Hochmuth.[34]

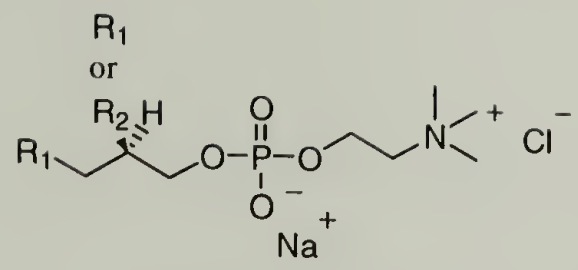


SOPC or DOPC

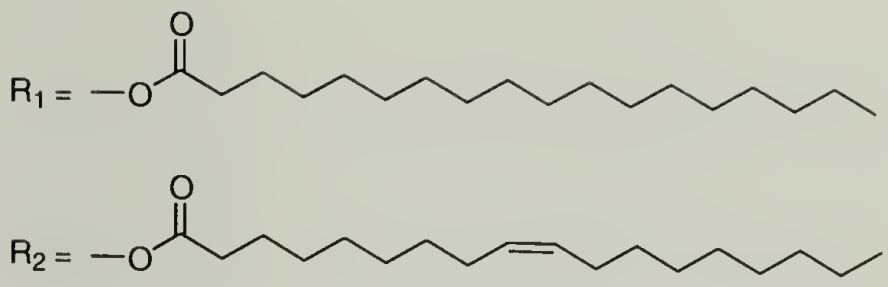


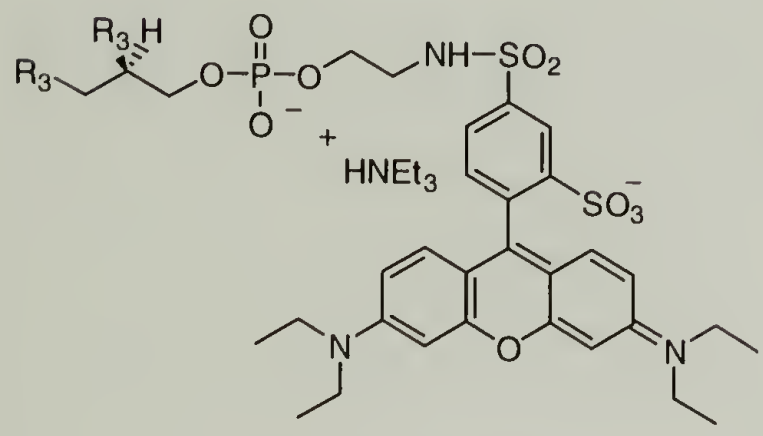


Rhodamine DPPE

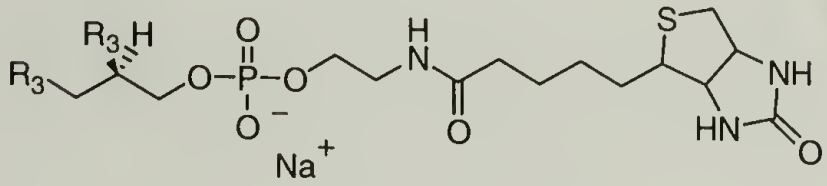


Biotinylated DPPE

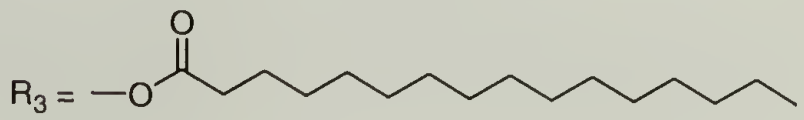


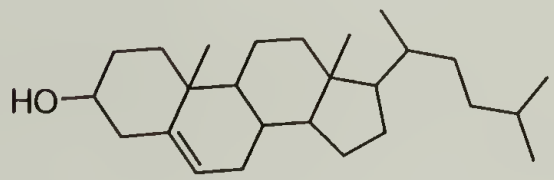


Cholesterol

Figure 1.3 Chemical structures of the lipids used to construct the giant vesicles.

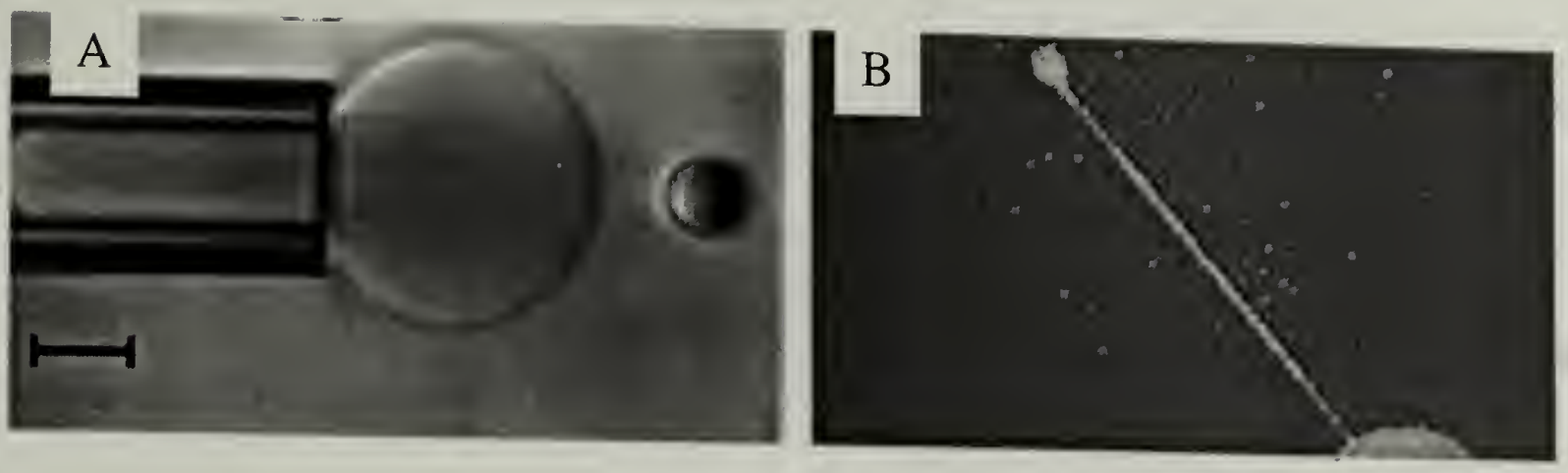


Figure 1.4 Video microscope images of a lipid bilayer vesicle (diameter ~20 microns) held by micropipette suction and tethered to a solid microsphere (diameter ~4 microns) by an invisible nanotube of bilayer (diameter ~40 nanometers) pulled from the vesicle surface. (A) A bright-field image shows only the vesicle and microsphere. The difference in index of refraction between the sucrose contained in the vesicle and the glucose in the exterior solution allows the bilayer (~3 nanometers thick) vesicle to be observed clearly with Hoffman modulation contrast optics. (B) Epiillumination is used to excite fluorescence from labeled lipids doped on the bilayer, revealing the bilayer tube (diameter ~40 nanometers) emanating from the vesicle. The vesicle was withdrawn from adhesive contact with the microsphere to produce the 50-micron-long tube. The cross section of the bilayer tube (which remains continuous with the vesicle surface) is an order of magnitude smaller than the apparent diffraction-limited thickness seen in the fluorescence image. Scale bar, 10 microns.

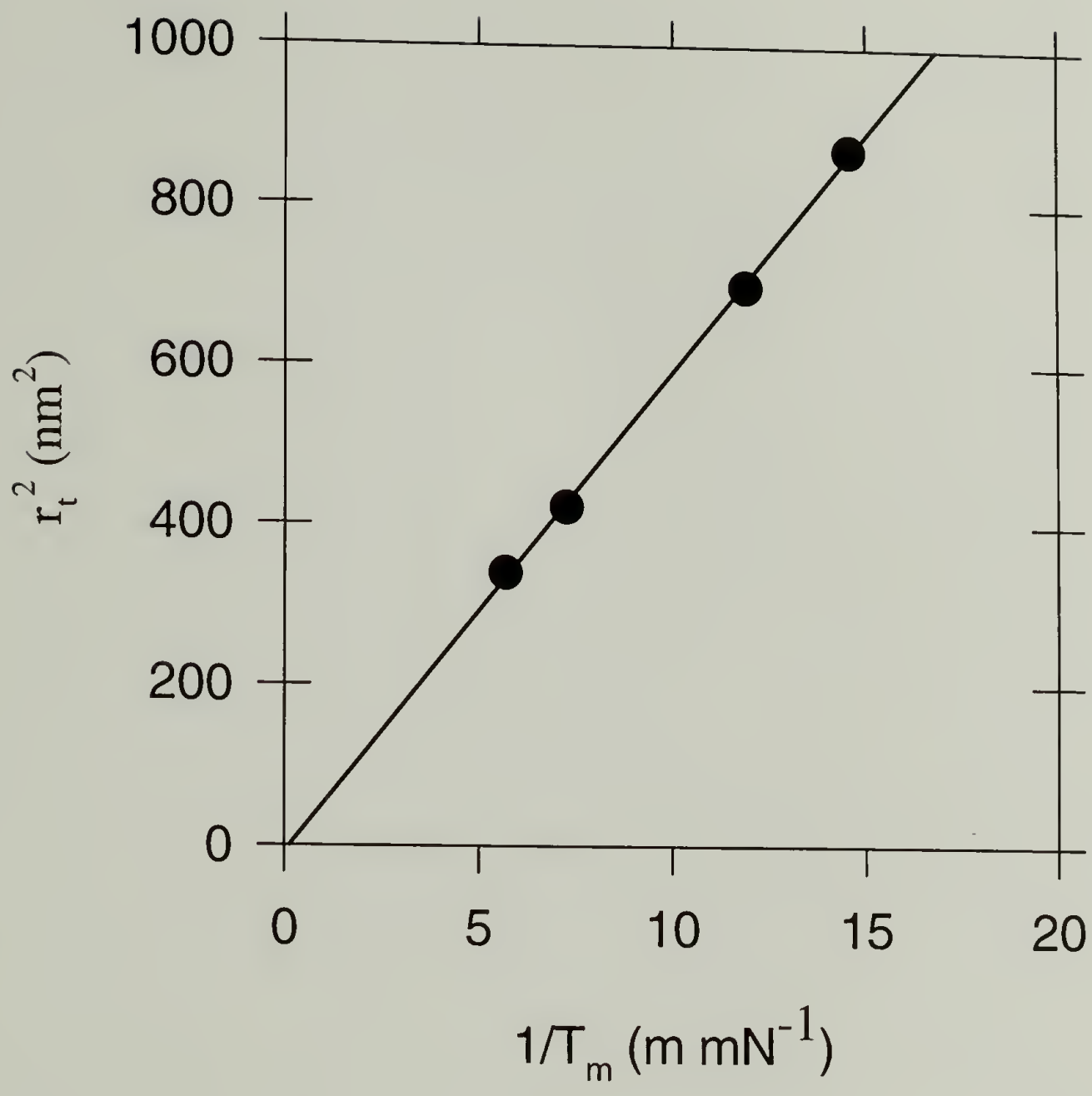


Figure 1.5 Values of the square of the nanotube radius are plotted as a function of bilayer tension. The proportionality between the square of the tube radius and the reciprocal tension is one-half the bending or curvature elasic modulus of the bilayer, which yields $k_c$ ~ $10^{-19}$ N-m.[27]

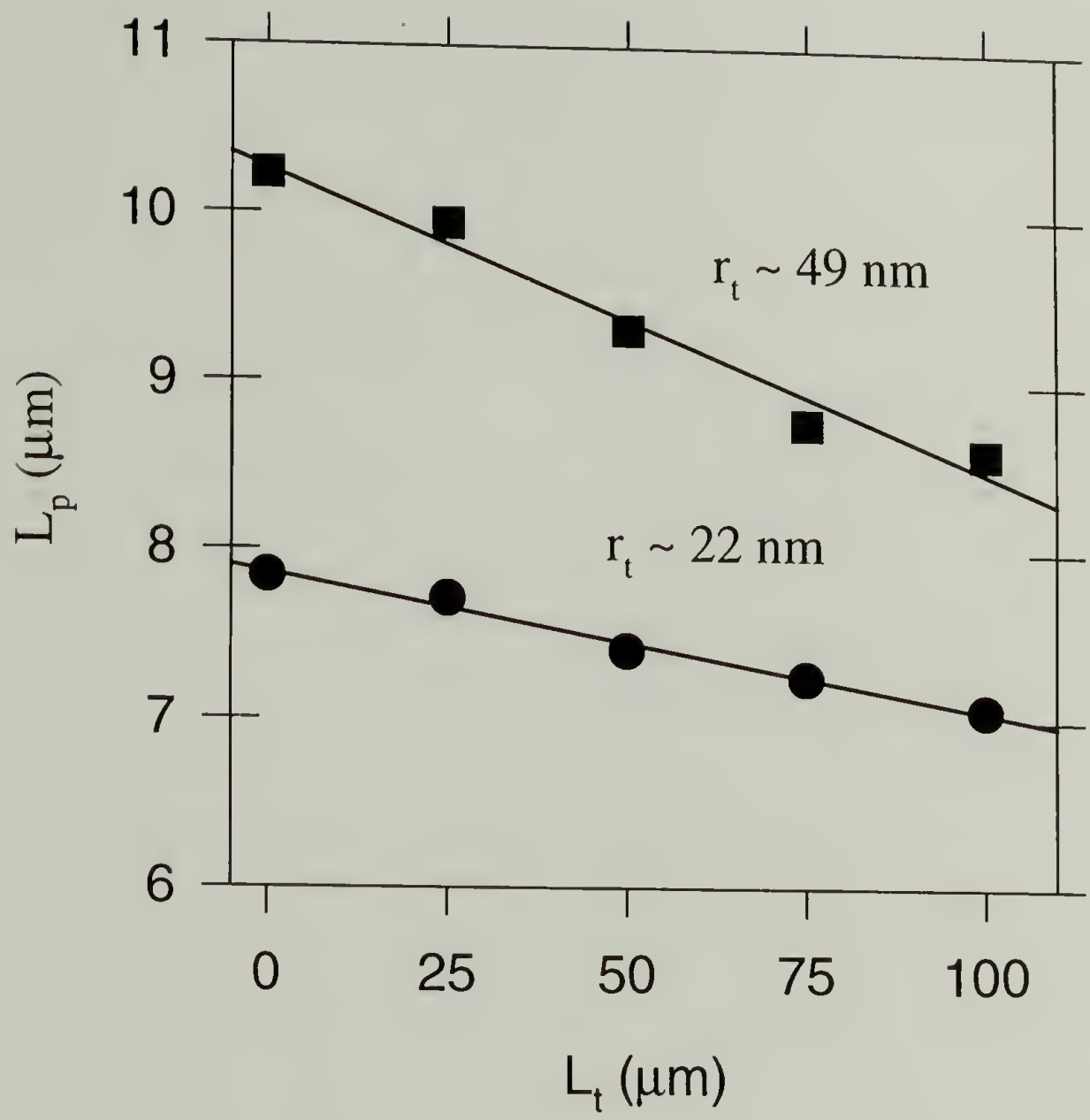


Figure 1.6 Control of nanotube diameter by pipette suction applied to a bilayer vesicle made from pure SOPC. Plots of vesicle projection length $L_p$ inside the pipette versus nanotube length $L_t$ as the vesicle was retracted from the adhesive surface at two levels of bilayer tension (set by pipette suction pressure). The slope of each plot yields the mean nanotube radius $r_t$.

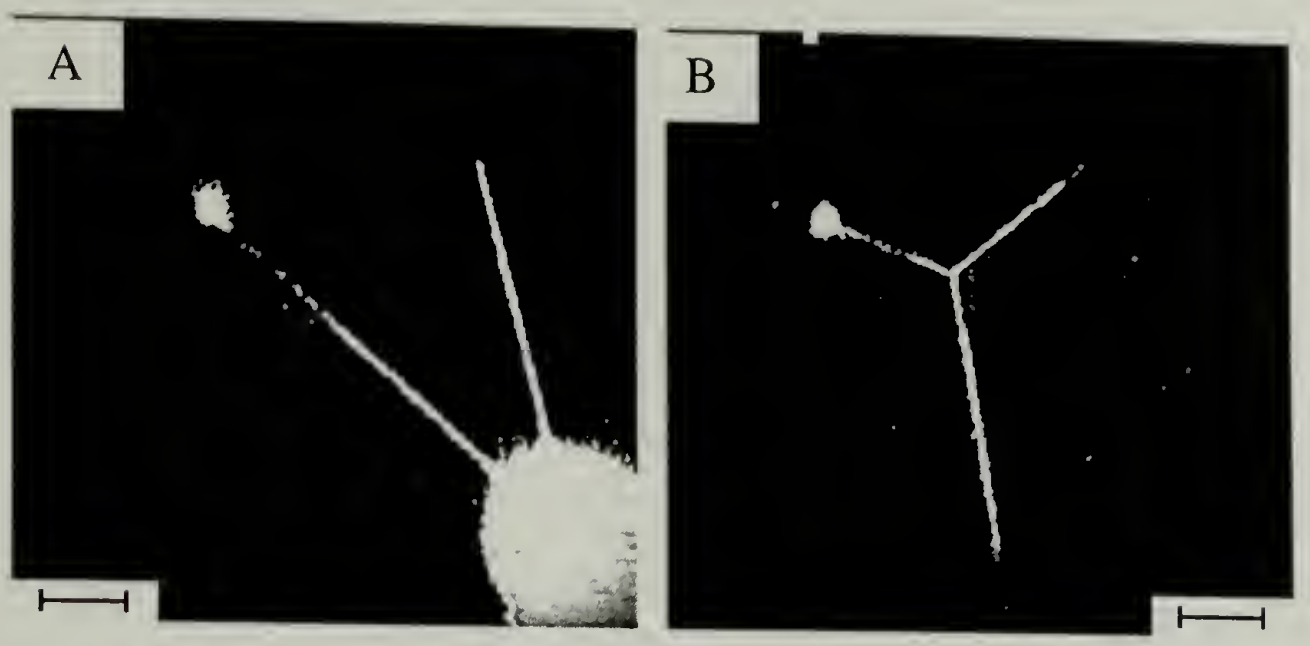


Figure 1.7 Fluorescence microscope images of the manipulation sequence used to create a confluent junction of nanotubes (diameter ~ 40 nm). (A) First, two or more nanotubes are drawn successively from separate regions of the feeder vesicle surface. (B) Next, the vesicle is pulled away and the bilayer tubes slide over the fluid surface to coalesce at a perfect triangular junction, which implies that all three segments have the same bilayer tension and cross-sectional dimension. The procedure can be repeated to create an array of nanotube junctions. Scale bars, 10 μm.

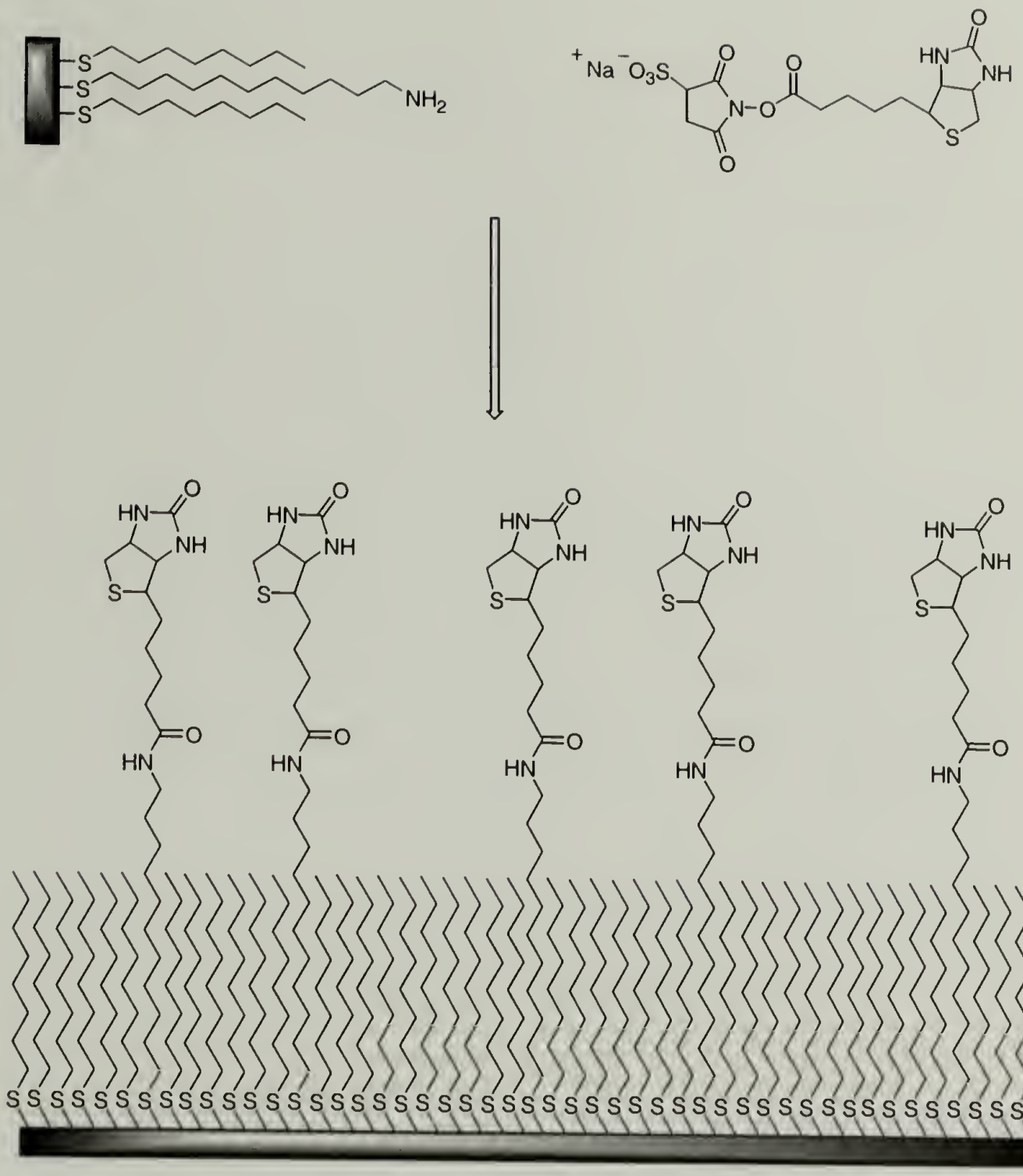


Figure 1.8 A schematic illustration of the biotinylated monolayer. The mixed SAM is prepared by adsorbing a mixture of amine-terminated thiol and disulfide to the gold contact, then, activated biotin is reacted with the amine, giving a supported monolayer which preferentially binds avidin.

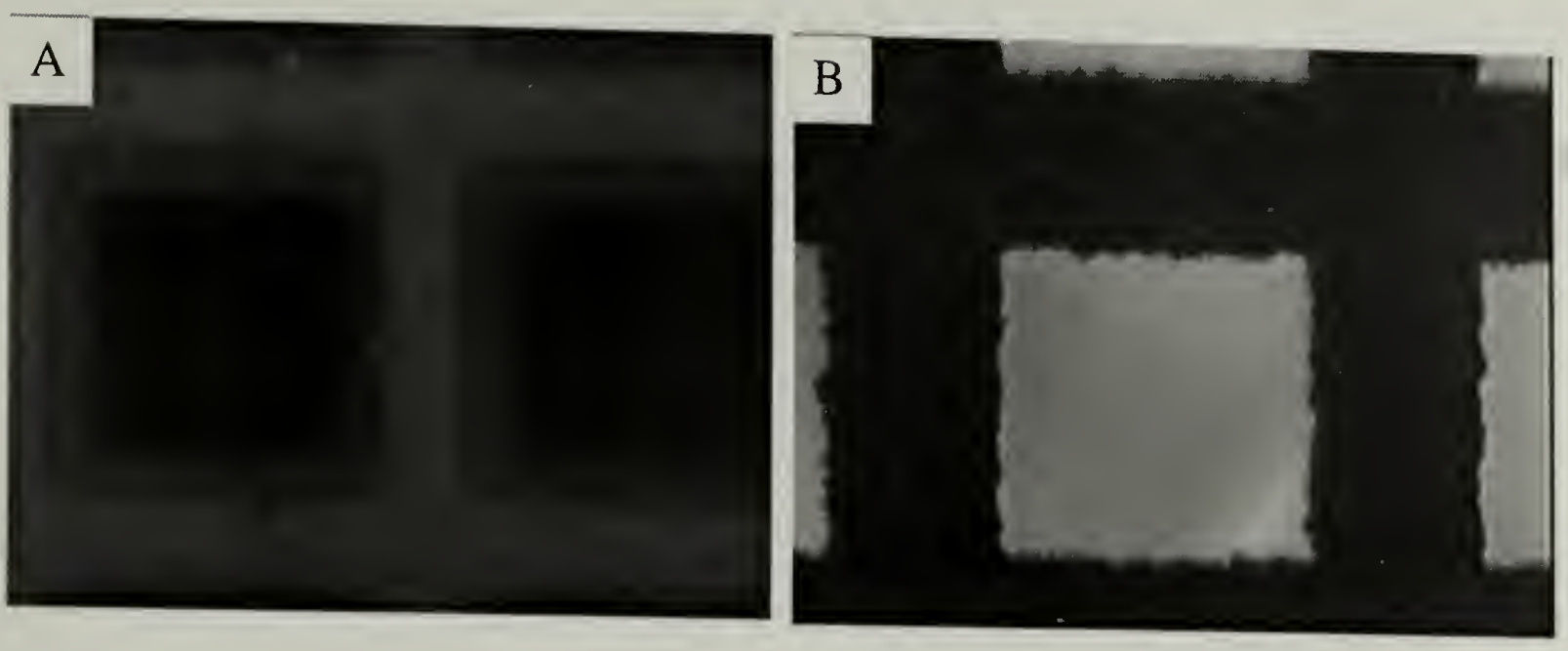


Figure 1.9 A gold TEM grid with a bound layer of fluorescein-labeled avidin. (A) A fluorescence image reveals the adsorbed layer of avidin through the luminescence of the fluorescent protein. (B) Shows the bright-field image of same region as in A.

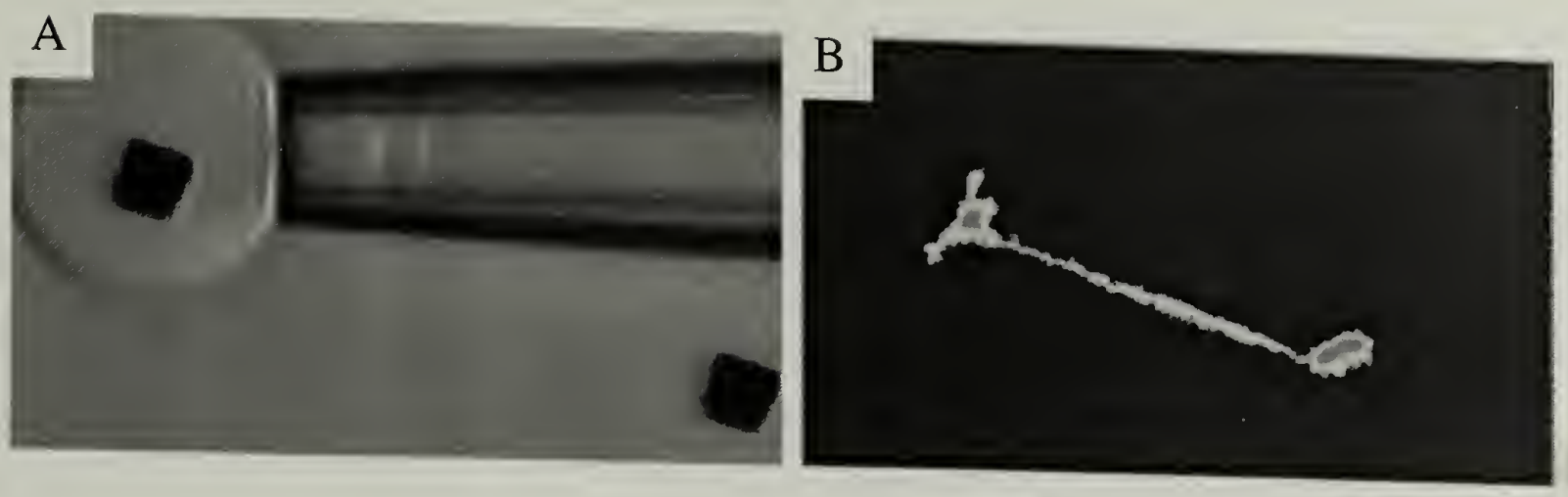


Figure 1.10 A nanotube drawn between 5 μm gold contacts deposited on glass. (A) The surface of a 20 μm aspirated vesicle is adsorbed to one of the two gold pads that are separated by 30 μm; the attached nanotube is optically invisible in bright field. (B) The fluorescence image of the same field of view after the feeder vesicle has been removed reveals the nanoscale conduit through the luminescence of a fluorescent lipid doped in the nanotube wall.

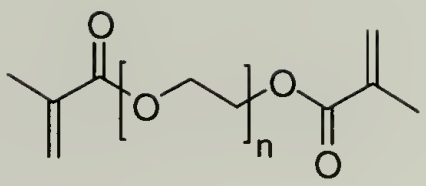

Poly(ethylene glycol) 1000 Dimethacrylate (n ≈ 23)

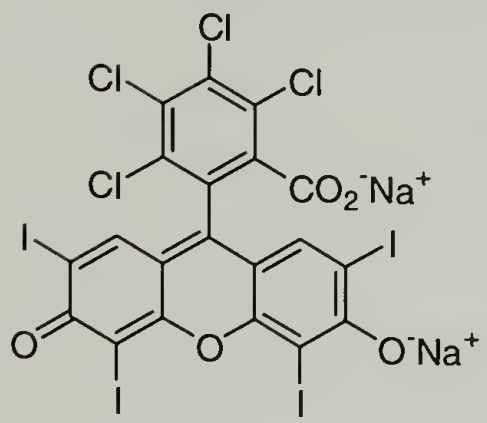

Rose Bengal

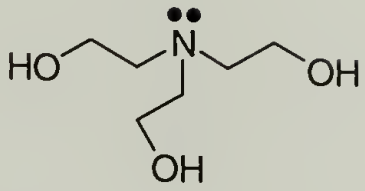

Triethanolamine

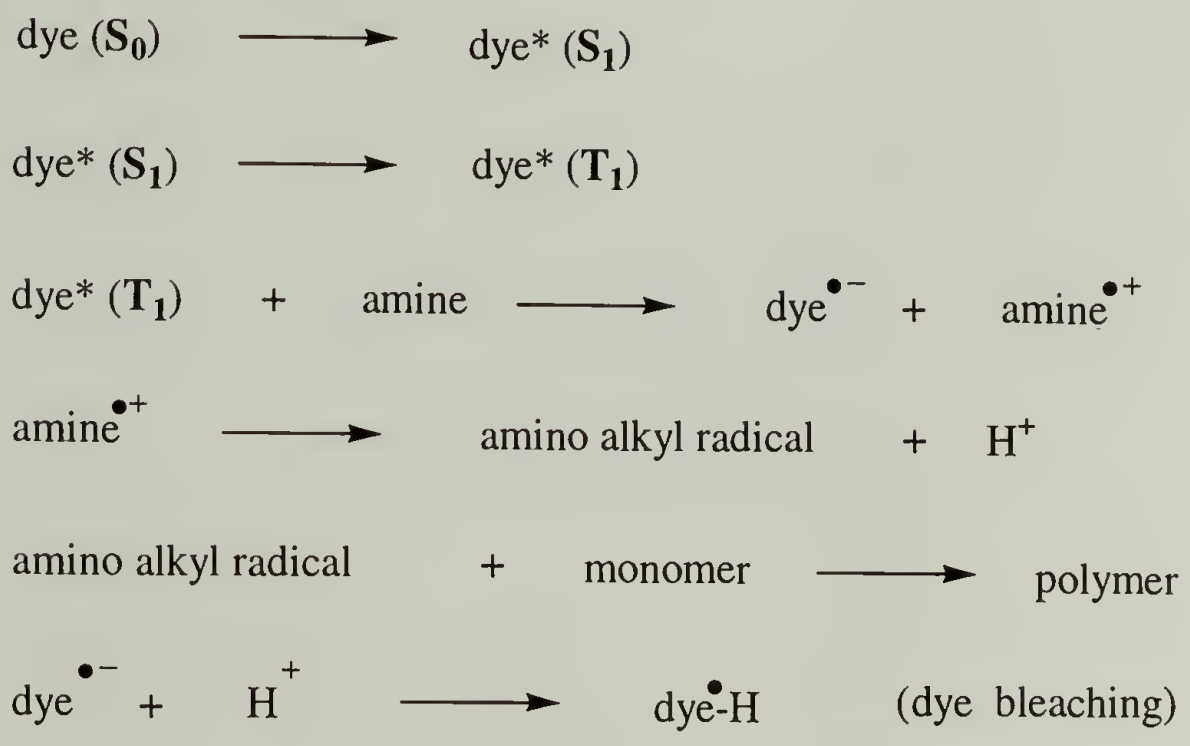


Figure 1.11 The photochemical polymerization reaction used to stabilize nanotube structures. The PEGDMA is confined by the lipid bilayer, and is crosslinked by radicals generated by the dye-sensitized photooxidation of triethanolamine. Rose bengal is included as a photosensitizer.

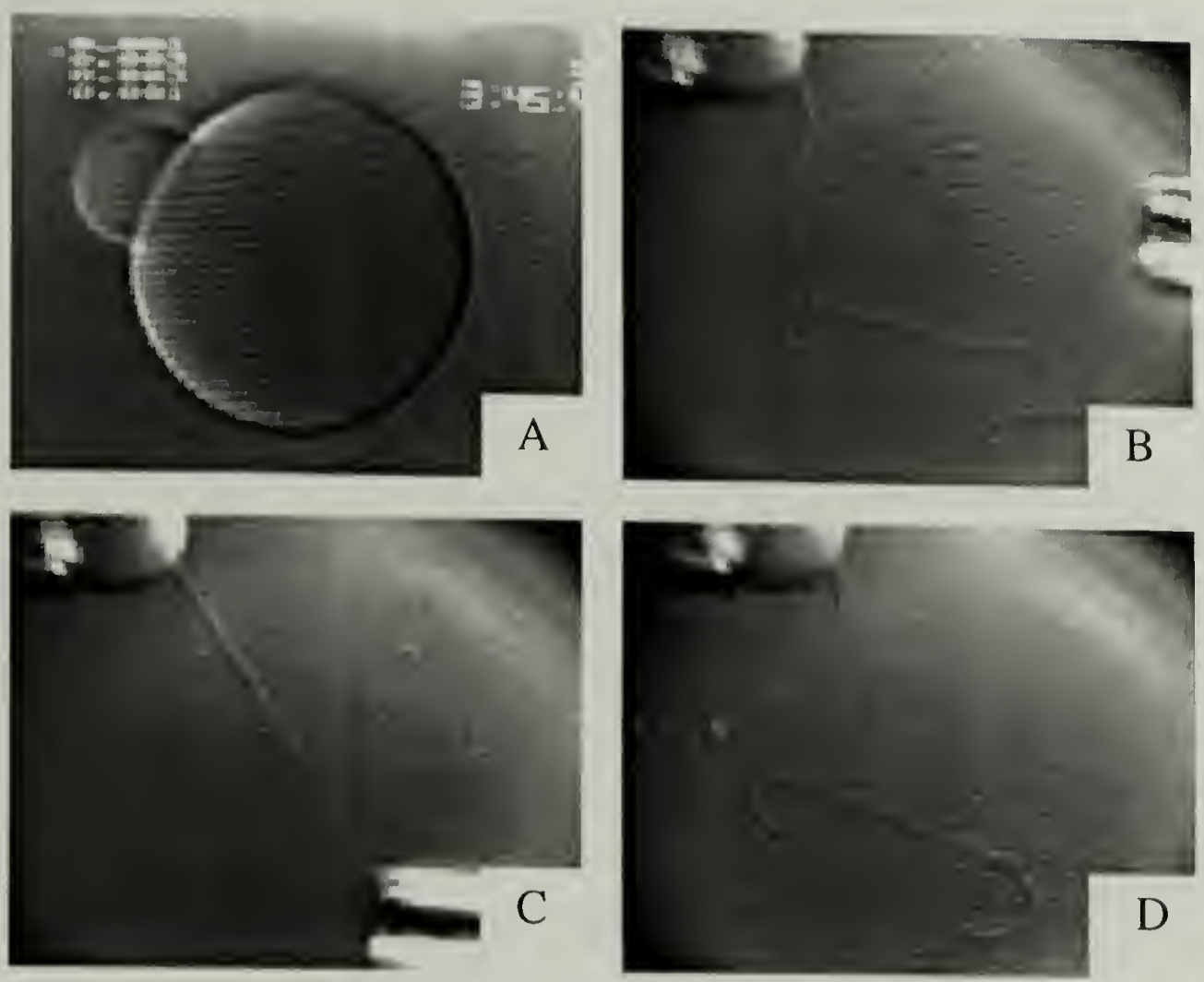


Figure 1.12 Bright-field video images of rigid casts of vesicle and tube shapes after photopolymerization. (A) The cross-linked PEGDMA replica of a bilayer vesicle (diameter 20 μm) aspirated initially into a micropipette. (B) The cross-linked PEGDMA core of a large bilayer tube (diameter ~ 0.5 to 1 μm) connected to the polymerized feeder vesicle. (C) A small-bore pipette pulls on the polymerized cylinder to demonstrate its mechanical strength. (D) After release, the tube relaxes and coils loosely like a flexible "rope".

## References


1) Martin, C. R. "Nanomaterials: A Membrane-Based Synthetic Approach," *Science* **1994**, *266*, 1961-1966.

2) Gref, R.; Minamitake, Y.; Peracchia, M. T.; Trubetskoy, V.; Torchilin, V.; Langer, R. "Biodegradable Long-Circulating Polymeric Nanospheres," *Science* **1994**, *263*, 1600-1603.

3) Parthasarathy, R.; Martin, C. R. "Synthesis of Polymeric Microcapsule Arrays and Their Use for Enzyme Immobilization," *Nature* **1994**, *369*, 298.

4) Lehn, J.-M. "Perspectives in Supramolecular Chemistry- From Molecular Recognition Towards Molecular Information Processing and Self-Organization," *Angew. Chem. Int. Ed. Engl.* **1990**, *29*, 1304-1319.

5) Mirkin, C. A.; Ratner, M. A. "Molecular Electronics," *Annu. Rev. Phys. Chem.*, **1992**, 43, 719-754.

6) Smith, R. C.; Fischer, W. M.; Gin, D. L. "Ordered Poly (*p*-phenylenevinylene) Matrix Nanocomposites via Lyotropic Liquid-Crystalline Monomers," *J. Am. Chem. Soc.* **1997**, *119*, 4092-4093.

7) Nostrum, C. F. v.; Picken, S. J.; Schouten, A. -J.; Nolte, R. J. M. "Synthesis and Supramolecular Chemistry of Novel Liquid Crystalline Crown Ether-Substituted Phthalocyanines: Toward Molecular Wires and Molecular Ionoelectronics," *J. Am. Chem. Soc.* **1995**, *117*, 9957-9965.

8) Bumm, L. A.; Arnold, J. J.; Cygan, M. T.; Dunbar, T. D.; Burgin, T. P.; Jones, L.; Allara, D. L.; Tour, J. M.; Weiss, P. S. "Are Single Molecular Wires Conducting?," *Science* **1996**, *271*, 1705-1707.

9) Reiser, A. *Photoreactive Polymers: The Science and Technology of Resists*, John Wiley & Sons: New York, 1989.

10) Wallraff, G. M.; Allen, R. D.; Hinsberg, W. D.; Simpson, L. L.; Kunz, R. R. "Designing Tomorrow's Photoresists," *Chemtech* **1993**, *23*, 22-30.

11) Cerrina, F. and Marrian, C., Eds., *Materials-Fabrication and Patterning at the Nanoscale*, Materials Research Society: Pittsburgh, 1995.

12) Tolles, W. M. in *Nanotechnology: Molecularly Designed Materials*, Eds., Chow, G. -M. and Gonsalves, K. E., American Chemical Society: Washington, D. C., 1996, pp. 1-18.

13) Whitesides, G. W.; Mathias, J. P.; Seto, C. T. "Molecular Self-Assembly and Nanochemistry: A Chemical Strategy for the Synthesis of Nanostructures," *Science* **1991**, *254*, 1312-1319.

14) Dai, H.; Wong, E. W.; Lieber, C. M. "Probing Electrical Transport in Nanomaterials: Conductivity of Individual Carbon Nanotubes," *Science* **1996**, *272*, 523-526.

15) Baum, R. "Nanotube Characterization," *Chem. Eng. News* **1998**, *76*, 6.

16) Iijima, S. "Helical Microtubules of Graphitic Carbon," *Science* **1991**, *354*, 56-58.

17) Schnur, J. M. "Lipid Tubules: A Paradigm for Molecularly Engineered Structures," *Science* **1993**, *262*, 1669-1676.

18) Kulkarni, V. S.; Anderson, W. H.; Brown, R. "Bilayer Nanotubes and Helical Ribbons Formed by Hydrated Galactosylceramides: Acyl Chain Headgroup Effects," *Biophys. J.* **1995**, *69*, 1976-1986.

19) Snow, E. S.; Campbell, P. M. "AFM Fabrication of Sub-10-Nanometer Metal-Oxide Devices with in Situ Control of Electrical Properties," *Science* **1995**, *270*, 1639-1641.

20) Tonucci, R. J.; Justus, B. L.; Campillo, A. J.; Ford, C. E. "Nanochannel Array Glass," *Science* **1992**, *258*, 783-785.

21) Crommie, M. F.; Lutz, C. P.; Eigler, D. M. "Confinement of Electrons to Quantum Corrals on a Metal Surface," *Science* **1993**, *262*, 218-220.

22) Martin, C. R. "Template Synthesis of Electronically Conductive Polymer Nanostructures," *Acc. Chem. Res.* **1995**, *28*, 61-68.

23) Blackshear, P. L. in *Biomechanics: Its Foundations and Objectives*, Eds., Fung, Y. C., Perrone, N., Anliker, M., Prentice-Hall, Inc.: Englewood Cliffs, N. J., 1972, pp. 501-528.

24) Hochmuth, R. M.; Mohandas, N.; Spaeth, E. E.; Williamson, J. R.; Blackshear, P. L. "Surface Adhesion, Deformation and Detachment at Low Shear or Red Cells and White Cells," *Trans. Am. Soc. Artif. Intern. Organs* **1972**, *18*, 420.

25) Hochmuth, R. M.; Mohandas, N.; Blackshear, P. L. "Measurement of the Elastic Modulus for Red Cell Membrane Using Fluid Mechanical Technique," *Biophys. J.* **1973**, *13*, 747-762.

26) Hochmuth, R. M.; Wiles, H. C.; Evans, E. A.; McCown, J. T. "Extensional Flow of Erythrocyte Membrane from Cell Body to Elastic Tether," *Biophys. J.* **1982**, *39*, 83-89.

27) Evans, E.; Yeung, A. "Hidden Dynamics in Rapid Changes of Bilayer Shape," *Chem. Phys. Lipids* **1994**, *73*, 39-56.

28) Waugh, R. E. "Surface Viscosity Measurements from Large Bilayer Vesicle Tether Formation," *Biophys. J.* **1982**, *38*, 29-37.

29) Hochmuth, R. M.; Shao, J. Y.; Dai, J.; Sheetz, M. P. "Deformation and Flow of Membrane into Tethers Extracted from Neuronal Growth Cones," *Biophys. J.* **1996**, *70*, 358-369.

30) Evans, E.; Rawicz, W. "Entropy-Driven Tension and Bending Elasticity in Condensed-Fluid Membranes," *Phys. Rev. Lett.* **1990**, *64*, 2094-2097.

31) Green, N. M. "Avidin," *Adv. Protein Chem.* **1975**, *29*, 85-133.

32) Hochmuth, R. M.; Evans, E. A. "Extensional Flow of Erythrocyte Membrane from Cell Body to Elastic Tether I. Analysis," *Biophys J.* **1982**, *39*, 71-81.

33) Rand, R. P.; Burton, A. C. "Mechanical Properties of the Red Cell Membrane I. Membrane Stiffness and Intracellular Pressure," *Biophys. J.* **1964**, *4*, 115-135.

34) Waugh, R. E.; Hochmuth, R. M. "Mechanical Equilibrium of Thick, Hollow, Liquid Membrane Cylinders," *Biophys. J.* **1987**, *52*, 391-400.

35) Hochmuth, R. M.; Evans, E. A.; Wiles, H. C.; McCown, J. T. "Mechanical Measurement of Red Cell Membrane Thickness," *Science* **1983**, *220*, 101-102.

36) Williams, L. M.; Evans, S. D.; Flynn, T. M.; Marsh, A.; Knowles, P. F.; Bushby, R. J.; Boden, N. "Kinetics of the Unrolling of Small Unilamellar Phospholipid Vesicles onto Self-Assembled Monolayers," *Langmuir* **1997**, *13*, 751-757.

37) Porter, M. D.; Bright, T. B.; Allara, D. L.; Chidsey, C. E. D. "Spontaneously Organized Molecular Assemblies. 4. Structural Characterization of n-Alkyl Thiol Monolayers on Gold by Optical Ellipsometry, Infrared Spectroscopy, and Electrochemistry," *J. Am. Chem. Soc.* **1987**, *109*, 3559-3568.

38) Bain, C. D.; Biebuyck, H. A.; Whitesides, G. M. "Comparison of Self-Assembled Monolayers on Gold: Coadsorption of Thiols and Disulfides," *Langmuir* **1989**, *5*, 723-727.

39) Anseth, K. S. K., Lauren M.; Walker, Teri A.; Anderson, Karin J.; Bowman, Christopher N. "Reaction Kinetics and Volume Relaxation during Polymerizations of Multiethylene Glycol Dimethacrylates," *Macromolecules* **1995**, *28*, 2491-2499.

40) Hershfield, M. S.; Buckley, R. H.; Greenberg, M. L.; Melton, A. L.; Schiff, R.; Hatem, C.; Kurtzberg, J.; Markert, M. L.; Kobayashi, R. H.; Kobayshi, A. L.; Abuchowski, A. "Treatment of Adenosine Deaminase Deficiency with Polyethylene Glycol-Modified Adenosine Deaminase," *N. Engl. J. Med.* **1987**, *316*, 589-596.

41) Eaton, D. F. "Dye Sensitized Photopolymerization," *Adv. Photochem.* **1986**, 13, 427-487.

42) Baral, S.; Schoen, P. "Silica-Deposited Phospholipid Tubules as a Precursor to Hollow Submicron-Diameter Silica Cylinders," *Chem. Mater.* **1993**, *5*, 145-147.

43) Archibald, D. D.; Mann, S. "Template Mineralization of Self-Assembled Anisotropic Lipid Microstructures," *Nature* **1993**, *364*, 430-433.

44) Lago, R. M.; Tsang, S. C.; Lu, K. L.; Chen, Y. K.; Green, M. L. H. Filling "Carbon Nanotubes with Small Palladium Metal Crystallites: The Effect of Surface Acid Groups," *J. Chem. Soc., Chem. Commun.* **1995**, no. 13, 1355-1356.

45) Tsang, S. C.; K., C. Y.; Harris, P. J. F.; Green, M. L. H. "A Simple Chemical Method of Opening and Filling Carbon Nanotubes," *Nature* **1994**, *372*, 159-162.

46) Nivarthi, S. S.; McCormick, A. V.; Davis, H. T. "Evidence for Single File Diffusion of Ethane in the Molecular Sieve $AlPO_4$-5," *Chem. Phys. Lett.* **1994**, *247*, 596.

47) Gupta, V.; Nivarthi, S. S.; Keffer, D.; McCormick, A. V.; Davis, H. T. "Evidence of Single-File Diffusion in Zeolites," *Science* **1996**, *274*, 5285.

# CHAPTER 2

# PREPARATION AND OSMOTIC STABILITY OF POLYMERIZED PHOSPHOLIPID VESICLES

## Introduction

This chapter represents a continuation of our studies on using biomembranes as templates for photopolymerization. Ringsdorf and coworkers first demonstrated the concept of polymerizing entrapped monomer in the interior compartment of a phospholipid vesicle for the purpose of stabilization.[1] This method lead to the formation of crosslinked polymer networks that were faithful replicas of the bilayer template, micron-sized spherical vesicles. The authors argued that polymerization of liposome-encapsulated monomer could possibly lead to a robust drug delivery system, as the gelled particles might be more stable than non-polymerized vesicles under physiological conditions. Prior to our investigation, there were no studies that determined the effect of lumenal polymerization on the membrane. Hence, the goal of this chapter is to ascertain the state of the membrane after the lumen has been polymerized. In the course of these studies, we have also probed the effects of polymerization on vesicles that were composed of polymerizable lipids and that also had entrapped monomer. We were particularly interested in determining if the encapsulated hydrogel remained surrounded by a semi-permeable membrane, or if the polymerization process altered the bilayer, causing temporary or permanent defects. Defects in the membrane would result in leakage of initially entrapped solutes, and as such, the barrier properties of the

polymerized vesicles would be substantially compromised. Hence, we have measured the permeability characteristics of polymerized and non-polymerized vesicles as a function of osmotic gradients, to address the question whether photopolymerization affects the membrane barrier properties and to determine if polymerization stabilizes the membrane toward osmotic stress.

Like living cells, synthetic vesicles are osmotically active because they have a semi-permeable membrane that is not a perfect barrier. The transfer of solutes like salt and sugar across the membrane is kinetically very slow, whereas water diffuses quite rapidly.[2] If the solutions on opposite sides of the membrane have different concentrations, there will be a net osmotic flux of water in the direction of higher solute concentration. A variety of techniques have been used to study the osmotic properties of phospholipid vesicles, including photon correlation spectroscopy, electron microscopy and measurement of the release of initially entrapped solutes.[3-6] These studies have clearly shown that vesicles subjected to large hypoosomotic gradients (the concentration of solutes inside the vesicle is greater than in the external solution) become stressed. This is caused by the rapid influx of water, and eventually the liposomes develop transient pores that allow the release of vesicle volume. Osmotic lysis occurs after the maximal membrane tension is exceeded.[6] We have measured the osmotic release of $Ca^{2+}$ and the self-quenching dye calcein from polymerized vesicles to determine if a semi-permeable membrane surrounds the polymer network, and if the photopolymerization of the gel stabilizes the response of the membrane toward osmotic stress.

The polymerization of vesicle-encapsulated monomer is one method that might possibly stabilize liposomes; however, the most studied stabilization process that has

been investigated is the polymerization of lipids that form the bilayer sheath of the vesicle.[7-15] We have explored a combination of these two strategies, specifically, vesicles were doped with a polymerizable lipid that was designed to copolymerize with the vesicle-entrapped monomer. We have prepared two polymerizable lipids which each have similar molecular architecture, that is, a reactive methacryloyl group is separated from the lipid amphiphile by a short poly(ethylene glycol) spacer group. The rationale for the inclusion of polymerizable lipids in combination with encapsulated monomer was based on the desire to create covlent grafts between the membrane surface and the entrapped polymer network.

## Experimental Section

### General Procedures

$^1$H NMR spectra were recorded in chloroform-*d* on a Bruker DPX-300 spectrometer at 300 MHz. All δ values were given in ppm downfield from tetramethylsilane. Infrared samples were cast as films on NaCl plates and were measured on a Perkin Elmer 1600 FT-IR instrument. TLC was performed with Whatman aluminum backed silica gel plates and compounds were visualized by iodine, ninhydrin (to detect primary amines) and molybdate (to detect phosphorus). UV-VIS spectra were measured with a Beckman DU-7 spectrophotometer. All pH values were measured on a Corning 155 pH/ion meter.

Solvents and Reagents

All materials were used as received. Stearoyl-oleoyl phosphatidylcholine (SOPC), dioleoyl phosphatidylcholine (DOPC) and egg phosphatidylcholine (EPC) were purchased from Avanti Polar Lipids, Inc. (Alabaster, AL). Cholesterol, chloroform-*d*, acrylamide, N,N'-methylene-bisacrylamide, poly(ethylene glycol) methacrylate (MW ≈ 360, PEG 360 MA), N,N'-carbonyl diimidazole (CDI), triethylamine and sodium chloride were purchased from Aldrich Chemical Co. (Milwaukee, WI). Calcium chloride, ethylenediaminetetraacetic acid (EDTA), toluene, alumina (neutral, activity I), and chloroform (HPLC grade) were purchased from Fisher Scientific (Fair Lawn, NJ). Triton X-100, calcein, Sephadex G-75, Sepharose CL-6B and 4-(2-hydroxyethyl)-1-piperazineethanesulfonic acid (HEPES) were purchased from Sigma Chemical Co. (St. Louis, MO). Poly(ethyleneglycol) dimethacrylate (MW ≈ 1000, PEGDMA) and poly(ethylene glycol) methacrylate (MW ≈ 400, PEG 400 MA) were purchased from Polysciences, Inc. (Warrington, PA). The inhibitor 2,2-diphenyl-1-picryl-hydrazyl (DPPH) was purchased from Eastman Kodak Co. (Kingsport, TN). Calcium Green-5N was purchased from Molecular Probes (Eugene, OR) and Irgacure 2959 was a gift from Ciba-Geigy Corp. (Hawthorne, NY).

Synthesis

DOPE PEG 360 MA. The (imidazoylcarbonyl)oxy derivative of PEG 360 MA was prepared in a one-step conversion by treating PEG 360 MA (1.24 g, 3.46 mmol) dissolved in freshly distilled toluene (1.5 ml) with CDI (0.504 g, 3.11 mmol). After stirring for thirty minutes at 60 °C, the derivatized PEG was mixed with DOPE (0.500 g,

0.672 mmol), that had been dissolved in 7 ml of toluene, and then with TEA (0.315 g, 3.11 mmol). The stable radical DPPH (13 mg, 0.033 mmol) was added as a polymerization inhibitor. The suspension was stirred and maintained at 55 °C overnight in a nitrogen-filled roundbottom flask. During this time, the reaction mixture formed a clear solution. TLC ( eluent: $CHCl_3$/MeOH/$H_20$ 65/25/4 v/v/v) showed complete disappearance of the ninhydrin-positive DOPE ($R_f \approx 0.5$) with the appearance of a new phosphorus positive product ($R_f \approx 0.7$) (Note: The molybdate spray was prepared by a published protocol[16]). After the toluene was evaporated by a stream of nitrogen, the crude mixture was dissolved in a minimal amount of chloroform, treated with additional DPPH (3 mg, 0.008 mmol), and purified by column chromatography (solid phase: alumina (75 g); eluent: $CHCl_3$/MeOH 95/5 100 ml; followed by $CHCl_3$/MeOH/$H_20$ 88/12/0.6 300 ml; then $CHCl_3$/MeOH/$H_20$ 65/25/4 100 ml) to afford a 62 % yield. From $^1$H NMR (300 MHz, $CDCl_3$): dioleoyl δ 0.88 (t, 6H, -$CH_3$), 1.2-1.6 (44H, -$CH_2$-), 1.95-2.1 (m, 8H, allylic -C<u>H</u>$_2$CH=CHC<u>H</u>$_2$-), 2.2-2.4 (m, 4H, -OCC<u>H</u>$_2$-), 5.3 (m, 4H, vinyl -CH=CHC-), glycero-phosphoethanolamine 3.3-3.4 (m, 2H, -NHC<u>H</u>$_2$CH$_2$O-), 3.85-4.0 (m, 2H, -NHCH$_2$C<u>H</u>$_2$O-), 4.3 (m, 2H, -PO$_4$C<u>H</u>$_2$CH(OCO-)(CH$_2$OCO-)), 4.4 (m, 2H, -PO$_4$CH$_2$CH(OCO-)(C<u>H</u>$_2$OCO-)), 5.2-5.3 (m, $^1$H, PO$_4$CH$_2$C<u>H</u>(OCO-)(CH$_2$OCO-)), PEG 3.6-3.8 (m, -CH$_2$CH$_2$O-), 4.2 (m, 2H, -C<u>H</u>$_2$OCONH-), methacrylate 1.9 (s, 3H, -$CH_3$), 5.6 and 6.1 (2H, =$CH_2$). IR ($cm^{-1}$): 3348, 3251, 1721,1531. Anal calcd for $C_{60}H_{113}NaNO_{18}P$ C, 60.74%; H, 9.26%; N, 1.18% found C, 60.59%; H, 9.14%; N, 1.24%.

<u>DSPE PEG 400 MA</u>. The synthesis of DSPE PEG 400 MA was essentially identical to that of DOPE PEG 360 MA. After the coupling reaction, the unreacted PEG

400 MA-(imidazoylcarbonyl)oxy derivative was removed from the crude mixture by addition of a tenfold excess of cold acetone, and after storage at -20 °C overnight, the lipid precipitated. The lipid was collected by centrifugation and dried *in vacuo* at room temperature. Further purification to remove non-functionalized lipid was accomplished by column chromatography (eluent: $CH_2Cl_2$/MeOH gradient on a silica gel column) to give a 20 % yield. $^1$H NMR (300 MHz, $CDCl_3$): distearoyl δ 0.8 -0.9 (t, 6H, -$CH_3$), 1.2-1.7 (60H, -$CH_2$-), 2.2-2.4 (m, 4H, -$OCCH_2$-), glycero-phosphoethanolamine 3.3-3.4 (m, 2H, -$NHC\underline{H}_2CH_2O$-), 3.8-4.0 (m, 2H, -$NHCH_2C\underline{H}_2O$-), 4.3 (m, 2H, -$PO_4C\underline{H}_2CH(OCO$-)($CH_2OCO$-)), 4.4 (m, 2H, -$PO_4CH_2CH(OCO$-)($C\underline{H}_2OCO$-)),), 5.2 (m, $^1$H, $PO_4CH_2C\underline{H}(OCO$-)($CH_2OCO$-)),), PEG 3.6-3.8 (m, -$CH_2CH_2O$-), 4.2 (m, 2H, -$C\underline{H}_2OCONH$-), methacrylate 1.9 (s, 3H, -$CH_3$), 5.6 and 6.1 (2H, =$CH_2$). IR ($cm^{-1}$): 3348, 3251, 1721, 1531. Anal. calcd for $C_{62}H_{121}NaNO_{19}P$ C, 60.12%; H, 9.85%; N, 1.13% found C, 59.93%; H 9.66%; N, 1.25%.

Vesicle Preparation

The type of lipid used in each preparation varied upon the experiment, however, the same methods were used to prepare all of the vesicle samples. Specifically, a $CHCl_3$ solution of lipid was evaporated to dryness in a glass test tube using a stream of $N_2$, then with high vacuum for 2 hours in constant darkness. Multilamellar vesicles were prepared by hydrating the lipid film to 20 mg/ml with the appropriate aqueous buffer. After repeated vortexing, the multilamellar vesicles were subjected to five freeze/thaw cycles. Each cycle consisted of a 5-minute freeze in liquid $N_2$, followed by a 10-minute thaw in warm tap water. Large unilamellar vesicles were prepared by extruding the resulting

multilamellar vesicles at least 10 times through two stacked polycarbonate filters (Nucleopore, Pleasanton, CA) with 100 nm diameter pores at 22 °C using a Lipex Extruder (Lipex Biomembranes, Inc., Vancouver, Canada).

## Osmotic Release

Osmolality Measurements. The osmolality of all aqueous solutions was measured at least three times using a Precision Systems, Inc. 5004 MicroOsmette freezing point osmometer (Natick, MA). Solutions with osmolalities greater than 200 mOsm/kg were diluted by two-fold with deionized water.

Osmotic Release of Liposome-Encapuslated Solutes. Osmotic lysis was followed by measuring the release of either $Ca^{2+}$ or a self-quenching dye calcein that was initially entrapped by the lipid bilayer. The details of calcium and calcein leakage experiments are given below.

Calcium Leakage Assay. Extruded vesicles of the appropriate lipid composition were prepared at 20 mg/ml with a solution that contained 150 mM $CaCl_2$ in 2.2 M NaCl and 50 mM HEPES at pH 7.4 (designated throughout this chapter as "HEPES buffer"). The total osmolality of the HEPES buffer was 4680 mOsm/kg. For those experiments where the interior compartment of the vesicle was polymerized, the HEPES buffer also contained 100 mM PEGDMA and 4.5 mM Irgacure 2959 (total osmolality 4807 mOsm/kg). A 1.5 ml aliquot of the extruded vesicles was passed down a Sephadex G-75 size exclusion column (1.5 X 17 cm) pre-equilibrated with a calcium free isoosmotic solution. [Note: The Sephadex G-75 was swollen overnight in 2.3 M NaCl, 50 mM

HEPES at pH 7.4 or 2.4 M NaCl, 50 mM HEPES at pH 7.4 where the former buffer was used for vesicles hydrated in HEPES buffer only and the latter when the vesicles were hydrated with HEPES buffer and the polymerizable solutes. Just prior to use, the hydrated gel was degassed for 30 min.] The elution profile was monitored by optical density (which is sensitive for vesicle elution) and the vesicle containing fractions were combined (~ 4 ml) and polymerized according to the procedure below. Steady-state fluorescence measurements were performed in 1-cm poly(methyl methacrylate) (PMMA) cuvettes using a Perkin Elmer MPF-66 fluorescence spectrophotometer. Emission and excitation slits were both set to 5 nm. Cuvettes were prepared by diluting 3 ml of buffered saline solutions of various osmolalities at 22 °C with 25 µl of 50 µg/ml (42 µM) calcium green-5N, then, 40 µL of the vesicle suspension. Calcium green-5N is a calcium chelator that upon binding exhibits an increase in fluorescence emission intensity with little shift in wavelength. Measuring the fluorescence emission at 531 nm, with excitation at 488 nm, the free calcium concentration can be determined using the following equation:

$$\left[Ca^{2+}\right] = K_d \frac{\left[F - F_{\min}\right]}{\left[F_{\max} - F\right]}$$

where F is the fluorescence intensity of the indicator at experimental calcium levels, $F_{min}$ is the fluorescence intensity in the absence of calcium and $F_{max}$ is the fluorescence intensity of the calcium-saturated probe. The $K_d$ is the dissociation constant for the probe and calcium.[17] The absolute value of $K_d$ for the indicator depends upon environmental conditions such as pH, temperature and ionic strength (e.g., 10 µl of 50 µg/ml calcium green-5N in 2 ml of 50 mM HEPES, pH 7.4 gives a fluorescence of 328.7 a.u., whereas

the same amount of indicator in 2 M NaCl, 50 mM HEPES gives a fluourescence of 115.1 a.u.). The amount of calcium released was measured by dividing the fraction of calcium released due to osmotic lysis by the amount of calcium released upon the addition of a sufficient amount of Triton X-100 to cause the complete solubilization of the vesicles (Note: The amount of Triton X-100 that completely solubilized all of the vesicles was determined experimentally by titrating the vesicle suspensions with small aliquots of 50 mg/ml Triton X-100 (~ 40 μl of 50 mg/ml Triton X-100 for 3 ml samples. The volumes of Triton X-100 used did not affect the fluorescence intensity.)

In these studies, it is important to use water that is not contaminated with calcium ions. Calcium 'free' water was obtained from a purification system consisting of two ion-exchange cartridges and was analyzed prior to use. Those samples of water that exhibited a fluorescence intensity less than 100 a.u. when made 42 μM in Calcium Green-5N were used in further experiments. All solutions were prepared in containers that were rinsed in the following protocol: 3X with pure water, 3X with boiling 5 mM $Na_2EDTA$, 2X with pure water, 3X with 10 % $HNO_3$, and again 6X with water.

Calcein Leakage Assay. Calcein loaded vesicles of EPC and cholesterol (2:1 mol ratio) were prepared by extrusion of a 20 mg/ml lipid suspension of a 200 mM solution of the dye in HEPES buffer (total osmolality 4961 mOsm/kg). The polymerizable vesicular suspensions also contained 4.5 mM of the photoinitiator Irgacure 2959 in 1.25 M acrylamide and 60 mM N,N'-methylene-bisacrylamide (total osmolality 5776 mOsm/kg). Non-entrapped solutes were exchanged with NaCl and HEPES by passing a 0.75 ml aliquot of the lipid suspension over an osmotically balanced Sepahadex G-75 gel

filtration column (1.5 X 10 cm). After polymerization, the vesicle suspension was diluted by a factor of 10,000 in an osmotically balanced buffer containing NaCl and 50 mM HEPES, pH 7.4 in order prevent detector saturation. Cuvettes for fluorescence measurements were prepared by adding 3 ml of the vesicle suspension to a disposable 1-ml PMMA cuvette. The fluorescence intensity at 520 nm was recorded at 22 °C under excitation at 495 nm. Maximum fluorescence intensity was obtained by the addition of 40 µl of a 5 % solution of Triton X-100.

Photopolymerization of Vesicles

A 2-ml aliquot of the calcein loaded vesicles was irradiated for 40 minutes in a 1-cm quartz cuvette with an Oriel 60064 100 W high pressure mercury arc lamp ($2.7 \times 10^5$ mW at 5 cm). All of the other vesicle samples, i.e., those without calcein, were photopolymerized by the following method: A 2.5 ml aliquot of the lipid suspension was added to a microscale quartz immersion photochemical reactor assembly (Ace Glass, Vineland, NJ) and irradiated for 30 min with a 254 nm UVP Pen-Ray lamp (4500 $mW/cm^2$ at 2.5 cm[18]).

Electron Microscopy

The vesicle suspensions used for the electron microscopy studies were prepared at a concentration of 5 mg/ml. Detergent treatment consisted of adding 5 µl of Triton X-100 to 500 µl of vesicles (~ 17 mM Triton X-100).

Freeze Fracture Microscopy. A drop of sample was placed in a low well specimen carrier such that a hemispherical drop of liquid was above the carrier rim. With forceps, the sample was plunged into liquid $N_2$ cooled propane and transferred to a Balzers freeze fracture apparatus, where the freeze fracture specimen stage was pre-cooled to -150 °C. The frozen sample was fractured at -100 °C, followed by a 2 min etch (knife temperature ≈ -196 °C) and then shadowed with Pt/C at 1900V (≈ 2 nm thickness measured by quartz balance) at an angle of 45°, followed immediately by C deposition at 2400V (≈ 20 nm thickness). The samples were warmed to room temperature in the freeze fracture unit under vacuum. The fracture replicas were floated off onto chromic acid (5 % w/v potassium dichromate in 50 % sulfuric acid) times ranging from 1 hour to overnight, then washed with doubly distilled water and picked up with bare copper 400 mesh grids. Fracture replicas were examined under a Philips CM/D transmission electron microscope operated at 100 kV.

Negative Stain Microscopy. Carbon grids were cleaned in a plasma for 20 seconds to remove static charges. Several 25 µl 2 % osmium tetroxide solutions (aqueous) were prepared from a stock 4 % osmium tetroxide solution that had been stored at room temperature. The 4 % solution was chilled on ice prior to dilution to prevent evaporation. Sample staining was carried out by placing a 25 µl drop of 2 % osmium tetroxide on a piece of parafilm, then, 25 µl of the sample was added to the drop and a clean carbon grid was placed on top of this drop for 2 minutes. After 2 minutes, the grid was washed by dabbing it on 3 water droplets and while holding with locked forceps a drop of 1 % uranyl acetate was placed on the grid for 30 seconds. The uranyl acetate

solution was wicked away with small triangular pieces of filter paper. The sample grid was left to dry in a petri dish for 5 - 10 minutes before examination. Stained samples were examined using a Philips CM/D transmission electron microscope operated at 100 kV.

Dynamic Light Scattering

The sample, contained in a 4 ml borosilicate tube (Fisher Scientific, Fair Lawn,NJ), consisted of 20 µl of the lipid suspension in 2 ml of filtered deionized water. Samples with detergent were prepared by first mixing 100 µl of vesicles with 20 µl of a 5 % Triton X-100, then, this solution was diluted to 2 ml with deionized water. All of the samples were then placed in a thermostatted sample holder at 25 °C. The light source, a Coherent Innova 70 Argon ion laser of wavelength 514.4 nm was focused onto the sample and scattered light was detected at a 90° scattering angle with a Thorn EMI photomultiplier tube (model QL30F15/RFI, Middlesex, England). Autocorrelation was performed by an ALV-5000 digital autocorrelator (Langen, Germany) and particle sizes were calculated with the ALV5000E software package.

Vesicles prepared by repeated extrusion through 100 nm pores have unimodal size distributions and the autocorrelation function C(t) is a single, decaying exponential function, with a characteristic decay time $\tau$ that is inversely proportional to the diffusivity, that is,

$$C(t) = A\exp(-2DQ^2t) + 1$$

$$D = kT/6\pi\eta R_h$$

where A is an instrumental constant and Q is the scattering wavevector magnitude. D is the particle diffusivity where *k* is Boltzmann's constant, T the temperature in Kelvins, η the shear viscosity of the solvent (water), and the quantity $R_h$ is the average hydrodynamic radius of the particles.

The average diffusion coefficient was calculated by averaging 3 successive autocorrelation functions, each with the same sampling time and experimental duration. We have used the method of cumulants[19] to determine vesicle size. Cumulants is a gaussian least-squares fit of a quadratic or cubic function of t to ln [C(t)-1]. This analysis yields the mean diameter (the first cumulant) for the vesicles and a polydispersity index for the distribution. The values for the refractive index and viscosity of the medium were those of pure water at 25 °C.

## Results and Discussion

### Polymerization of Liposome-Entrapped Monomer

Freeze-Fracture Characterization of Polymerized Vesicles. UV irradiation of extruded vesicles filled with multi-functional monomer and photoinitiator resulted in the formation of crosslinked gels in the interior compartment of the vesicles (Figure 2.2). The vesicles were prepared from a mixture of DOPC and cholesterol (3:2 w/w) in 100 mM PEGDMA and 4.5 mM Irgacure 2959 in water. Irgacure 2959, (4-(2-hydroxyethoxy) phenyl-(2-hydroxypropyl)ketone), is a water soluble photoinitiator that undergoes Norrish type I cleavage when exposed to UV radiation (Figure 2.1).[20] The extruded vesicles were passed over an osmotically balanced Sepharose CL-6B size exclusion column to

exchange the non-entrapped PEGDMA and Irgacure 2959 with sucrose. Fractions containing lipids were combined and polymerized for 30 minutes in a microscale immersion well photoreactor with a low pressure mercury arc pen-ray lamp.

Figures 2.2 A and B are freeze fracture replicas of the irradiated vesicles. Figure 2.2 B shows the effect of the addition of a quantity of Triton X-100 that was sufficient to dissolve vesicles that were not subjected to photopolymerization (based on results from optical density measurements - data not shown). The spherical particles in Figure 2.2 A and B have diameters in the 60 - 80 nm range, which is the expected size range for vesicles prepared by extrusion through 100 nm diameter pores.[21] The presence of spherical particles on the fracture surface of samples treated with Triton X-100 suggests that the vesicle lumen has polymerized and that UV irradiation results in the formation of detergent-insoluble gel particles.

Dynamic Light Scattering Analysis of Polymerized Vesicles. Table 2.1 summarizes the results from dynamic light scattering, showing the hydrodynamic radii of polymerized vesicles suspended in pure deionized water and in a concentration of Triton X-100 that solubilized non-irradiated samples. Also shown as a control is the radius of vesicles that were prepared in deionized water (no entrapped solute). CONTIN analysis was used to invert the autocorrelation function to confirm that the particle size distribution was unimodal. Neither monomer nor photopolymerization has a large effect on the average diameter of vesicles; vesicles prepared in pure water essentially are the same size. Polymerization of the confined monomer is confirmed by the presence of particles after addition of detergent. Vesicles that had not been irradiated were

transformed into mixed micelles upon the addition of Triton X-100. Unfortunately, the mixed micelles were too small to be detected by the dynamic light scattering apparatus. However, Triton X-100 and lipid mixed micelles have been reported to have a hydrodynamic radius of about 3.3 nm.[22] Finally, the formation of acrylamide gel particles demonstrates that monomers, in addition to macromonomers, can be entrapped in the inner compartment for a sufficient amount of time to allow for lumenal polymerization.

Negative Stain Electron Microscopy of Polymerized Vesicles. The effects of polymerization on the lipid bilayer were observed by negative-stain transmission electron microscopy. Figure 2.3 A is a negative-stain micrograph of polymerized DOPC:cholesterol (2:1 mol ratio) vesicles that were prepared in an aqueous solution that contained 100 mM PEGDMA and 4.5 mM Irgacure 2959. Prior to polymerization, the vesicles were passed over a gel filtration column to exchange the nonentrapped solutes with sucrose. The sample was irradiated for 30 min with a low pressure mercury arc lamp. The uranyl acetate stain reveals a folded membrane "skin" that outlines all of the gelled vesicles. The excellent contrast seen in Figure 2.3 A is attributed to the high concentration of uranyl acetate that accumulates on the wrinkled membrane interface. Figure 2.3 B is a negatively stained electron micrograph of the same sample of polymerized vesicles but with a sufficient amount of Triton X-100 to dissolve the bilayer membrane (determined by optical density measurements- data not shown). There is a striking difference in the level of staining between the two samples, which is attributed to the dissolution of the phospholipid membrane. It is clear that uranyl acetate does not

accumulate at the surface of neutral PEGDMA hydrogel as efficiently as it does at the lipid membrane interface. It seems clear that the vinyl groups found in the hydrophobic region of the lipid bilayer do not react to any great extent with the propagating polymer radicals because the membrane appears to be completely solubilized by the addition of detergent. Finally, these results suggest that it is likely the polymerized vesicles can encapsulate water soluble molecules after polymerization of the interior compartment because the gels appear to remain surrounded by the lipid bilayer.

Osmotic Lysis of Vesicle-Entrapped Acrylamide Hydrogels. The release of vesicle-entrapped solutes was measured as a function of transmembrane osmotic gradients to determine if the polymerized vesicles remained osmotically active and if the polymerization of the lumen altered the membrane response to osmotic stress. In Figure 2.4, calcein dye was used as a marker to monitor osmotic lysis, and release is reported as an increase in fluorescence emission as the dye is diluted into the extravesicular space.[23] The osmotic lysis experiments were carried out with EPC:cholesterol (1:1 mol ratio) vesicles prepared by extrusion through 100 nm pores. The non-polymerized vesicles were prepared in a solution of high osmolality that contained 200 mM calcein dissolved in HEPES buffer. The polymerized vesicles were prepared in HEPES buffer with 1.25 M acrylamide in 0.06 M N,N'-methylene-bisacrylamide and 4.5 mM Irgacure 2959. The vesicles were polymerized by irradiation for 40 minutes with a high pressure mercury arc lamp. The applied osmotic differential was the difference between the osmolality of the dilution buffer (HEPES, pH 7.4 buffered solution with varying amounts of NaCl) and the osmolality of the buffer used to prepare the vesicles. For both samples, there was no

significant release until the osmotic strength of the extravesicular medium is ~2000 mOsm/kg *less* concentrated than the vesicle interior, then, further increases in the hypoosmotic gradient result in the release of more entrapped calcein. Figure 2.4 shows the polymerized vesicles released *less* calcein than the non-polymerized vesicles at the same applied osmotic gradient. The polymerized vesicles have to be diluted into a buffer that is ≈ 1000 mOsm/kg less concentrated than the buffer that causes the same percent release from the non-polymerized vesicles. This apparent increased resistance to osmotic stress is most likely due to the decrease in the osmolality of the vesicle interior upon polymerization as opposed to an increase in mechanical stability of the membrane. If all the entrapped monomer reacted, the osmotic strength of the interior would decrease by ≈ 1000 mOsm/kg, which would account for the observed shift in the data. Therefore, the decrease in calcein release is not a consequence of increased membrane stability, rather it is caused by the large decrease in the osmolality of the entrapped buffer due to the depletion of monomer during polymerization. As a result of these observations, acrylamide will be replaced with PEGDMA, as the macromonomer at the same weight percent in solution has an osmolality of only 116 mOsm/kg compared with that of acrylamide which has an osmolality of approximately 1000 mOsm/kg.

Mui *et. al.*[24] carried out cryo-electron microscopy studies that demonstrated vesicles prepared by extrusion in the presence of impermeant solutes were not spherical, hence, the vesicles had excess membrane surface area. Exposure of these vesicles to a hypoosmotic gradient caused the volume to surface area ratio to increase, thus the vesicles took in a small volume of water before the membrane experienced an increase in tension. In this earlier study, the authors found that 100 nm vesicles did not release any

contents until the hypoosmotic gradient was about 1700 mOsm/kg, which is in agreement with our results (Figure 2.4).

Osmotic Lysis of Vesicle-Entrapped PEG-Methacrylate Hydrogels. We have examined the release from 100 nm polymerized DOPC:cholesterol (55:45 mol ratio) vesicles prepared by extrusion in HEPES buffer that contained 100 mM PEGDMA, 4.5 mM Irgacure 2959 and 150 mM $CaCl_2$.

Figure 2.5 shows the percentage loss of $Ca^{2+}$ from the polymerized vesicles as a function of the applied hypoosmotic gradient. The release of $Ca^{2+}$ was measured using the fluorescent indicator, Calcium Green-5N. Upon binding $Ca^{2+}$, the indicator exhibits an increase in fluorescence emission intensity. Shown for reference is the osmotic release of calcein from EPC:cholesterol vesicles that were not polymerized (same data as in Figure 2.4). The polymerized and non-polymerized vesicles exhibited identical release of entrapped solutes at the same applied hypoosmotic gradient. [Note: Calcein could not be used in experiments that included PEGDMA as the dye and macromonomer were immiscible]. As seen in the previous experiments (Figure 2.4), vesicle contents were not released until the applied osmotic differential exceeded 1700 mOsm/kg.

It is clear from these results that a cross-linked poly(ethylene glycol)-methacrylate gel entrapped in the interior compartment of a vesicle does not alter the membrane sensitivity towards a hypoosmotic gradient, nor does the polymerization process cause defects in the membrane. This is consistent with the results from the liposome-encapsulated acrylamide experiments, where the polymerization of vesicles did not result in particles that were more resistant toward osmotic stress. An encapsulated gel lacks the

ability to stabilize the membrane because, as shown by TEM experiments, the vesicle bilayer is not incorporated in the polymer gel. After polymerization, the osmotic activity of the vesicle is still regulated by the bilayer membrane, whose properties remain unaffected by lumenal polymerization.

## Osmotic Lysis of Vesicles with Polymerizable Lipids

Our observations have shown that an entrapped hydrogel does not alter the osmotic activity of the vesicle because it is decoupled from the bilayer membrane. The hydrogel is only encapsulated by the bilayer and does not affect membrane barrier properties. However, covalent linkage of the membrane to the encapsulated gel might impart some unique material properties to the lipid bilayer. Initially, we hypothesized that an anchored membrane might resist osmotic lysis since the membrane is stabilized by a polymer network. To test this hypothesis, we designed a polymerization process that would result in the copolymerization of liposome-encapsulated hydrophilic monomer with a polymerizable lipid in the vesicle sheath.

Polymerizable Lipid. In order to create an anchored membrane, the hydrophilic surface of the vesicle must be made reactive toward the propagating free radicals inside. With that in mind, two phospholipid analogs with PEG spacer groups were prepared. Each was designed to have the amphiphilic part of the molecule separated from the reactive methacryloyl group by a short PEG chain. The function of the hydrophilic PEG spacer group is to extend the methacrylate away from the membrane interface, so that it may copolymerize with the vesicle-entrapped monomer.

The general synthetic approach used to prepare the polymerizable phospholipid analogs is outlined in Figure 2.6, and is based on previously reported strategies that were used to prepare PEG-grafted lipids.[24] Briefly, the terminal hydroxyl group of PEG methacrylate was treated with CDI to convert it into an amine reactive (imidazoylcarbonyl)oxy derivative, which was then reacted with a phosphatidyl-ethanolamine (PE) to give a lipid-PEG MA conjugate.

In preliminary vesicle studies with the saturated DSPE polymerizable analog (DSPE PEG 400 MA), we found it was difficult to extrude multilamellar vesicles composed from mixtures of phosphatidylcholine (PC), DSPE PEG 400 MA, and very small amounts of cholesterol (< 10 mol %). The second polymerizable lipid, DOPE PEG 360 MA, which is the unsaturated derivative of DSPE PEG 400 MA, could be easily extruded at room temperature using moderate pressures (~ 200 psi) in lipid mixtures with up to 45 mol % cholesterol. This behavior is most likely due to the low phase transition temperature (-16 °C) of the DOPE amphiphile and the good miscibility of DOPE with DOPC.

In certain applications, it is desirable to have cholesterol in the bilayer because of its ability to increase membrane cohesiveness. Compared to cholesterol-free vesicles, those with cholesterol exhibit higher membrane surface tension and decreased solute permeability (Note: The effect of cholesterol is more pronounced in vesicles that are composed from saturated lipids.).[25] In this chapter, we have purposely prepared vesicles with cholesterol in all of the osmotic lysis experiments, thus, all of the samples with a polymerizable lipid were prepared with DOPE PEG 360 MA. For the sake of continuity,

the osmotic release results with vesicles prepared from DSPE PEG 400 MA are summarized in the appendix.

Osmotic Lysis of Vesicles with an Anchored Membrane. The effect of anchoring the vesicle bilayer to the encapsulated gel on the osmotic stability of the membrane was measured by monitoring the release of $Ca^{2+}$ as a function of the osmotic differential. Figure 2.7 shows the percentage loss of $Ca^{2+}$ from UV irradiated extruded DOPC:cholesterol:DOPE PEG 360 MA (45:45:10 mol ratio) vesicles that were prepared in HEPES buffer with 100 mM PEGDMA, 4.5 mM Irgacure 2959 and 150 mM $CaCl_2$. When the vesicles were exposed to UV irradiation, the membrane was completely *destabilized* resulting in the near quantitative release of the entrapped solutes. These unexpected results were not due to diffusion of $Ca^{2+}$ through the bilayer membrane, as the permeability of the polymerizable vesicles that were not irradiated is extremely low. Evidence for this is shown in Figure 2.7. Since non-irradiated vesicles essentially showed no leakage of $Ca^{2+}$ 24 hours after the vesicles were passed over an osmotically balanced size exclusion column, it is clear the photoinduced release of vesicle contents is caused by polymerization that takes place at the membrane interface as those vesicles without DOPE PEG 360 MA showed no contents release upon exposure to UV radiation.

Even more surprising was our observation that UV irradiation of vesicles that were prepared from a mixture of DOPC:cholesterol:DOPE PEG 360 MA (45:45:10 mol ratio) *without* entrapped PEGDMA also resulted in the photoinduced release of $Ca^{2+}$ (Figure 2.8). These results were unexpected since it is generally recognized that polymerization of the lipid bilayer in vesicles is an effective method to stabilize

liposomes and decrease their solute permeability.[9] Furthermore, in chapter 3, we will discuss the results of a series of experiments that were designed to elucidate the mechanism for the photoinduced release of vesicle contents.

## Conclusions

The experiments described here provide the first direct evidence that a bilayer membrane used as a template for photopolymerization remains intact. After polymerization, the cross-linked polymer network remains surrounded by a semi-permeable membrane that shows negligible permeability towards osmotic solutes like salt and fluorescent dyes. The vesicle encapsulated hydrogel is "decoupled" from the membrane, that is, it is not covalently bound to the membrane, meaning the lipid bilayer can be stripped away by the addition of detergent, leaving a water swellable gel replica of the vesicle capsule. We found polymerization of the vesicle lumen did not effect the osmotic properties of the bilayer membrane because the polymer network is unable to prevent the catastrophic aerial strains that develop in the membrane brought about by the large influx of water. It was thought the lack of stabilization was due to the fact the polymer network and the membrane were not covalently attached. To test this, we prepared two polymerizable lipids that would anchor the membrane to the internal polymer network. Surprisingly, in all of the tests where the polymerizable lipids were incorporated in the membrane, we found that polymerization resulted in the complete destabilization of the membrane and the near quantitative release of all of the entrapped solutes. Importantly, the release of contents was observed in tests where there was no entrapped monomer, i.e. polymerization of DOPE PEG 360 MA doped membranes was

sufficient to cause the release of vesicle entrapped solutes. These results represent a new approach to the photoinduced release of contents of lipid vesicles.

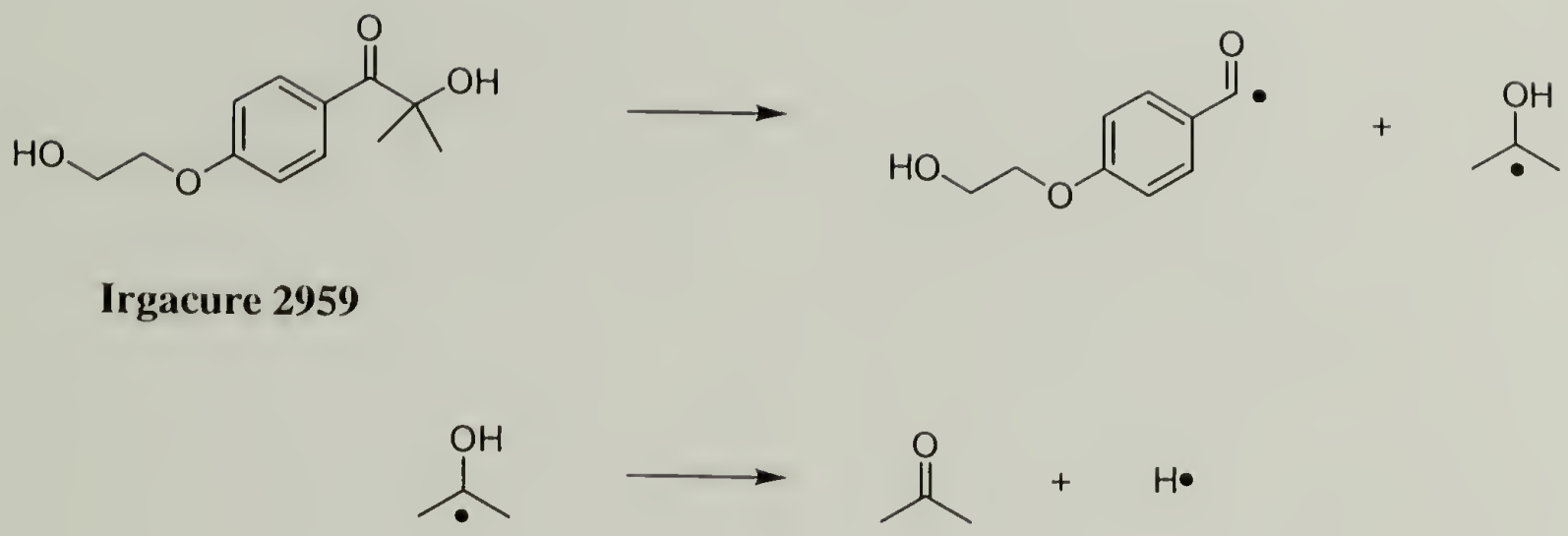


**Irgacure 2959**

Figure 2.1 The Norrish type I cleavage reaction of Irgacure 2959. Absorption of UV radiation ($\lambda < 350$ nm) results in homolytic cleavage between the carbonyl group and the adjacent $\alpha$ carbon atom. The isopropanol radical rearranges to give acetone and a hydrogen atom.[20]

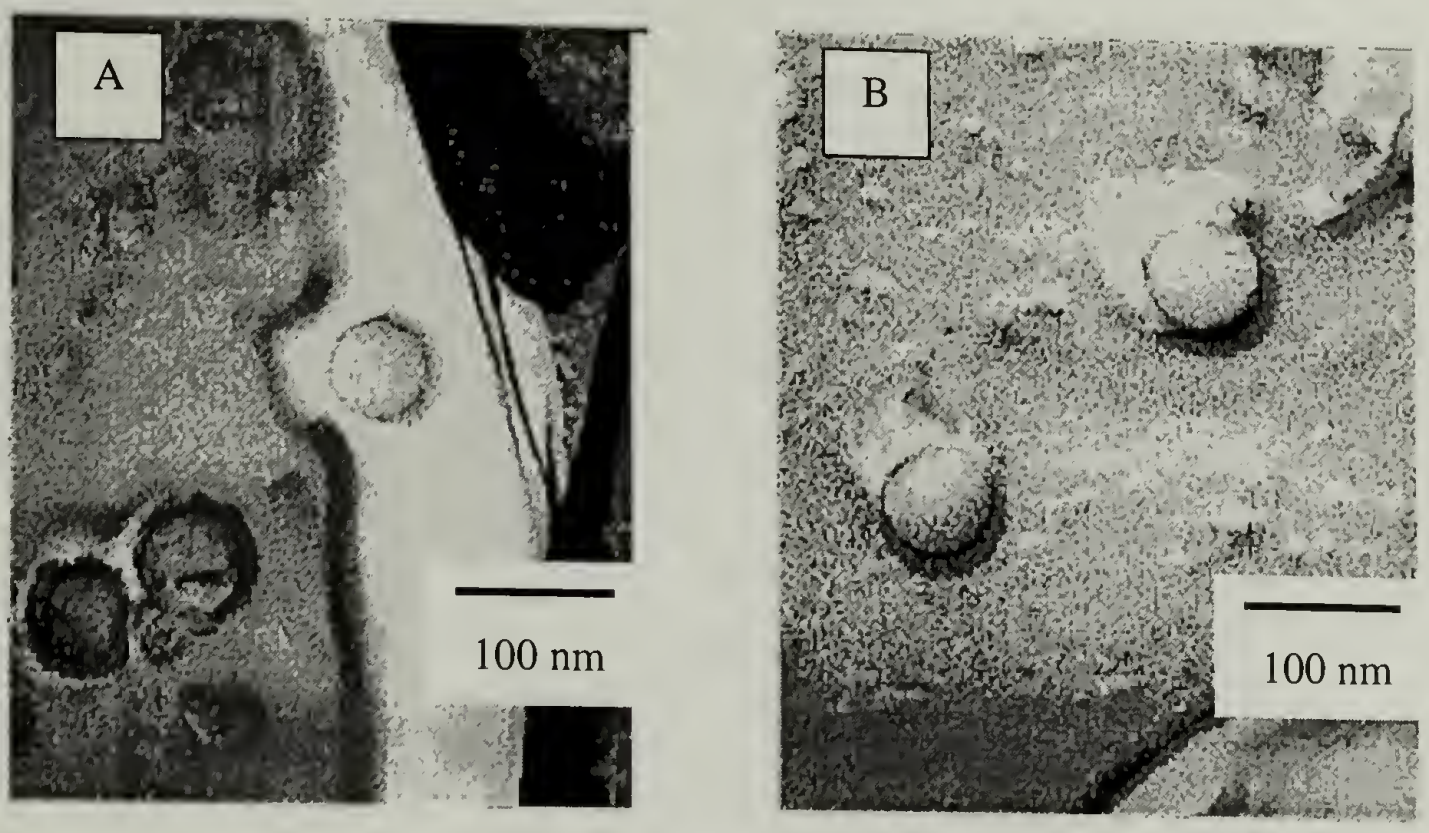


Figure 2.2 Freeze-fracture micrographs of polymerized, large unilamellar vesicles. The vesicles were prepared from a mixture of DOPC and cholesterol (3:2 w/w) in 100 mM PEGDMA and 4.5 mM Irgacure 2959 in water. (A) The fracture replica of irradiated vesicles reveals smooth spherical structures that have 100 nm diameters. (B) The same vesicles as in A but with detergent triton X-100 added.


A

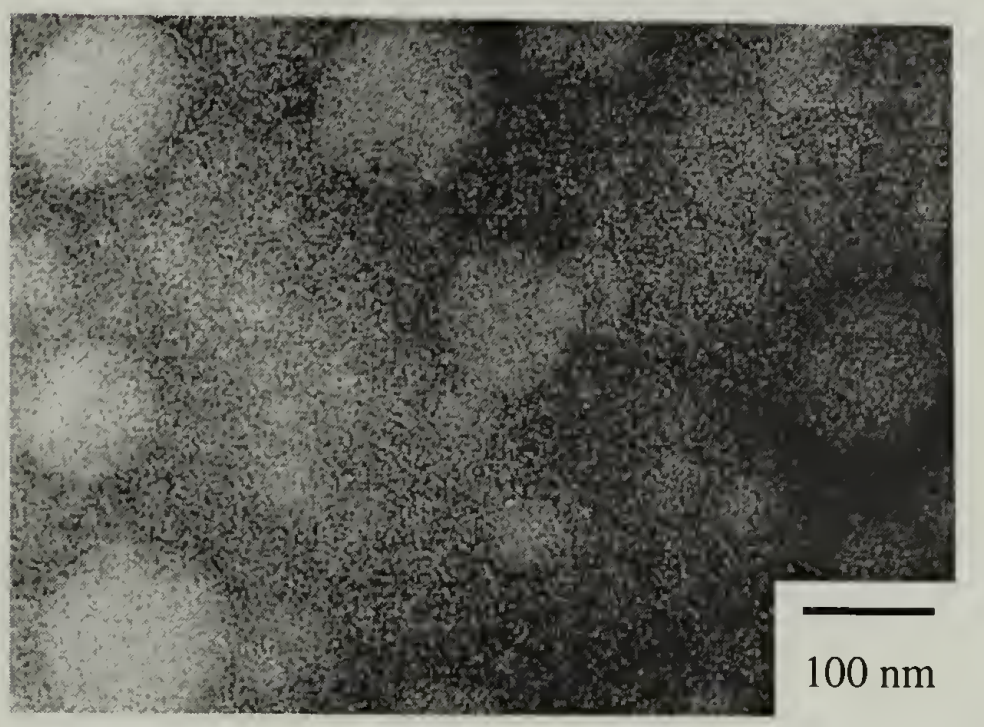


B

Figure 2.3 Effects of detergent on irradiated 2:1 DOPC:cholesterol (mol ratio) vesicles with entrapped 100 mM PEGDMA and 4.5 mM Irgacure 2959. (A) Polymerized large unilamellar vesicles. (B) The same vesicles after treatment with Triton X-100.

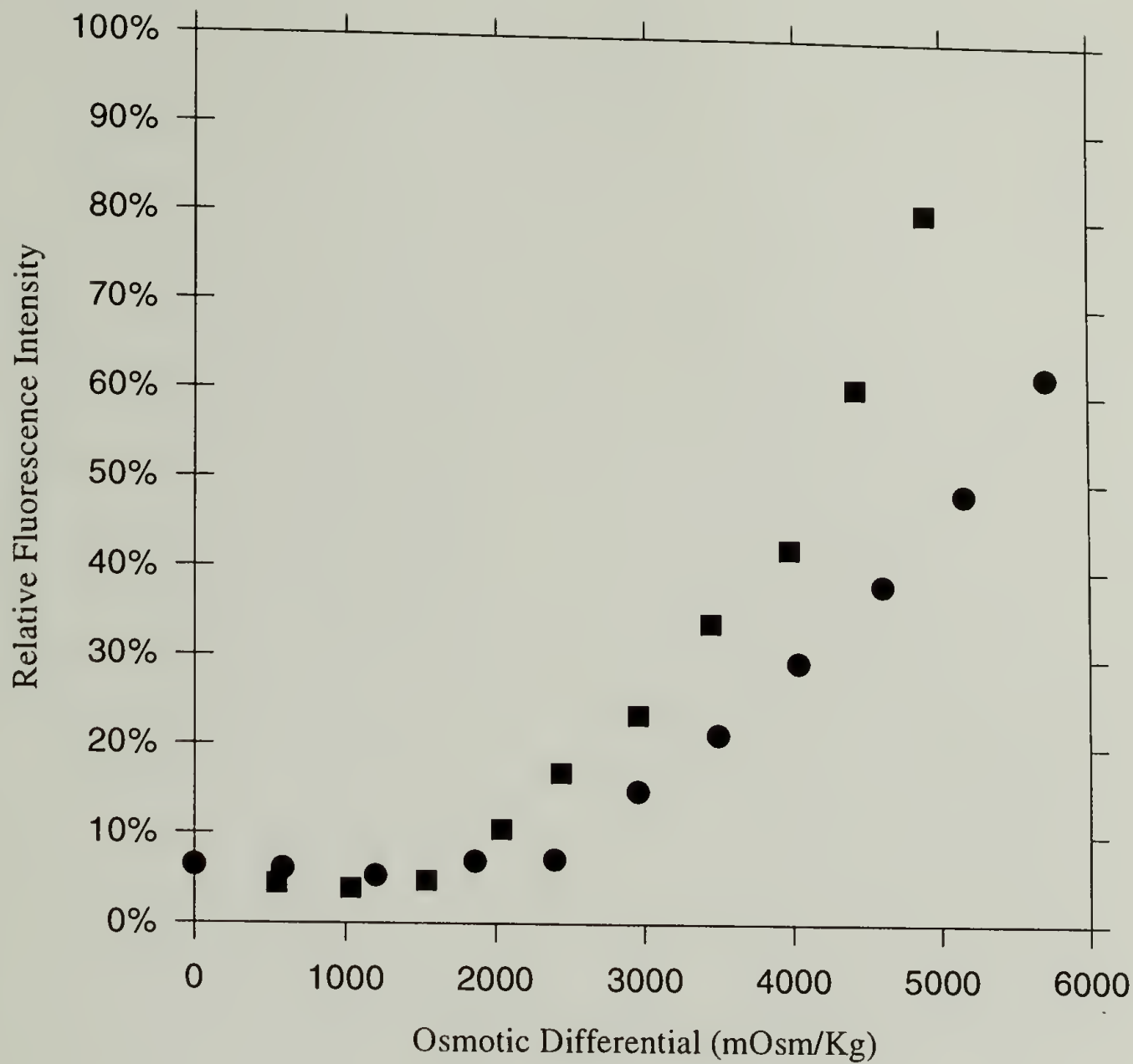


Figure 2.4 Effect of polymerization on the osmotic release of calcein from 100 nm phospholipid vesicles. Both samples of vesicles were prepared from a mixture of EPC and cholesterol (1:1 mol ratio) that contained 200 mM calcein in 2.2 M NaCl and 50 mM HEPES, pH 7.4, but (●) also contained 1.25 M acrylamide, 0.06 M N,N'-methylene-bisacryamide and 4.5 mM Irgacure 2959. This sample was irradiated for 40 minutes with a high pressure mercury arc lamp. (■) Control vesicles that were not irradiated. The relative calcein fluorescence was measured as a function of the osmotic differential.

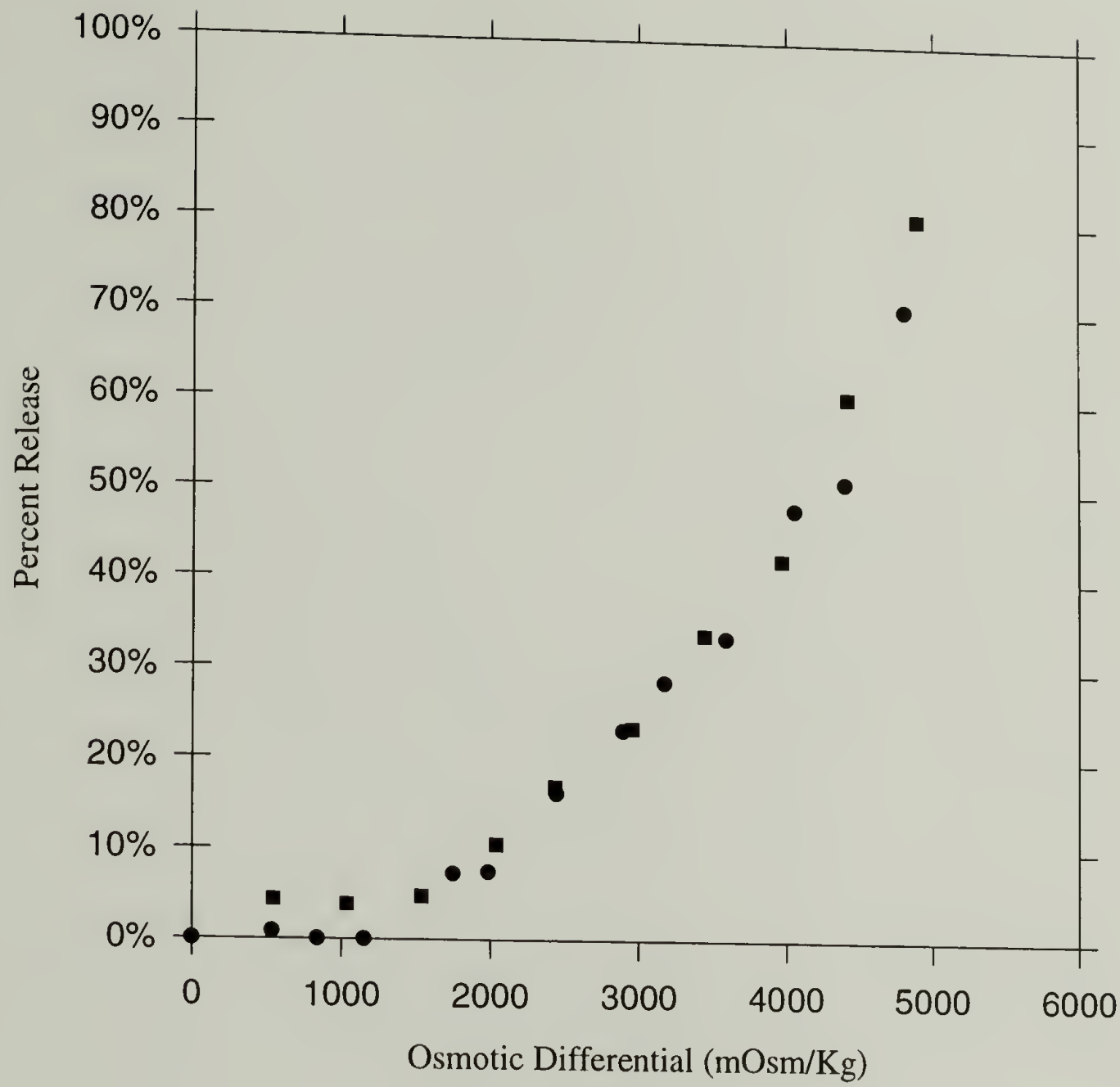


Figure 2.5 Osmotic leakage of $Ca^{2+}$ from extruded DOPC:cholesterol (55:45) vesicles (●) prepared in 100 mM PEGDMA, 150 mM $CaCl_2$, 4.5 mM Irgacure 2959 in HEPES buffer and irradiated for 30 minutes with a pen-ray mercury lamp. $Ca^{2+}$ in the surrounding medium was measured using the fluorescent dye, calcium green-5N. (■) Non-irradiated EPC:cholesterol (1:1) that contained 200 mM calcein in HEPES buffer. The relative calcein fluorescence was measured as a function of the osmotic differential.

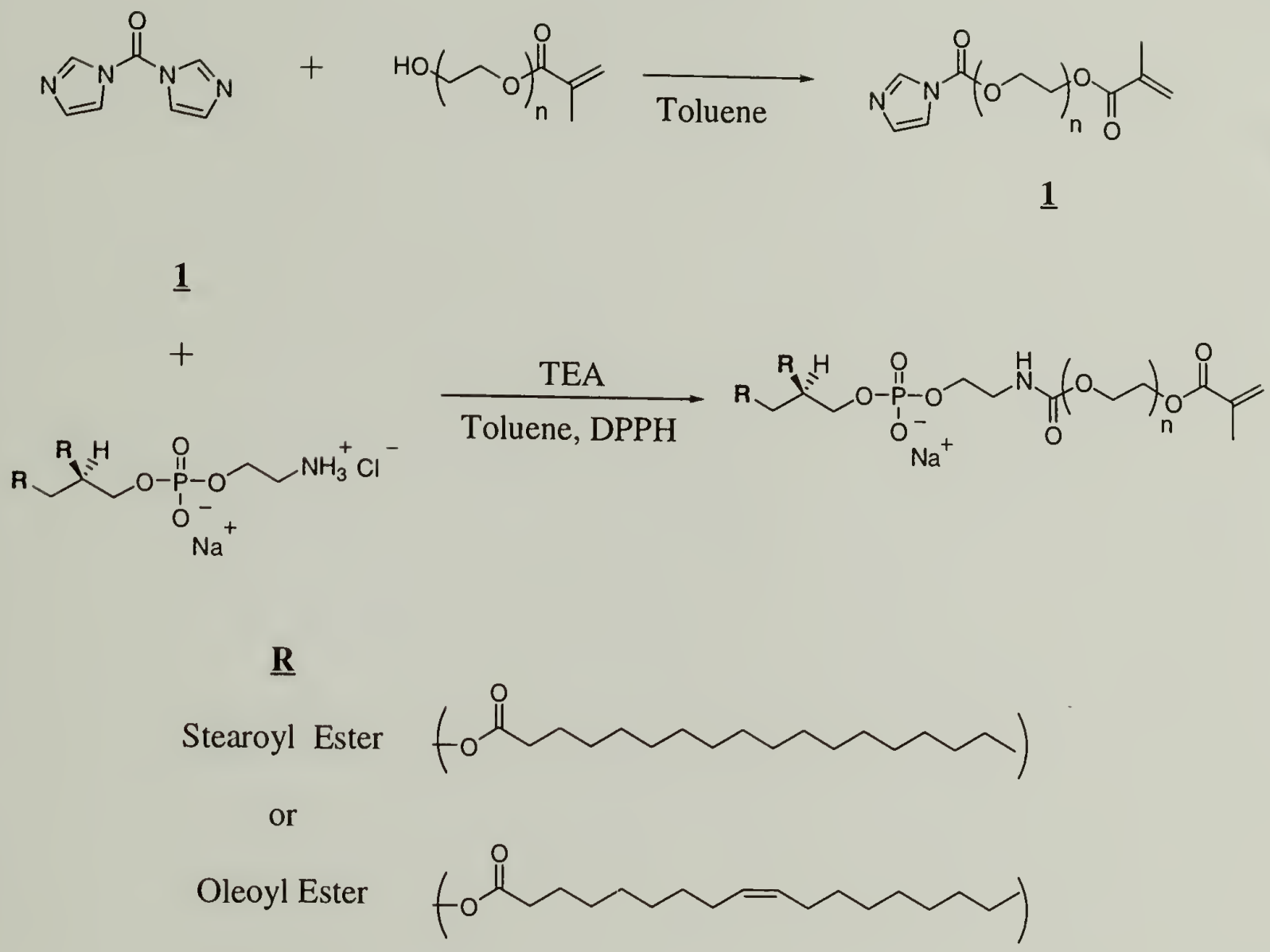


Figure 2.6 Synthetic pathways leading to polymerizable lipids where n ≈ 7 - 8.

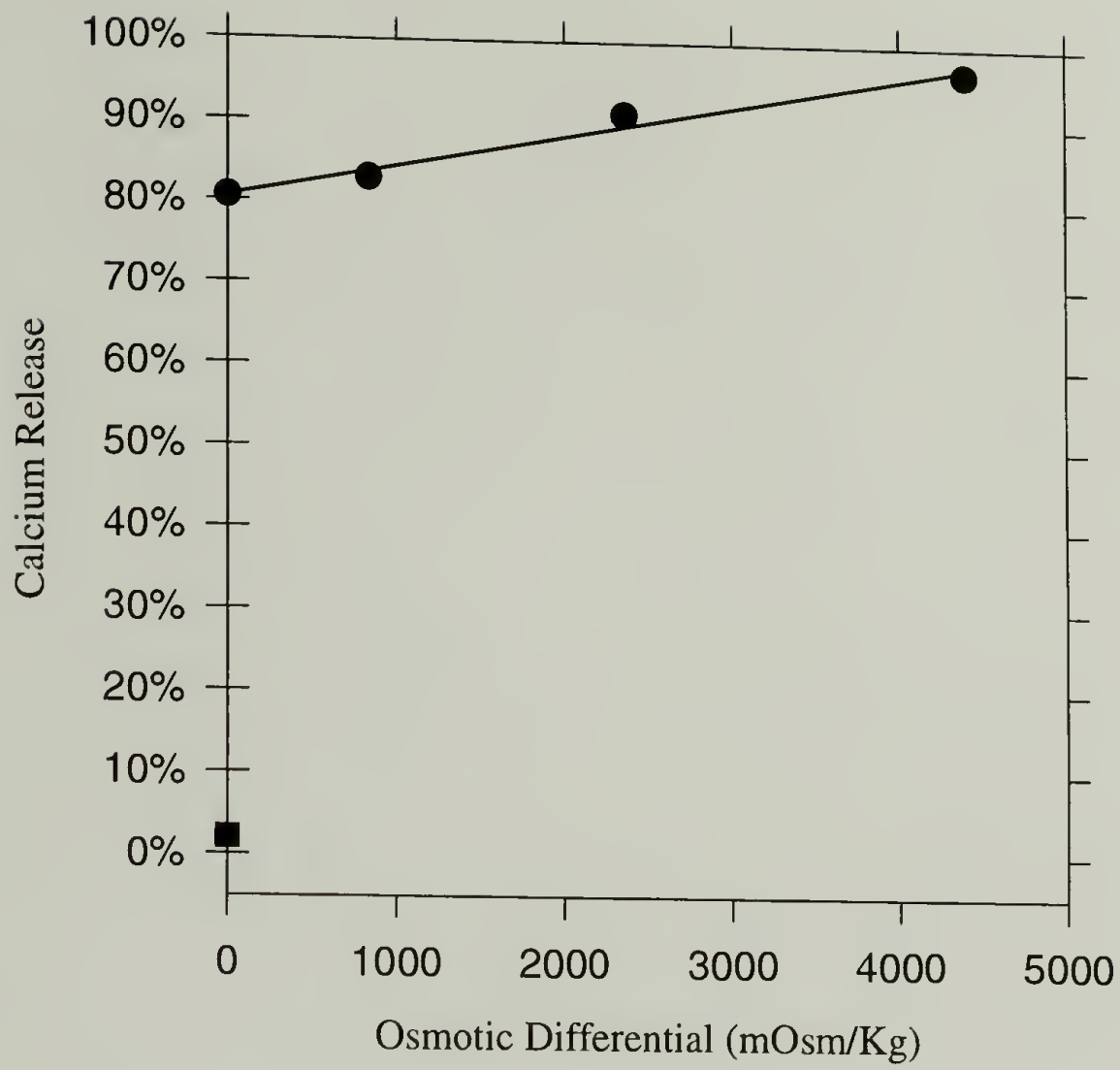


Figure 2.7 Influence of UV irradiation of extruded DOPC:Cholesterol:DOPE PEG 360 MA (45:45:10) vesicles with entrapped 100 mM PEGDMA on the osmotic leakage of $Ca^{2+}$. Extruded vesicles were loaded with 100 mM PEGDMA, 4.5 mM Irgacure 2959 and 150 mM $CaCl_2$ in HEPES buffer. Vesicles were irradiated (●) for 30 minutes with a pen-ray mercury lamp. (■) Vesicles that were not polymerized; the measurement was taken 24 hrs after the vesicles were passed over a gel filtration column. $Ca^{2+}$ in the surrounding medium was measured using the fluorescent dye, calcium green-5N.

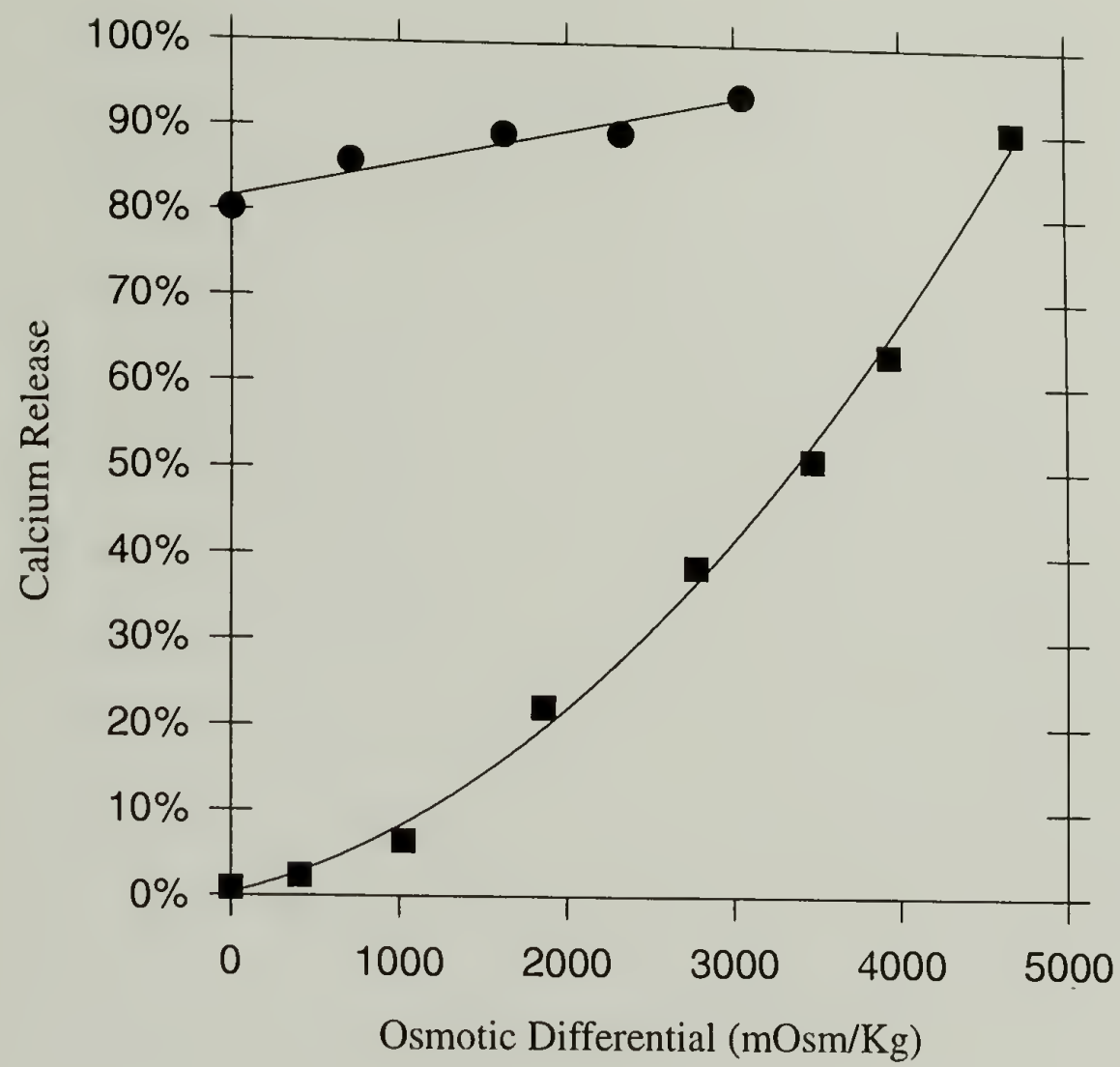


Figure 2.8 Influence of osmotic differential on extruded DOPC:cholesterol: DOPE PEG 360 MA (45:45:10) vesicles prepared in HEPES buffer with 4.5 mM irgacure 2959 and 150 mM $CaCl_2$. (●) Vesicles were irradiated for 30 minutes with a pen-ray mercury lamp. (■) Vesicles were not irradiated. $Ca^{2+}$ in the surrounding medium was measured using the fluorescent dye, calcium green-5N.

Table 2.1 Summary of results of dynamic light scattering of vesicles.

| Sample | Entrapped Solutes | Cumulant $R_H$ (nm) | CONTIN $R_H$ (nm) |
|---|---|---|---|
| Irradiated[a,b] | | 56 | 55 |
| Irradiated[a,b] + Triton X-100 | 100 mM PEGDMA 4.5 mM Irgacure 2959 | 39 | 39 |
| Irradiated[a,c] | 940 mM acrylamide 43 mM N,N-methylene-bisacrylamide | 60 | 55 |
| Irradiated[a,c] + Triton X-100 | Irgacure 2959 | 46 | 40 |
| Not Irradiated[d] | none | 47 | 44 |

[a] Irradiated for 30 min. with a low pressure mercury arc lamp. [b] Lipid composition: SOPC. [c] Lipid composition: EPC:cholesterol (2:1 mol ratio). [d] Lipid composition: DOPC:cholesterol (2:1 mol ratio).

## References


1) Torchilin, V. P.; Klibanov, A. L.; Ivanov, N. N.; Ringsdorf, H.; Schlarb, B. "Polymerization of Liposome-Encapsulated Hydrophilic Monomers," *Makromol. Chem., Rapid Commun.* **1987**, *8*, 457-460.

2) Jain, M. K.; Wagner, R. C. *Introduction to Biological Membranes*, John Wiley & Sons: New York, 1980.

3) Rutkowski, C. A.; Williams, L. M.; Haines, T. H.; Cummins, H. Z. "The Elasticity of Synthetic Phospholipid Vesicles Obtained by Photon Correlation Spectroscopy," *Biochemistry* **1991**, *30*, 5688-5696.

4) Ertel, A.; Marangoni, A. G.; Marsh, J.; Hallet, F. R.; Wood, J. M. "Mechanical Properties of Vesicles I. Coordinated Analyses of Osmotic Swelling and Lysis," *Biophys. J.* **1993**, *64*, 426-434.

5) Hallett, F. R.; Marsh, J.; Nickel, B. G.; Wood, J. M. "Mechanical Properties of Vesicles II. A Model for Osmotic Swelling and Lysis," *Biophys. J.* **1993**, *64*, 435-442.

6) Mui, B. L. S.; Cullis, P. R.; Evans, E. A.; Madden, T. D. "Osmotic Properties of Large Unilamellar Vesicles Prepared by Extrusion," *Biophys. J.* **1993**, *64*, 443-453.

7) Dorn, K.; Patton, E. V.; Klingbiel, R. T.; O'Brien, D. F.; Ringsdorf, H. "Molecular Weight of Polymers from Methacryloyl Lipids in Bilayer Membranes," *Makromol. Chem., Rapid Commun.* **1983**, *4*, 513-517.

8) Dorn, K.; Klingbiel, R. T.; Specht, D. P.; Tyminski, P. N.; Ringsdorf, H.; Obrien, D. F. "Permeability Characteristics of Polymeric Bilayer Membranes from Methacryloyl and Butadiene lipids," *J. Am. Chem. Soc.* **1984**, *106*, 1627-1633.

9) Ringsdorf, H.; Schlarb, B.; Venzmer, J. "Molecular Architecture and Function of Polymeric Oriented Systems: Models for the study of Organization, Surface Recognition, and Dynamics of Biomembranes," *Angew. Chem. Int. Ed. Engl.* **1988**, *27*, 113-158.

10) Regen, S. L. C., Bronislaw; Singh, A. "Polymerized Vesicles," *J. Am. Chem. Soc.* **1980**, *102*, 6638-6640.

11) Regen, S. L.; Singh, A.; Oehme, G.; Singh, M. "Polymerized Phosphatidylcholine Vesicles. Synthesis and Characterization," *J. Am. Chem. Soc.* **1982**, *104*, 791-795.

12) Lamparski, H.; O'Brien, D. F. "Two-Dimensional Polymerization of Lipid Bilayers: Degree of Polymerization of Sorbyl Lipids," *Macromolecules* **1995**, *28*, 1786-1794.

13) Lee, Y. -S.; Yang, J.-Z.; Sisson, T. M.; Frankel, D. A.; Gleeson, J. T.; Aksay, E.; Keller, S. L.; Gruner, S. M.; O'Brien, D. F. "Polymerization of Nonlamellar Lipid Assemblies," *J. Am. Chem. Soc.* **1995**, *117*, 5573-5578.

14) O'Brien, D. F. in *Encyclopedia of Polymer Science and Engineering*, Eds., Mark, H. F.; Bikales, N. M.; Overberger, C. G.; Menges, G. J., John Wiley & Sons: New York, 1989, pp. 108-135.

15) Okahata, Y.; Kunitake, T. "Formation of Stable Monolayer Membranes and Related Structures in Dilute Aqueous Solution from Two-Headed Ammonium Amphiphiles," *J. Am. Chem. Soc.* **1979**, *101*, 5231-5234.

16) Ellingson, J. S.; Lands, W. E. M. "Phospholipid Reactivation of Plasmalogen Metabolism," *Lipids* **1968**, *3*, 111-120.

17) Grynkiewicz, G.; Poenie, M.; Tsien, R. "A New Generation of Calcium Indicators with Greatly Improved Fluorescence Properties," *J. Biol. Chem.* **1985**, *260*, 3440-3450.

18) You, H.; Tirrell, D. A. "Photoinduced, Polyelectrolyte-Driven Release of Contents of Phosphatidylcholine Bilayer Vesicles," *J. Am. Chem. Soc.* **1991**, *113*, 4022-4023.

19) Koppel, D. E. "Analysis of Macromolecular Polydispersity in Intensity Correlation Spectroscopy: The Method of Cumulants," *J. Chem. Phys.* **1972**, *57*, 4814-4820.

20) Chang, C. H.; Mar, A.; Tiefenthaler, A.; Wostratzky, D. in *Handbook of Coatings Additives: Volume 2*, Ed., Calbo, L. J., Marcel Dekker, Inc.: Monticello, 1992, pp. 1-43.

21) Hope, M. J.; Bally, M. B.; Webb, G.; Cullis, P. R. "Production of Large Unilamellar Vesicles by a Rapid Extrusion Procedure. Characterization of Size Distribution, Trapped Volume and Ability to Maintain a Membrane Potential," *Biochim. Biophys. Acta* **1985**, *812*, 55-65.

22) Edwards, K.; Almgren, M.; Bellare, J.; Brown, W. "Effects of Triton X-100 on Sonicated Lecithin Vesicles," *Langmuir* **1989**, *5*, 473-478.

23) Allen, T. M. in *Liposome Technology Vol. 3*, Ed., Gregoriadis, G., CRC: Boca Raton, 1984, pp. 177-182.

24) Zalipsky, S. "Functionalized Poly (ethylene glycol) for Preparation of Biologically Relevent Conjugates," *Bioconjugate Chem.* **1995**, *6*, 150-165.

25) Needham, D.; Nunn, R. S. "Elastic Deformation and Failure of Lipid Bilayer Membranes Containing Cholesterol," *Biophys. J.* **1990**, *58*, 997-1009.

# CHAPTER 3

# PHOTOINDUCED, POLYMERIZATION-DRIVEN RELEASE OF CONTENTS FROM BILAYER VESICLES

## Introduction

The biomembrane is the site of many complex cellular processes. These include functions related to transport of metabolites, ions and proteins; cellular recognition and integration; and cell signaling. It is the membrane proteins that modulate these functions in response to environmental stimuli, such as changes in ion concentrations, pH and the binding of ligands to membrane receptors. At the molecular level, a membrane behaves like a two-dimensional fluid, consisting primarily of phospholipid, cholesterol and protein molecules. Currently, there is not one model which mimics the complex machinery associated with the biological membrane; however, significant progress has been made in controlling membrane structure and permeability using simple membrane models. A liposome, or vesicle, is a synthetic, cell-like capsule that has been a useful model system in the investigation of biomembranes. Phospholipids that are dispersed in excess water spontaneously assemble into a closed bilayer, and like the plasma membrane, the vesicle bilayer serves as an effective barrier to the movement of ions and hydrophilic molecules between the inner aqueous compartment and the external solution. The impetus to study membrane models is the potential application of lipid vesicles in imaging, drug delivery and biosensing.

Because lipid vesicles are composed of the same materials as cellular membranes, they have been used in therapeutic applications such as gene therapy and drug delivery.[1] Engineering such a delivery system is an intricate task, as its ultimate goal is to have a vesicle use environmental cues to deliver its contents specifically to the receiving compartment of its target. Therefore, it is important to develop strategies to modulate membrane permeability by physiologically relevant stimuli.

In the course of our investigation into the osmotic behavior of polymerized vesicles, we observed the release of contents from mixed polymerizable lipid vesicles after exposure to ultraviolet (UV) radiation. Figure 3.1 shows the molecular structures for the prepared lipids. Each lipid has a methacrylate functionalized poly(ethylene glycol) grafted to a phospatidylethanolamine derivative, that is dioleoyl phosphatidylethanolamine (DOPE PEG 360 MA) and distearoyl phosphatidylethanolamine (DSPE PEG 400 MA). The design rationale was to develop lipids that would copolymerize with monomer dissolved in the inner aqueous compartment. Therefore, the function of the PEG spacer group was to extend the methacryloyl group into the aqueous solution away from the membrane interface in order to facilitate copolymerization with monomer entrapped in the internal aqueous compartment. As the results herein demonstrate, vesicles with as little as 10 mol % DOPE PEG 360 MA quantitatively release entrapped solutes when exposed to UV irradiation. We have used a fluorescent calcium indicator to characterize the leakage of contents from extruded vesicles. The ability to modulate membrane permeability with light creates the possibility for applications in therapeutics, imaging and biosensors.

In therapeutics, liposome based technologies have been used to treat fungal infections,[2] to diagnose and treat cancer,[3,4] and to carry DNA into cells for gene therapy.[5,6] Appropriately designed vesicle systems improve drug efficacy by increased time in circulation and specific targeting of affected tissues. In each of these systems, a process had to be developed to trigger the release of therapeutic agents at an optimized rate and at the correct target. The concepts and strategies for effecting triggered release from pH- or immunosensitive vesicles have recently been reviewed in the literature,[5-7] and thus will not be discussed in this chapter; however, a brief survey of techniques that have been used to trigger the release of vesicle contents by the action of light will be given in the next section.

## Photoinduced Release of Contents from Bilayer Vesicles

In view of the many technological applications of phospholipid vesicles, it is necessary to develop versatile methods to control the leakage rate of entrapped substances from liposomes. We have investigated the triggered release of contents by UV irradiation. This approach seems promising as the intensity of light can easily be controlled by an external source, and can be used to treat regions of the body, which are accessible by fiber optic endoscopes. The subject of photoinduced reorganization of bilayer vesicles has recently been reviewed by O'Brien and Tirrell,[8] and as such, the following paragraphs will be limited to a brief survey of those experiments which provide added insight into our own results.

Photomodification of the Bilayer. In the early 1980's, Kunitake and associates were the first to report that unilamellar dipalmitoyl phosphatidylcholine (DPPC) vesicles could be made permeable by photoisomerization of an amphiphilic azobenzene (Figure 3.2) doped in the bilayer.[9] UV irradiation causes a *trans*-to-*cis* isomerization in the vesicular form of azobenzene, as evidenced by the decrease in the *trans*-azobenzene absorption at $\lambda$ = 358 nm. The authors characterized the effects of photoisomerization on mixed bilayers by osmotic shrinkage and the release of a fluorescent dye. In all cases, the *cis* form of the azo amphiphile resulted in increased membrane permeability, and the osmotic shrinkage rates were substantially increased (i.e., increased water permeability). The authors postulated that "channels" formed in the bilayer due to the large geometric change of the azobenzene moiety after UV irradiation.

Sato and coworkers[10] have demonstrated that it is possible to reversibly control the ion permeability of sonicated vesicles constructed from a mixture of dimyristoyl phosphatidylcholine (DMPC), dicetyl phosphate (DCP) and 4-octyl-4'-(5-carboxypentamethyleneoxy)azobenzene (8A5). As in the system described above, UV irradiation of dark-adapted liposomes caused *trans*-to-*cis* isomerization (Figure 3.3), which was followed by a decrease in the strong absorption peak of the *trans* form at $\lambda$ = 350 nm. The permeation of $K^+$ was shown to increase by approximately ~ 3 orders of magnitude after UV irradiation, compared with the permeability of the dark adapted vesicles. Evidence for the reversible control of ion permeability with UV irradiation was demonstrated by measuring $K^+$ leakage by cycling periods of irradiation and darkness. Stepwise increases in the permeability of the vesicles were observed (Figure 3.4), as

permeation of $K^+$ increased during UV irradiation and dropped to 'zero' during periods of darkness.

Kunitake and coworkers were the first to demonstate that the ion permeability could be controlled photochemically. Building on these results, Sato was able to engineer a synthetic vesicle with "channel-like" behavior that could be switched on or off by intermittent irradiation. Both of these experiments represent one general approach to induce bilayer reorganization photochemically, i.e., isomerization of an azobenzene chromophore incorporated in the bilayer.

Photomodification of the Polar Headgroup. The membrane consists of a hydrophobic bilayer and two polar surfaces. In the previous section, it was reported that vesicles were rendered permeable by photochemical alteration of the hydrophobic region of the bilayer. An equally attractive strategy is to photochemically alter the polar headgroups instead. Fuhrhop and coworkers,[11,12] used this general approach to disrupt vesicular aggregates with visible light. The authors prepared sonicated vesicles from benzenediazonium amphiphiles at low pH (Figure 3.5). Transmission electron microscopy of the lipid suspensions showed spherical structures of diameter 20-200 nm. With the addition of catalytic amounts of 5,10,15,20-porphinetetrakis(9-decenesulfonic acid), the vesicles could be quantitatively precipitated within 10 minutes of irradiation with a 60 W tungsten lamp. This work represented the first example of visible light induced bilayer reorganization.

Haubs and Ringsdorf[13,14] developed two techniques to photochemically alter the polar surfaces of the bilayer. Both methods increase the hydrophobicity of the lipid

headgroups, thus destroying the amphiphilic nature of the molecules and destabilizing the vesicular structure. The authors prepared single- and double-chained amphiphiles with a N-(1-pyridinio)amidate headgroup. The single $C_{25}$-alkyl chains and the double chain derivatives formed vesicles at low pH as evidenced by electron microscopy and encapsulation of a water-soluble dye. Continuous exposure of double chain N-(1-pyridinio)amidate vesicles to UV irradiation resulted in the clean conversion of the ylide to the 1,2-diazepine derivative, which is much less polar (Figure 3.6). These vesicles are metastable, and could be disrupted easily by mechanical agitation.

Haubs and Ringsdorf developed a second approach to headgroup modification.[14] They prepared a lipid with a quaternary ammonium salt headgroup, which can be photolysed in vesicular form to yield non-polar toluene derivatives (Figure 3.7). The double chain ammonium lipid formed liposomes as evidenced by electron microscopy and dye entrapment. The photolysis of the headgroup was further investigated by viewing giant vesicles constructed from the double chain ammonium lipid using a phase-contrast light microscope. At the beginning of UV exposure, membrane fluidity decreased as evidenced by the decrease in membrane fluctuations, then, after further irradiation, the vesicles were observed to shrink and ultimately collapse into microcrystals.

Photopolymerization-Induced Vesicle Leakage. A third strategy to modify membrane permeability is to exploit the tendency of certain lipids, particularly phosphatidylethanolamines (PE),[15,16] to form nonlamellar phases under physiological conditions. Therefore, processes that trigger the formation of a PE rich phase can be used to generate responsive synthetic vesicles. It was discovered that polymerization of two-

component vesicles, where only one of the lipid components was polymerizable, caused the lipids to phase separate into polymeric and monomeric rich phases.[17] If the non-polymerizable lipid is a PE, the formation of an enriched PE phase will induce a lamellar to inverted hexagonal phase transition. O'Brien and coworkers[18,19] were the first to exploit this in polymerizable vesicles, and demonstrated the concept by preparing stable two-component vesicles constructed from 2:1 mixtures of PE with the polymerizable SorbPC (Figure 3.8). An important feature of this design is that SorbPC is able to stabilize PE bilayers, as demonstrated by dye encapsulation. The photoinduced destabilization of PE/SorbPC membrane was verified by dye leakage after UV irradiation.

The membrane in the work described here is a ternary mixture of PC, cholesterol and DOPE PEG 360 MA, where the two non-polymerizable lipids tend to form lamellar phases in aqueous buffers. Clearly, membrane destabilization is not caused by lateral phase separation between polymerized and monomeric lipid molecules. It is interesting to note that a polymerizable lipid with similar structure has been synthesized before and shown to decrease the solute permeability in crosslinked vesicles.[20] Based on these observations, we have examined the ability of DOPE PEG 360 MA to cause the destabilization of phospholipid/cholesterol membranes upon UV irradiation. The primary objective of this study was to establish a tentative model that accounts for this new approach to the photoinduced release of contents of lipid bilayer vesicles.

## Experimental Section

### General Procedures

For a general section concerning spectroscopic and chromatographic techniques, see chapter 2.

### Solvents and Reagents

All materials were used as received. Dioleoyl phosphatidylcholine (DOPC), egg phosphatidylcholine (EPC) and distearoyl phosphatidylethanolamine-N-PEG-2000 (DSPE PEG 2000) were purchased from Avanti Polar Lipids, Inc. (Alabaster, AL). Cholesterol, deuterium oxide, and sodium chloride were purchased from Aldrich Chemical Co. (Milwaukee, WI). Calcium chloride, ethylenediaminetetraacetic acid (EDTA), manganese(ous) chloride, and chloroform (HPLC grade) were purchased from Fisher Scientific (Fair Lawn, NJ). Triton X-100, Sephadex G-75 and 4-(2-hydroxyethyl)-1-piperazineethanesulfonic acid (HEPES) were purchased from Sigma Chemical Co. (St. Louis, MO). Poly(ethylene glycol) 1000 dimethacrylate (PEGDMA) was purchased from Polysciences, Inc. (Warrington, PA). Irgacure 2959 was a gift from Ciba-Geigy Corp. (Hawthorne, NY).

### Synthesis

The procedures for the synthesis of DSPE PEG 400 MA and DOPE PEG 360 MA are discussed in chapter 2.

## Vesicle Preparation

Liposomes were prepared by drying a $CHCl_3$ solution of 60 mg of lipid first with a jet of $N_2$, then with high vacuum for 2 hours in constant darkness. Multilamellar vesicles (MLVs) were prepared by vortex mixing with 3 ml of the solution to be encapsulated, followed by repeated vortexing, and then 5 freeze/thaw cycles (5 minute freeze in liquid $N_2$, followed by a 10 minute thaw in warm tap water). Large unilamellar vesicles were then prepared by 10 extrusions through two stacked polycarbonate filters as described previously.[21]

## Photopolymerization of Giant Vesicles

For a description concerning the preparation and micromanipulation of giant vesicles, see chapter 1.

## Photopolymerization of Vesicles

Vesicles composed of DOPE PEG 360 MA, DOPC and cholesterol were prepared in 50 mM HEPES, pH 7.4, containing 4.5 mM irgacure 2959, 150 mM $CaCl_2$ and depending upon the experiment, 100 mM PEGDMA (Note: High concentrations of NaCl (~ 2 M) were used in the initial release experiments in conjunction with osmotic release studies). To remove nonentrapped solutes, the resulting large unilamellar vesicles (1.5 ml) were passed through a Sephadex G-75 size exclusion column (1.5 x 17 cm) pre-equilibrated with a calcium free HEPES buffer (50 mM, pH 7.4), that was osmotically balanced with the vesicles using NaCl. Vesicle fractions were collected based on absorbance measurements at 300 and 400 nm. A 2.5 ml aliquot of the lipid suspension

was added to a microscale quartz immersion photochemical reactor assembly (Ace Glass, Vineland, NJ) and irradiated for 30 min with a 254 nm UVP Pen-Ray lamp (4500 $mW/cm^2$ at 2.5 $cm^{22}$).

In these studies, it is important to use water that is not contaminated with calcium ions. Calcium 'free' water was obtained from a purification system consisting of two ion-exchange cartridges and was analyzed prior to use. Those samples of water that exhibited a fluorescence intensity less than 100 a.u. when made 42 μM in Calcium Green-5N were used in further experiments. All solutions were prepared in containers that were rinsed in the following protocol: 3X with pure water, 3X with boiling 5 mM $Na_2EDTA$, 2X with pure water, 3X with 10 % $HNO_3$, and again 6X with water.

Calcium Leakage Measurements

Steady-state fluorescence measurements were performed in 1-cm poly(methyl methacrylate) cuvettes using a Perkin Elmer MPF-66 fluorescence spectrophotometer. Emission and excitation slits were both set to 5 nm. Cuvettes were prepared by diluting 3 ml of an osmotically balanced buffer (50 mM HEPES (pH 7.4), NaCl ) with 25 μl of 50 μg/ml Calcium Green-5N (42 μM), then, 40 μL of the vesicle suspension. Calcium green-5N is a calcium chelator that shows an increase in fluorescence intensity upon calcium binding. By measuring the fluorescence emission at 531 nm, with excitation at 488 nm, one can determine the free calcium concentration from the following equation:

$$\left[Ca^{2+}\right] = K_d \frac{\left[F - F_{\min}\right]}{\left[F_{\max} - F\right]}$$

where F is the fluorescence intensity at 531 nm under illumination at 488 nm, $F_{min}$ and $F_{max}$ are determined from zero and saturating calcium concentrations and $K_d$ is the dissociation constant.[23] The fraction of calcium released is determined by dividing the calcium concentration measured after photoinduced lysis by the total concentration of calcium released caused by the addition of 40 µl of Triton X-100 (50 mg/ml).

## Dynamic Light Scattering

For a section concerning dynamic light scattering measurements, see chapter 2.

## Nuclear Magnetic Resonance Spectroscopy of Lipid Vesicles

High-resolution $^1H$ NMR spectroscopy was carried out on a Bruker DPX-300 instrument at room temperature. Extruded vesicles were prepared from a DOPC:cholesterol:DOPE PEG 360 MA (45:45:10 mol ratio) lipid mixture at 35 mg/ml in $D_2O$. Spectra were collected as the samples were titrated with small aliquots (10-20 µl) of a stock 12 mM $MnCl_2$ solution in $D_20$. The spectra were analyzed after 16 scans using a personal computer and the MestRe-C Magnetic Resonance Companion Version 1.5.0 software package (Santiago de Compostela, Spain).

# Results

## Osmotic Release of Vesicle Contents from PEG-Grafted Liposomes

As a control experiment, liposomes with DSPE PEG 2000 were subjected to osmotic lysis tests to determine if the PEG repeats interfere with the release studies by chelating free calcium. Figure 3.9 shows the increase in calcium release from

DOPC:cholesterol:DSPE PEG 2000 (53:45:2 mol ratio) vesicles as the osmotic strength of the external buffer decreases. The figure also shows results for a sample composed of vesicles prepared from a 55:45 mixture of EPC:cholesterol. The osmotic release profile for the PEG containing vesicles is consistent with the rupture behavior of the PEG free vesicles. This indicates the ethylene glycol repeats of the PEG do not bind $Ca^{2+}$ as strongly as the fluorescent indicator calcium green 5-N, and that PEG does not affect the calcium release measurement. (Note: EPC:cholesterol and DOPC:cholesterol vesicles exhibit similar osmotic release behavior.)

Photoinduced Release of Contents from Extruded Vesicles. Unfortunately, we found that lipid mixtures containing both DSPE PEG 400 MA and cholesterol were very difficult to extrude. Therefore, our discussions of the release of contents from extruded vesicles will be limited to those mixtures that contain DOPE PEG 360 MA as the polymerizable lipid. Table 3.1 summarizes the results of three photopolymerization experiments. In each experiment, the lipids were prepared at a concentration of 20 mg/ml lipid, passed through an osmotically balanced size exclusion column to exchange the non-entrapped solutes with a saline buffer solution, and irradiated for 30 minutes with a low pressure pen-ray mercury arc lamp. Only those lipid mixtures with DOPE PEG 360 MA (Table 3.1, samples 2 and 3) in the membrane exhibited release of vesicle contents upon UV irradiation. Destabilization of the membrane is triggered by UV irradiation of the lipid bound methacrylates, as those vesicles with entrapped PEGDMA but no DOPE PEG 360 MA in the membrane show no release (Table 3.1, sample 1). Also, since no $Ca^{2+}$ was released from sample 1, membrane destabilization is not likely to be caused by

photooxidation of the vinyl groups in the lipid backbone. Interestingly, samples 2 and 3 remained turbid (e.g. the optical density of 3 increased from 1.15 to 1.81 after irradiation) suggesting that large particles were still present in the suspension, and that leakage is not due to a vesicle to micelle transition.

That UV irradiation results in polymerization at the membrane interface is shown by $^1$H NMR spectroscopy. The Fourier transform $^1$H NMR spectra of a mixture DOPC:cholesterol:DOPE PEG 360 MA (45:45:10 mol ratio) lipids before and after irradiation are shown in Figure 3.10 A and B. The lipids were initially dissolved in 1 ml of $CDCl_3$, and the $^1$H NMR spectrum was recorded (Figure 3.10 A), then, the $CDCl_3$ was removed and multilamellar vesicles (MLVs) were prepared by dispersing the lipids in deionized water (20 mg/ml). Next, the MLVs were extruded and the resulting large unilamellar vesicles (100 nm) were irradiated for 30 minutes with a low pressure pen-ray mercury arc lamp. After UV irradiation, the sample was dried, resuspended in $CDCL_3$ and a second $^1$H NMR spectrum was recorded (Figure 3.10 B). The spectra revealed the disappearance of the methacryloyl vinyl protons upon irradiation, showing that polymerization has occurred and that the lipid vinyl protons are not affected by UV irradiation.

Polymerization Induced Shape Changes in Giant Vesicles

The direct observation of giant vesicles composed of DSPE PEG 400 MA and cholesterol with an optical microscope revealed photopolymerization-induced membrane shape changes. Figure 3.11 shows a sequence of images of an aspirated giant vesicle as it is being photopolymerized. The vesicle was composed of a 1:1 mixture of DSPE PEG

400 MA and cholesterol and was prepared in a solution of 50 mM PEGDMA and photoinitiator. Irradiation of the sample led to a striking effect; the giant vesicle ejected smaller vesicles from its outer surface and these small units diffused laterally across the entire membrane surface throughout the polymerization process, suggesting that membrane retained its fluid-like properties. The expulsion of the small vesicles is believed to have been triggered by photopolymerization at the membrane interface because: (i) it occurred within seconds after irradiation and (ii) it was not observed in irradiated control vesicles that did not contain DOPE PEG 360 MA. Also, giant vesicles that were prepared from cholesterol and DSPE PEG 400 MA (1:1 mol ratio), but without entrapped PEGDMA) did not eject small vesicles upon irradiation.

Finally, two vesicles with the same composition as above that did not have entrapped PEGDMA were brought into contact by micromanipulation. The juxtaposed vesicles were irradiated in an attempt to graft the two vesicles together with polymeric bridges. Images from video microscopy indicate there was not a significant amount of cross polymerization at the membrane/membrane interface because the two vesicles were easily pulled apart (images not shown). The absence of polymerization between two vesicles suggests that a suspension of extruded vesicles most likely will not aggregate due to vesicle grafting.

It seems clear grafting between the DSPE PEG 400 MA in the inner monolayer and the entrapped PEGDMA caused the ejection of the small vesicles. As DSPE PEG 400 MA copolymerizes with the entrapped PEGDMA, the surface area of the inner leaflet will decrease. We assume the grafts between the membrane and the entrapped gel couple the membrane to the loss of volume due to polymerization. We presume there is less area

being lost in the outer monolayer because there is no PEGDMA in the extravesicular medium. Consequently, the outer layer does not condense as much as the inner leaflet during photopolymerization, and yet it must cover as much area as the inner monolayer. The outer leaflet is under compression, and at some point, the membrane buckles and it undergoes a change in curvature forming small vesicles on the outer leaflet. This process might render the membrane leaky. This explanation assumes perturbation of the membrane is the direct result of asymmetric polymerization with respect to the two membrane interfaces. Such a model might explain photopolymerization-induced release of contents from 100 nm extruded vesicles if a mechanism for asymmetric polymerization can be shown.

Asymmetric Photopolymerization in Extruded Vesicles

Several experiments have been designed to ascertain if asymmetric polymerization across the bilayer membrane is responsible for the photoinduced release of contents from 100 nm extruded vesicles. The three possible ways that asymmetric polymerization can take in vesicles prepared from DOPE PEG 360 MA are: (1) Polymerization of vesicles where the concentration of PEGDMA in solution are not equal on the opposite sides of the membrane. (2) The concentration of photoinitiated radicals is not equally distributed between the vesicular and extravesicular media where the assumption is photogenerated radicals do not diffuse rapidly through the membrane. (3) The polymerizable lipid is not evenly distributed between the two monolayers because of bilayer curvature; that is, the outer leaflet could have a higher concentration of DOPE PEG 360 MA owing to its large headgroup.

Photoinduced Release of $Ca^{2+}$ from Polymerizable Vesicles with Entrapped PEGDMA. We have already ascertained that photopolymerization of 100 nm vesicles prepared from DOPC:cholesterol:DOPE PEG 360 MA (45:45:10 mol ratio) in 100 mM PEGDMA buffered solution (Sample no. 2, Table 3.1) results in the near quantitative release of contents. These results are consistent with the hypothesis that asymmetric polymerization causes leakage. Copolymerization between the membrane and entrapped monomer might be sufficient to cause membrane leakage, but it does not account for the photoinduced release of contents from vesicles that contain DOPE PEG 360 MA but not entrapped PEGDMA.

Effect of Photoinitiator on the Release of $Ca^{2+}$ from Polymerizable Vesicles. In all of the previous $Ca^{2+}$ release studies, the photoinitiator was systematically removed from the extravesicular medium by gel filtration chromatography. Figure 3.12 shows a typical elution profile as monitored by absorbance at 400 nm (which reports vesicle elution) and 300 nm (which reports vesicle and Irgacure 2959 elution). Two elution peaks are present in the chromatogram; the vesicles elute in fractions 14-22, whereas the non-entrapped solutes elute in fractions > 37. Immediately following the column purification, fractions containing vesicles were combined and irradiated for thirty minutes. The elution profiles clearly indicate that prior to polymerization the initiator is asymmetrically distributed across the membrane.

To determine how the unequal distribution of Irgacure 2959 influences the photopolymerization-induced release of contents from vesicles, we monitored the release

of $Ca^{2+}$ from several vesicle preparations where the initiator was systematically placed either symmetrically or asymmetrically across the vesicle bilayer. Figure 3.13 shows how the spatial distribution of photoinitiator affects the release of entrapped $Ca^{2+}$ from vesicles that were constructed from 45:45:10 DOPC:cholesterol:DOPE PEG 360 MA lipid mixtures. In the experiment where the photoinitiator was only in the external medium, the extruded vesicles were prepared in 150 mM $CaCl_2$ and 50 mM HEPES, pH 7.4 and passed through an osmotically balanced gel filtration column pre-equilibrated with 4.5 mM Irgacure 2959 in 0.2 M NaCl and 50 mM HEPES, pH 7.4. UV irradiation of this sample led to the quantitative release of the initially entrapped $Ca^{2+}$. The vesicles with photoinitiator distributed equally across the membrane were prepared in the same manner except that they were hydrated in an aqueous buffer that also contained 4.5 mM Irgacure 2959. UV irradiation of this lipid suspension led to similar results, that is, the quantitative release of $Ca^{2+}$ from the vesicles. In a control experiment, no photoinitiator was added to either the internal nor the external buffer, and still UV irradiation led to the release of nearly 60 % of the entrapped $Ca^{2+}$. That contents release is independent of the spatial distribution of photoinitiator is clear from these results, including the control experiment where there was no photoinitiator present and yet UV exposure led to the substantial release of entrapped $Ca^{2+}$. (Note: The implicit assumption that Irgacure 2959 does not permeate the membrane was never verified, that is, we never demonstrated the presence of an initiator concentration gradient across the membrane. These experiments were not conducted because of our observation that photopolymerization, and therefore $Ca^{2+}$ release, did not require the use of Irgacure 2959. Apparently, initiation by photolysis is sufficient to cause the polymerization of DOPE PEG 360 MA.[24] See Figure

3.10, where the disappearance of methacryloyl vinyl protons was effected by UV irradiation in the absence of photoinitiator.)

Characterization of the Asymmetric Distribution of DOPE PEG 360 MA in Curved Bilayers. The distribution of DOPE PEG 360 MA between the inner and outer leaflets of extruded vesicles was determined using $^1$H NMR spectroscopy of vesicle suspensions in the presence of paramagnetic ions. Extruded vesicles were made from a mixture of DOPC:cholesterol:DOPE PEG 360 MA (45:45:10, 35 mg/ml) in $D_2O$, and the $^1$H NMR spectrum of the suspension was recorded as the sample was titrated with 12 mM $MnCl_2$. Paramagnetic ions ($Mn^{2+}$, $Pr^{3+}$, $Eu^{3+}$ etc.) have been used to identify the head groups in the two monolayers of vesicle bilayers.[25-28] Figure 3.14 shows the $^1$H NMR spectra of a suspension of extruded vesicles. The most prominent signals were assigned to the aliphatic protons found in the hydrophobic region of the lipid bilayer, as well as the choline protons and the protons in the ethylene oxide repeats of the PEG spacer group.[25] In the NMR spectrum after the extravesicular medium was made 0.9 mM in $MnCl_2$ (Figure 3.14, top spectrum), the signals from the choline and PEG protons, as well as the HDO signal, were considerably broadened, whereas the signals from the nonpolar hydrocarbon chains were only slightly broadened. In these experiments, the signal intensity from the aliphatic proton peaks was used to normalize the intensities of the PEG and choline signals.

Figure 3.15 confirms that DOPE PEG 360 MA is asymmetrically distributed between the inner and outer leaflets in vesicles that were prepared from DOPC: cholesterol:DOPE PEG 360 MA (45:45:10 mol ratio, 82 nm average diameter from

dynamic light scattering). The sample was titrated with 12 mM $MnCl_2$, where the fraction of the signal that remained after the addition of $Mn^{2+}$ was calculated by dividing the normalized signal intensity by the normalized intensity of its corresponding peak prior to the addition of $Mn^{2+}$. After the lipid suspension was made ≈ 0.80 mM in $Mn^{2+}$, the addition of more $Mn^{2+}$ did not cause further loss in the intensities of the PEG and choline signals, hence, the titration curve reached a plateau at this concentration and the constant value for the fraction represents the amount of that lipid that lies in the inner leaflet. The data in Figure 3.15 clearly show that nearly 60 % of the DOPE PEG 360 MA lipid molecules are distributed in the vesicles outer leaflet, compared to 55 % for the phosphatidylcholine lipids (vesicle diameter 82 nm). The measured distribution of the DOPC is in good agreement with the calculated value of 54 % in the outer leaflet, based on a spherical vesicle with a 41 nm external radius and a 4 nm bilayer thickness. The difference between the distributions of DOPC and DOPE PEG 360 MA is due to the large headgroup of the latter and the packing constraints it causes in the highly curved membrane. As the vesicle diameter increases, the DOPE PEG 360 should become more equally distributed between the two leaflets, i.e., the signals for both of the headgroups will lose the same fraction of intensity at the end of the titration, since the packing constraints will decrease as the bilayer curvature increases. This is exactly what was found experimentally for 210 nm vesicles where the DOPC and DOPE PEG 360 MA lipid molecules were both distributed equally between the two leaflets (Figure 3.16). It must be noted that the addition of $Mn^{2+}$ resulted in more than a 50 % reduction in choline and PEG signals. For 200 nm vesicles with a 4 nm bilayer thickness, the calculated inner to outer ratio of surface area is 49:51, thus we expected the intensities of the choline and

PEG signals to decrease by approximately 50 %. Also, vesicles that are prepared by extrusion with 400 nm pores have been shown to be multilamellar meaning the signal losses should be less than 50%.[29] The discrepancy in the measured absolute spatial distributions most likely reflects the systematic error involved in measuring the area of the $^1$H NMR signals. However, the fact that the two signals approach the same value in the titration curve indicates that they are nearly equally distributed between the two monolayers.

Table 3.2 is a summary of the results of photoinduced release of $Ca^{2+}$ from vesicles with different radii. Both vesicle preparations were composed of DOPC, cholesterol and DOPE PEG 360 MA (45:45:10 mol ratio, respectively) and entrapped 150 mM $CaCl_2$ in 4.5 mM Irgacure 2959 and 50 mM HEPES, pH 7.4. The smaller vesicles were prepared by extrusion through 100 nm pores whereas the larger ones were extruded through 400 nm pores. Unfortunately, we were unable to prepare vesicles that had a larger average diameter than 170 nm in the presence of the ionic reaction buffer. The calculated ratio between the outer and inner surface is 1.1. After the small and large vesicles were UV irradiated for 30 min, both samples exhibited an increase in the extravesicular $Ca^{2+}$ concentration, though the larger vesicles (173 nm) released 62 % of the entrapped $Ca^{2+}$ compared to 100 % release of $Ca^{2+}$ by the 110 nm vesicles. The fact that the larger vesicles released a lower fraction of the entrapped solutes compared to the smaller vesicles is consistent with our hypothesis that the photoinduced release of contents is caused by asymmetric polymerization. However, a significant amount of $Ca^{2+}$ was released from the larger vesicles.

## Discussion

The results presented here demonstrate a new approach to the photoinduced release of contents from 100 nm extruded vesicles that were doped with 10 mol percent of DOPE PEG 360 MA, a polymerizable lipid. A suspension of vesicles was destabilized upon photopolymerization resulting in the near quantitative release of the entrapped solutes. This discovery was surprising because the polymerization of liposomes has been shown to reduce the permeability and enhance the chemical stability of the bilayer membrane.[30,31]

We have proposed that the membrane destabilization in 100 nm extruded vesicles could be caused by asymmetric polymerization across the membrane. As DOPE PEG 360 MA polymerizes in the membrane, we believe the area occupied by the phosphatidylethanolamine side group decreases. In fact, Ringsdorf and his coworkers[20] have studied the spreading behavior of the monomeric and polymeric monolayers of polymerizable amphiphiles with similarities to DOPE PEG 360 MA, and they observed a decrease in the area per molecule from 1.50 $nm^2$/molecule to 0.95 $nm^2$/molecule upon polymerization. Hence, as DOPE PEG 360 MA polymerizes in the bilayer, each leaflet tends to condense (Figure 3.17). Therefore, if the extent of polymerization is not the same at both monolayers, each leaflet will experience different degrees of lateral compression. Since each monolayer must cover the same amount of area, polymerization induced compression in one monolayer must be counteracted by compression in the other. As polymerization continues, most likely the monolayer where the polymerization is not as efficient buckles under the compressive stress. Such a model explains the ejection of

small vesicles from the surface of the giant vesicle in Figure 3.11. In the case of giant vesicles, the inner leaflet is believed to react more than the outer leaflet during photopolymerization due to the presence of 50 mM PEGDMA in the interior compartment, consequently resulting the *expulsion* of bilayer from the outer leaflet. We believe it is these photopolymerization induced membrane shape changes that render the membrane leaky.

The fact that extruded vesicles *without* entrapped monomer were rendered leaky upon photopolymerization suggests there are additional mechanisms for achieving differences in the degree of polymerization at the two leaflets. Results from $^{1}H$ NMR spectroscopy suggested bilayer curvature forced the polymerizable lipid to be partitioned into the outer leaflet in smaller vesicles, that is, as the vesicle curvature increased, the relative amount of DOPE PEG 360 MA in the inner leaflet increased. Therefore, in larger vesicles, there should be no mechanism for asymmetric polymerization between the two leaflets, and there should be reduced leakage upon photopolymerization. We found this to be true; larger vesicles released *less* entrapped $Ca^{2+}$ upon irradiation than smaller ones. However, the larger vesicles did release nearly 60 % of the entrapped solutes suggesting asymmetric polymerization may not be the correct model.

The proposed model does not explain why polymerization of sonicated vesicles composed of amphiphiles with polymerizable headgroups caused a *decrease* in solute permeability.[20] A second model for membrane destabilization can be postulated to explain photopolymerization-induced membrane destabilization. Polymerization of vesicles doped with DOPE PEG 360 MA results in the formation of a PEG-grafted hydrophobic polymer at the membrane interface. In fact, this polymer most likely has

surface-active properties, which may cause membrane insertion and release of vesicle contents. Optical density measurements and dynamic light scattering results polymerized vesicles indicate there are still large structures in the suspension, suggesting that photopolymerization does not cause a vesicle to micelle transition. There are several reports in the literature where low concentrations of detergent in the extravesicular medium trigger the release of vesicle contents by the formation of pores as opposed to complete solubilization.[32-35] It is not unreasonable that leakage could be caused by the accumulation of polymeric "surfactant" at the membrane interface.

Future Work

There are several aspects of the photopolymerization-induced release of contents from phosphatidylcholine vesicles which have not been fully addressed. Indeed, the mechanism of membrane destabilization has not been resolved. It is uncertain if the release of vesicle contents is due to bilayer curvature (asymmetric polymerization) or to the formation of a "polymeric surfactant" at the membrane interface. Measurement of the permeability of polymerized giant, single-walled vesicles in conjunction with micropipette techniques would certainly reveal if the "bilayer curvature" hypothesis is correct, as DOPE PEG 360 MA is expected to be distributed equally between the inner and outer monolayers of the bilayer. Specifically, one could pressurize a giant vesicle by micropipette aspiration, and then measure the change in the membrane projection length in the pipette to ascertain if the membrane becomes permeable during photopolymerization. The length of the membrane projection is sensitive to changes either in the membrane area, or in vesicle volume or both.[36] If, for example, the

projection length increases or if the vesicle flows continuously into the pipette due to the loss of vesicle volume, then clearly the photoinduced destabilization of the membrane is independent of the bilayer curvature and is most likely caused by the accumulation of the polymeric surfactant at the membrane interface. Furthermore, if the vesicle is loaded with a solution that has a refractive index that is different from that of the extravesicular medium, release of the internal solution from the pressurized vesicle can be visualized.[37] Also, if polymerization does not change membrane permeabilization (constant volume), then change in the projection length will reflect the area changes caused by the photopolymerization of DOPE PEG 360 MA.

We have not yet considered, in a systematic way, how the composition and mechanical properties of the fluid bilayer influence the photopolymerization-induced release of solutes. Both of our proposed models would tend to be affected by membrane cohesiveness, and it would be interesting to determine if whether our strategy can be used to release the contents from vesicles with various lipid compositions.

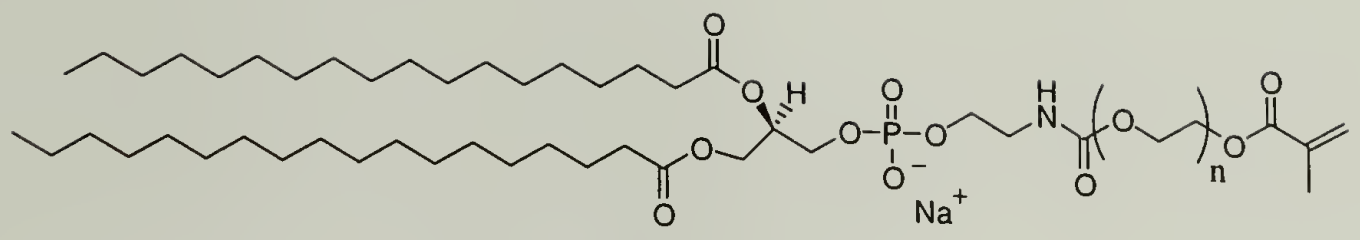


**DSPE PEG 400 MA**

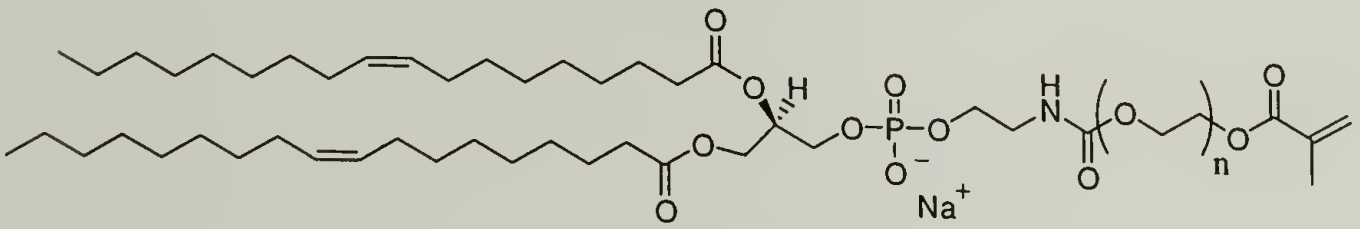


**DOPE PEG 360 MA**

Figure 3.1 The chemical structures of DSPE PEG 400 MA and DOPE PEG 360 MA where n ≈ 7 - 8 for both lipids.

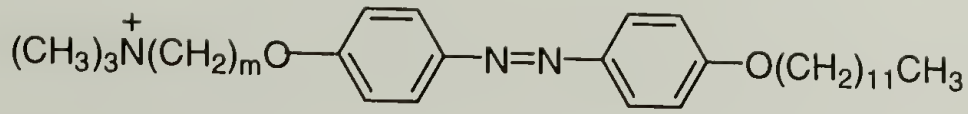


Figure 3.2 The chemical structure of the azobenzene amphiphile (m = 2 or 4) prepared by Kunitake et. al.[9]

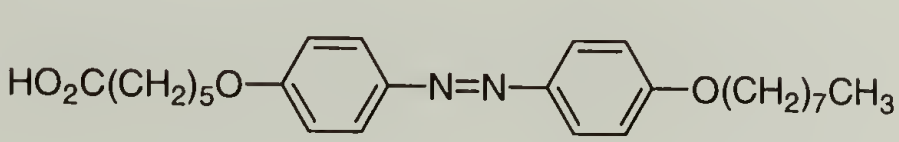


Figure 3.3 The azobenzene amphiphile 8A5 prepared by Sato and et. al.[10] used to photochemically control ion permeability in vesicle bilayers.

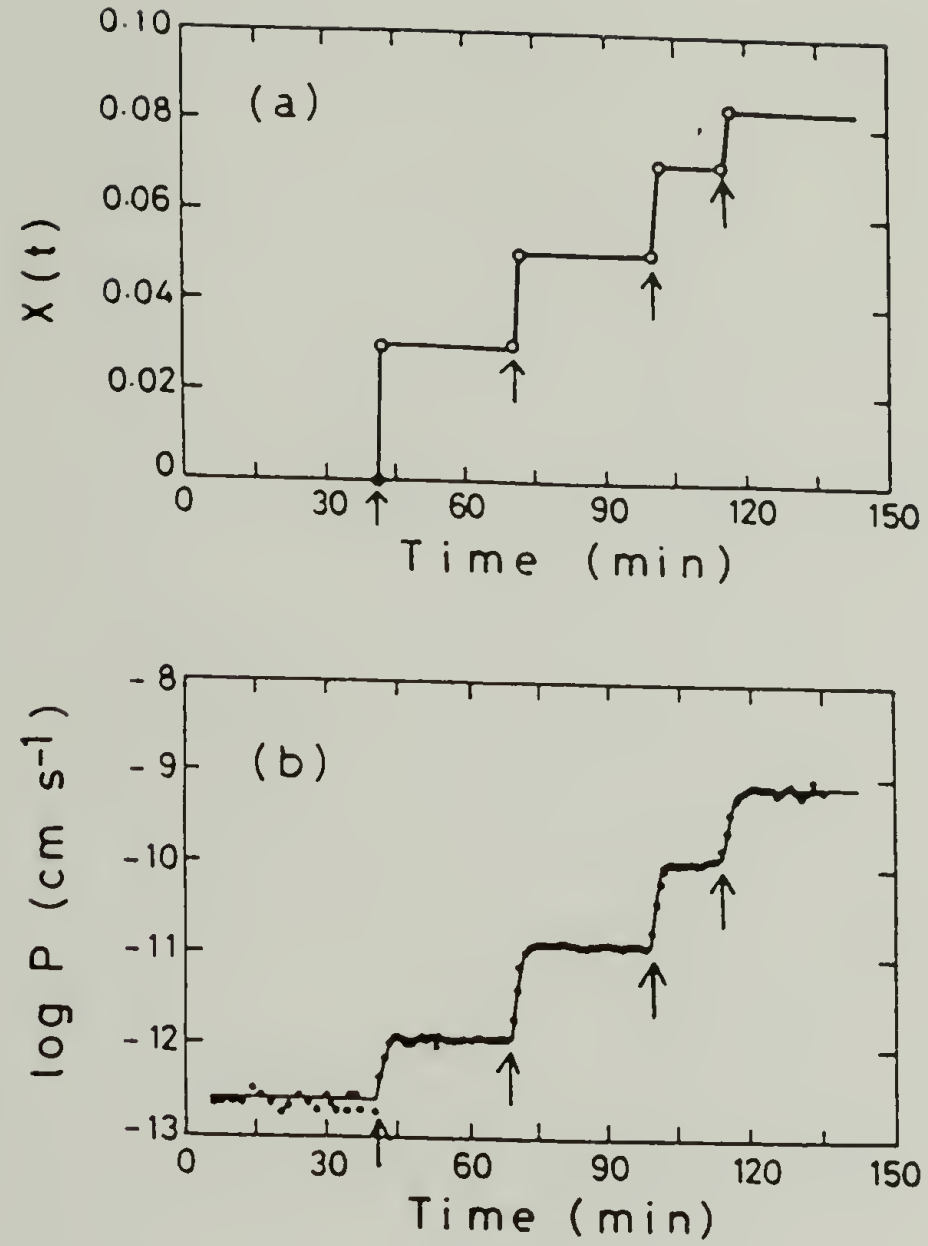


Figure 3.4 Variations of (a) X (t) ([*cis*-8A5]/[DMPC]) and (b) log (permeability coefficient, P) of the liposomal membrane with intermittent UV irradiation ($\lambda$ = 365 nm, Hg lamp). [DMPC]:[DCP] = 10:1 liposome dispersion with [8A5]/[DMPC] = 0.10. [DMPC] = 2.0 X $10^{-3}$ M. T = 288 K. UV irradiation periods: 40-41, 70-71, 100-101, and 115-116 min. Arrows indicate onset of UV irradiation for 1 min. Liposome dispersion is in the dark between 0 and 40, 41 and 70, 71 and 100, 101 and 115 and 116 and 150 min (taken from Sato *et. al.*[9])

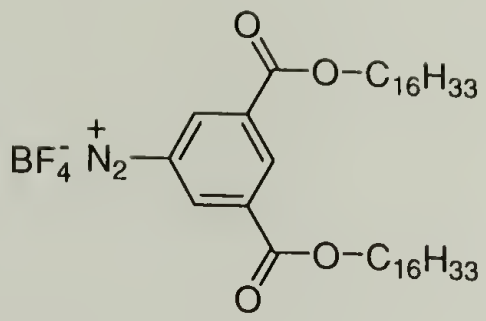


Figure 3.5 The chemical structure of the benzenediazonium amphiphile.[11,12]

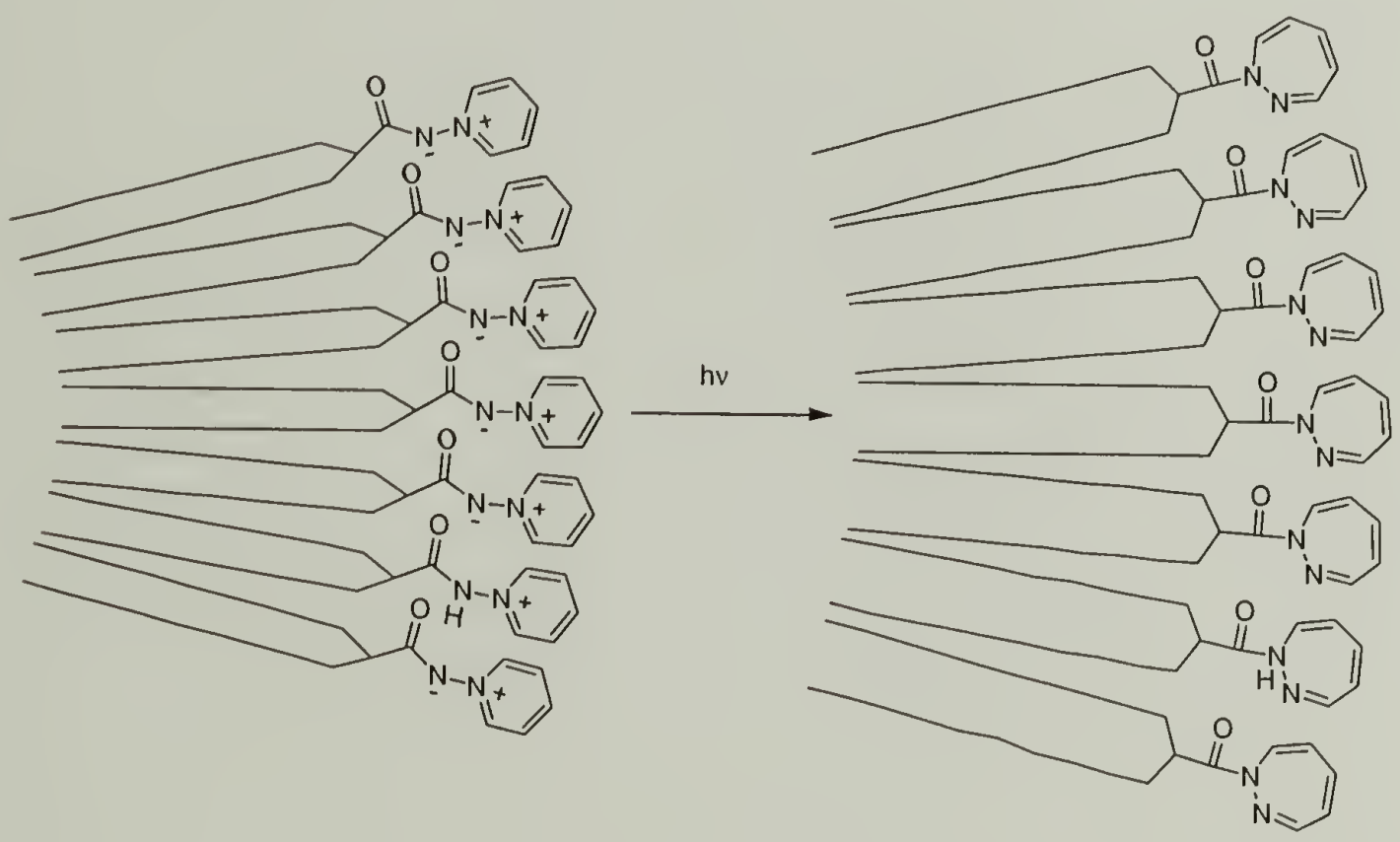


Figure 3.6 Schematic representation of one-half of a bilayer constructed from N-(1-pyridinio)-amidate amphiphiles. UV irradiation causes the ylide to rearrange to the less polar 1,2-diazepine derivative.[13]

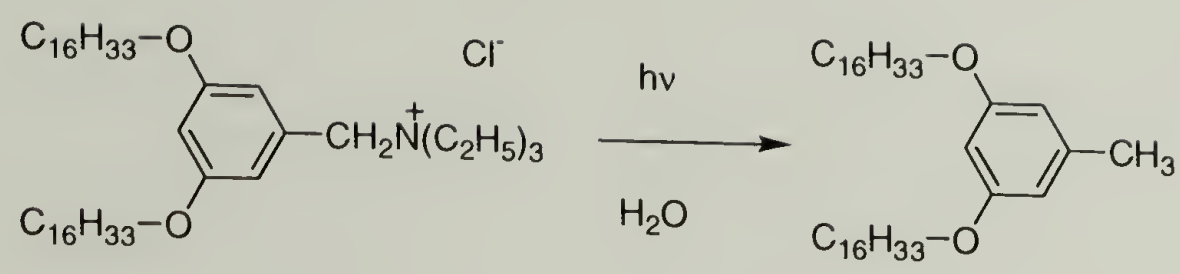


Figure 3.7 The photolysis of benzylammonium lipids.[14]

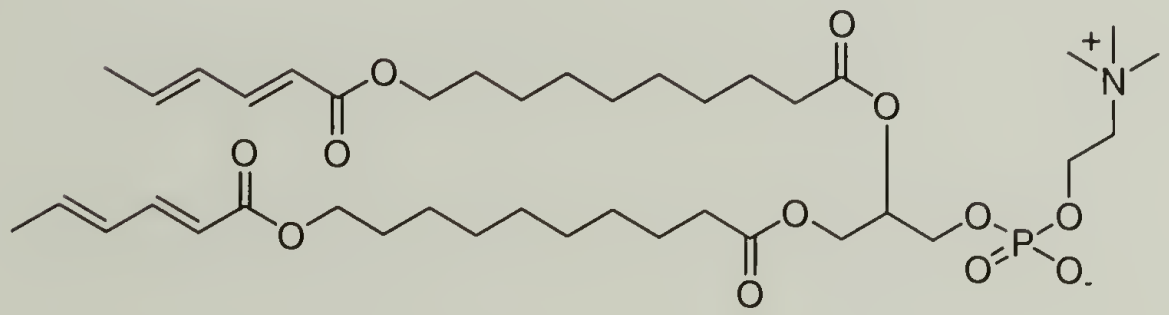


Figure 3.8 The chemical structure of SorbPC.[38]

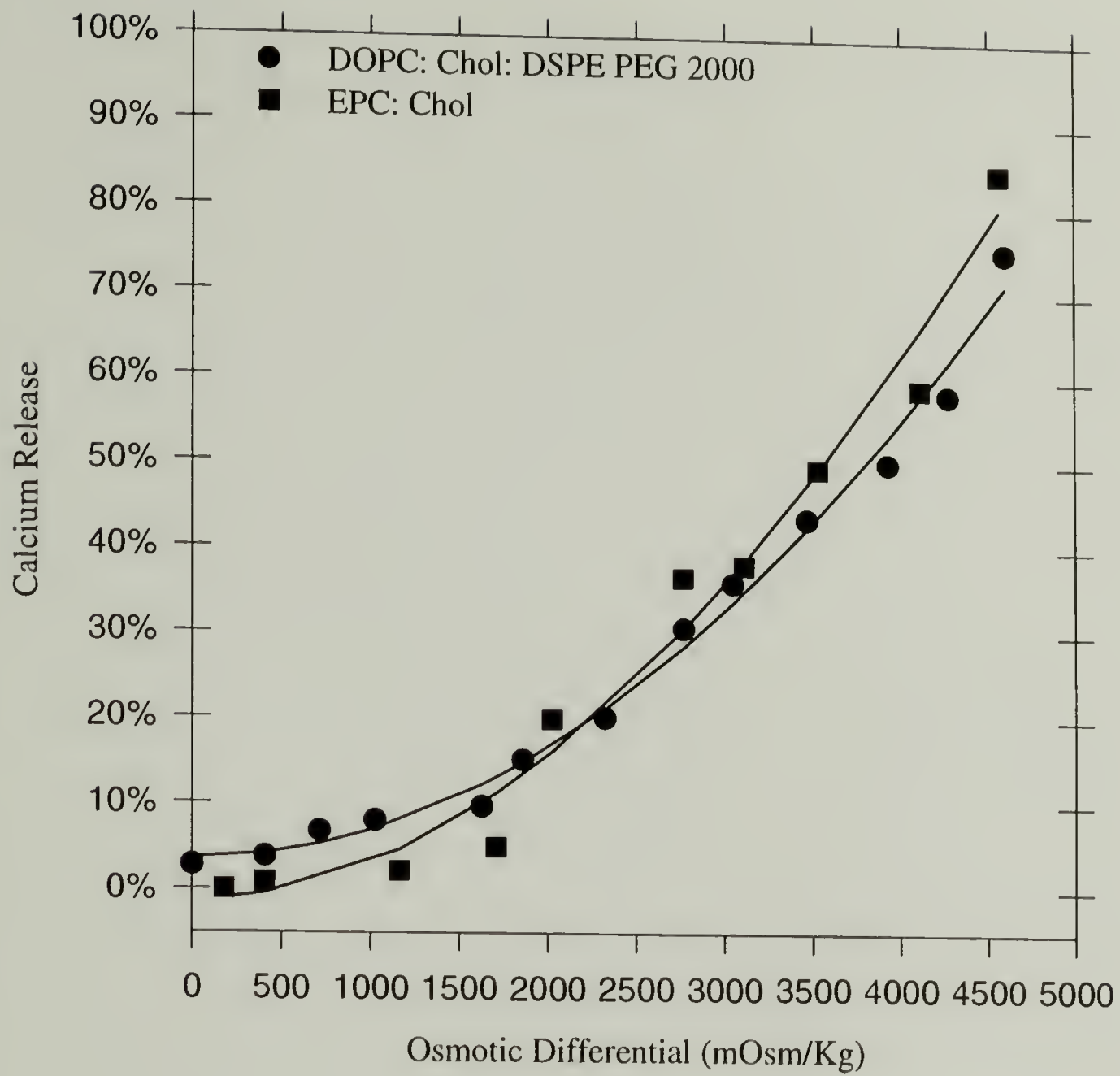


Figure 3.9 Influence of PEG on the release of $Ca^{2+}$ from osmotically stressed phospholipid vesicles. Extruded vesicles were loaded with 50 mM HEPES, 150 mM $CaCl_2$, 2.2 M NaCl, pH 7.4 and diluted into hypoosmotic NaCl buffers. (●) DOPC: cholesterol: DSPE PEG 2000 (53:45:2). (■) EPC: cholesterol (55:45).

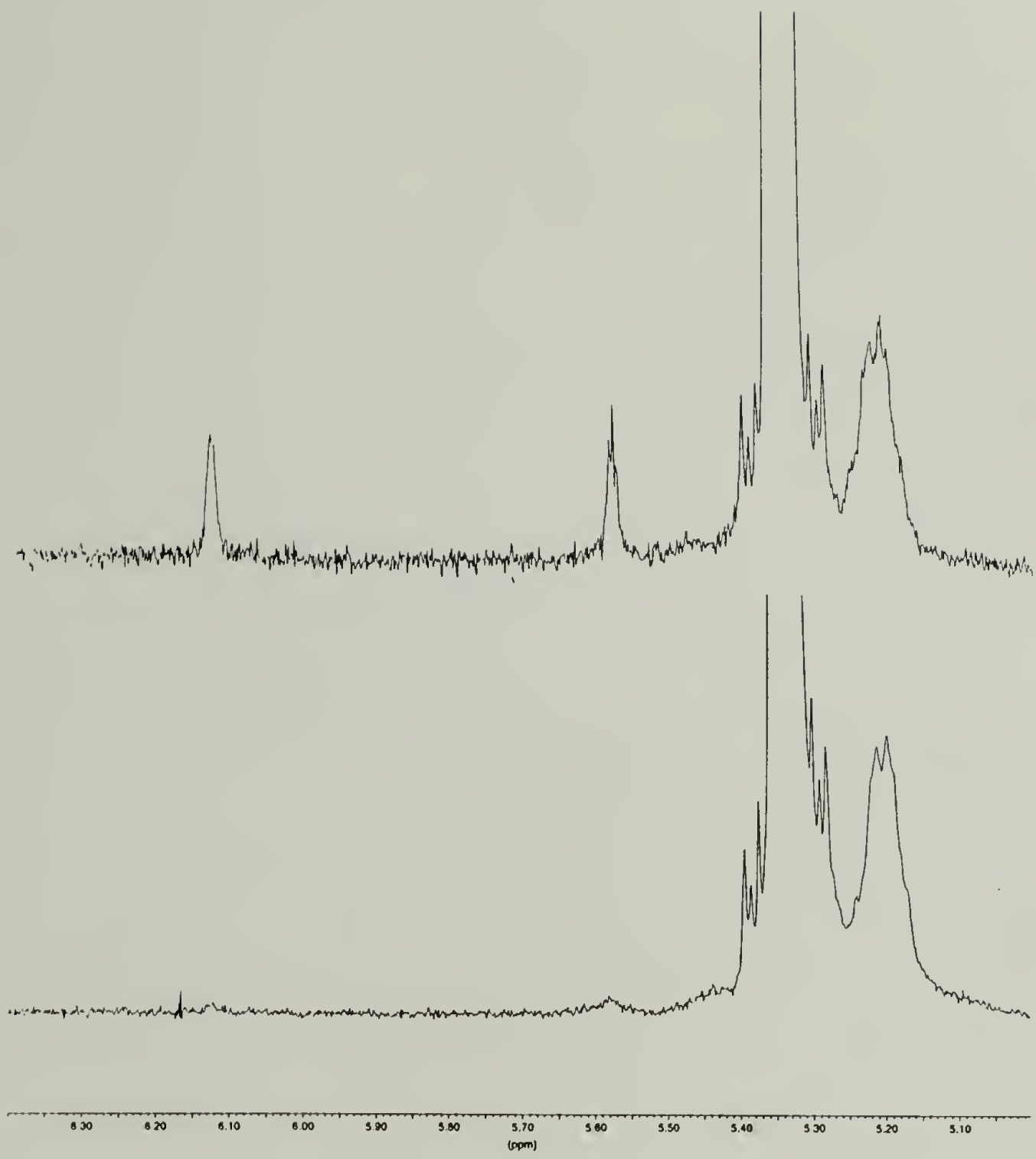


Figure 3.10 $^{1}H$ NMR spectra of non-irradiated (A) and irradiated (B) mixtures of DOPC:cholesterol:DOPE PEG 360 MA lipids in $CDCl_3$. Prior to vesicle formation, a NMR spectrum was recorded (A) of the lipids. The lipid mixture was then used to prepare 100 nm extruded vesicles (10 mg/ml) in deionized water and was irradiated for 30 minutes with a low pressure pen-ray mercury lamp. The water was removed and a second NMR spectrum was recorded in $CDCl_3$.

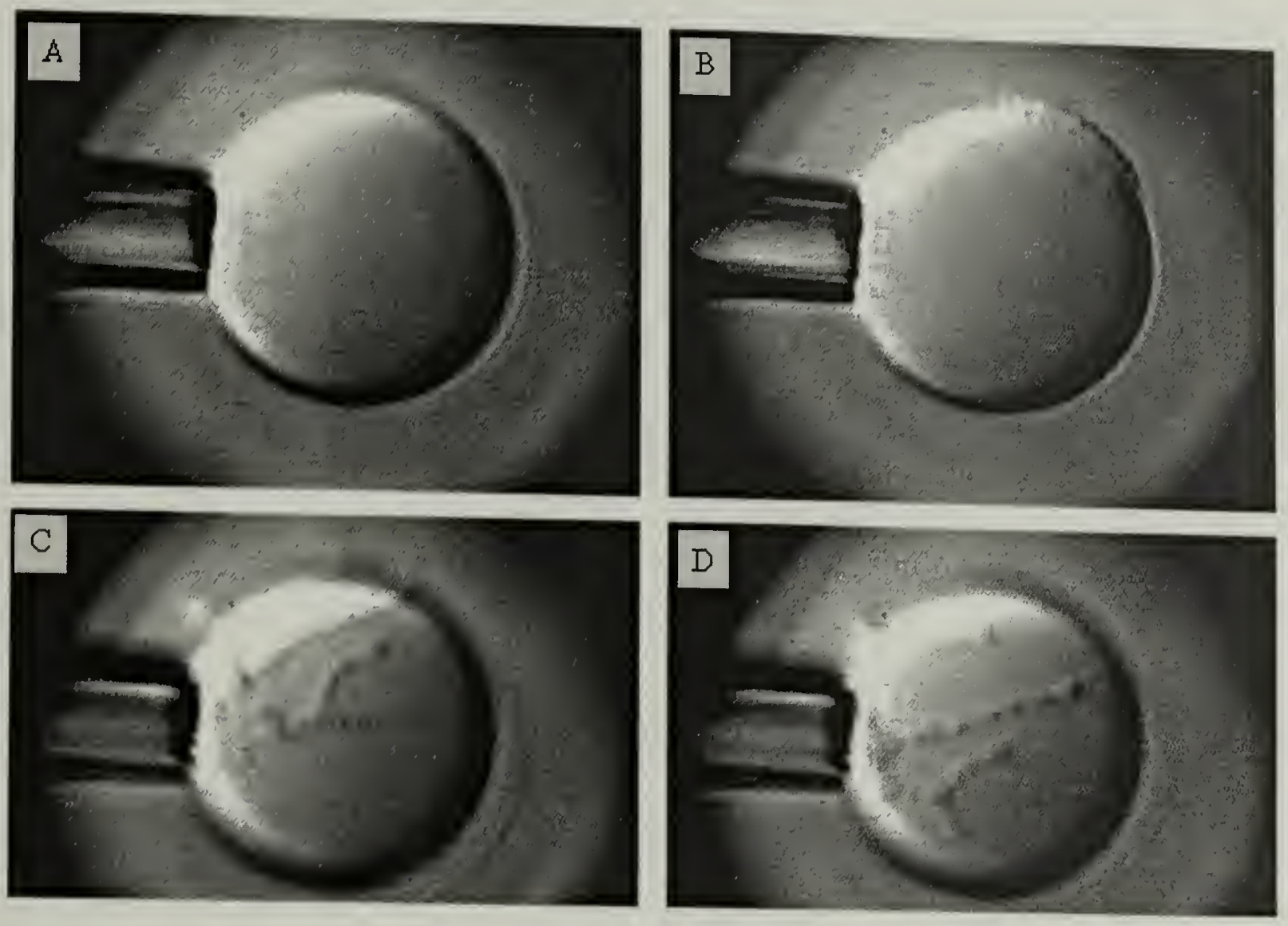


Figure 3.11 Videomicrographs of a micropipette-aspirated DSPE PEG 400/ cholesterol vesicle (diameter ~30 μm) loaded with 50 mM PEGDMA, 0.1 mM rose bengal and 100 mM TEOA. (A) Vesicle just prior to irradiation. (B) The vesicle is irradiated with the 514 nm-line of an argon ion laser. Small vesicles are ejected from the top right surface of the vesicle. (C and D) Images of the aspirated vesicle as it is polymerized. Throughout photopolymerization, small vesicles continue to pinch off from the outer lipid monolayer and slide across the surface.

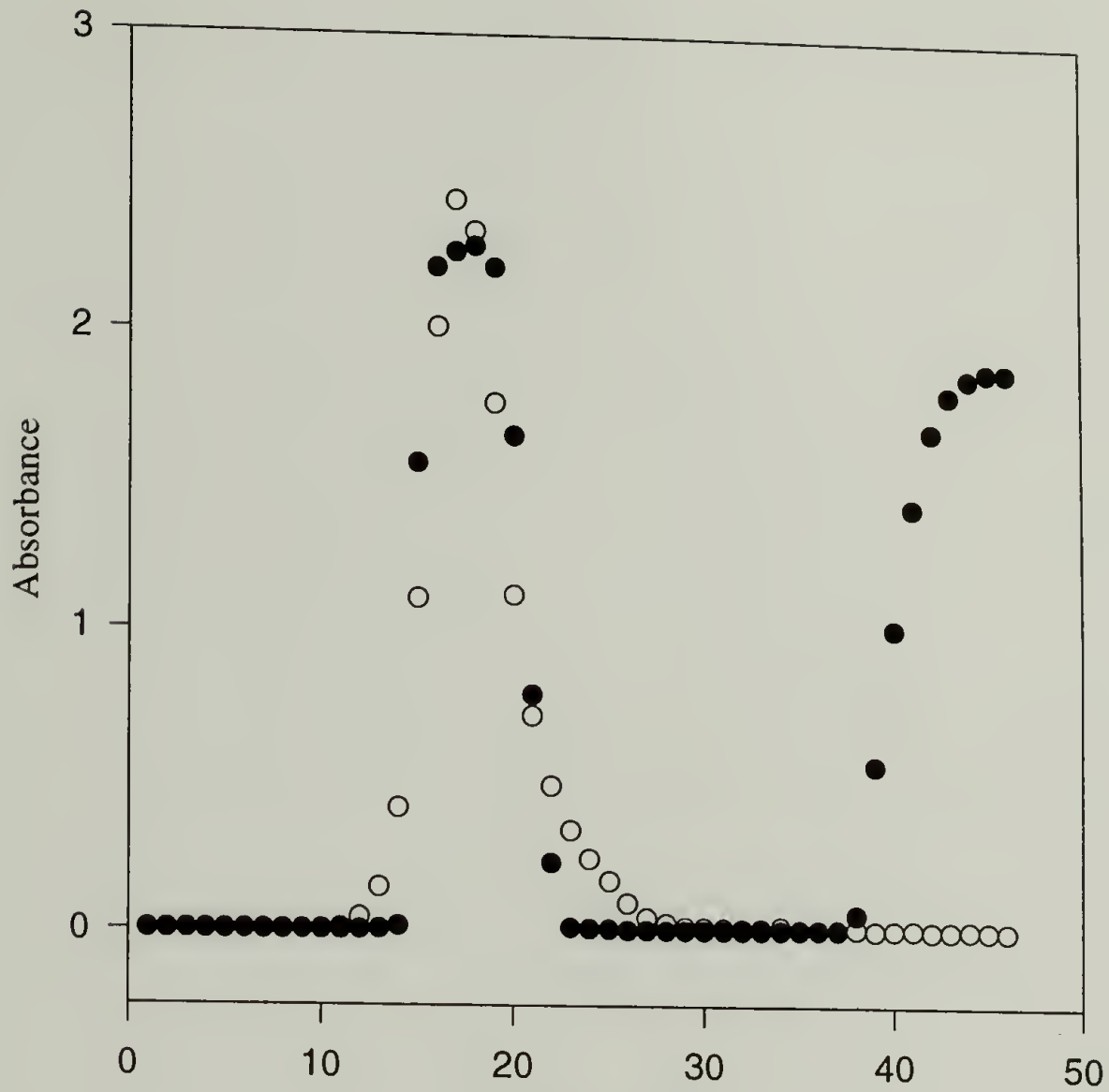


Figure 3.12 Sephadex G-75 chromatography of entrapped solute from extruded 45/45/10 DOPC/cholesterol/DOPE PEG 360 MA vesicles. Elution profiles were determined by measurements of optical density (○) at 400 nm and (●) and 300 nm to monitor elution

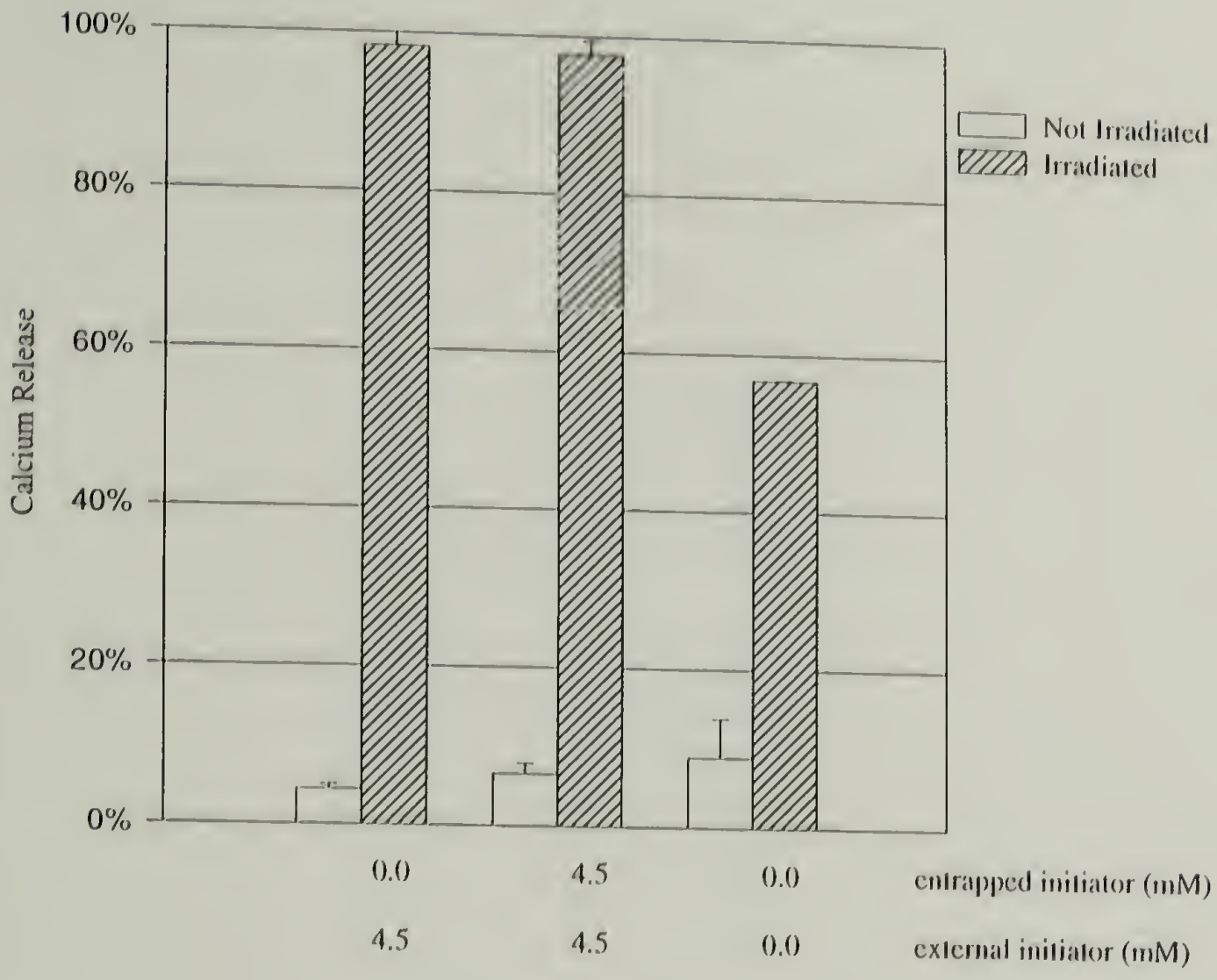


Figure 3.13 Dependence of photoinduced release on initiator. All of the vesicles were composed of DOPC/cholesterol/DOPE PEG 360 MA (45/45/10) and loaded with 150 mM $CaCl_2$, 50 mM HEPES, pH 7.4. Depending upon the experiment, Irgacure 2959 was (1) in the external buffer only, (2) equally distributed across the membrane or (3) not present. The bars represent percent release of $Ca^{2+}$ under the conditions indicated on the right. Each sample was irradiated for 30 minutes.

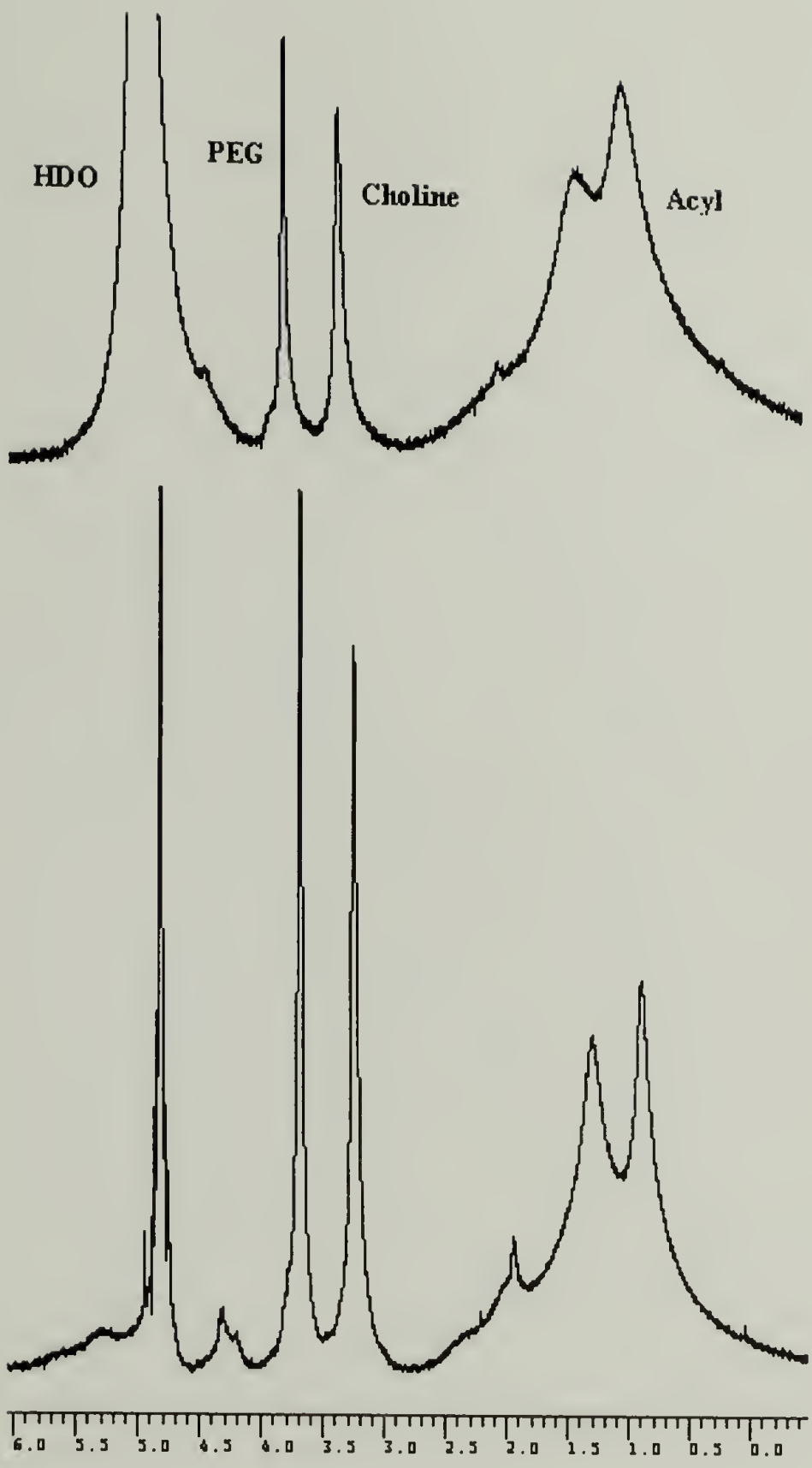


Figure 3.14 $^{1}$H NMR spectra of DOPC:cholesterol:DOPE PEG 360 MA unilamellar vesicles (Top) After and (Bottom) before the addition of $MnCl_2$.

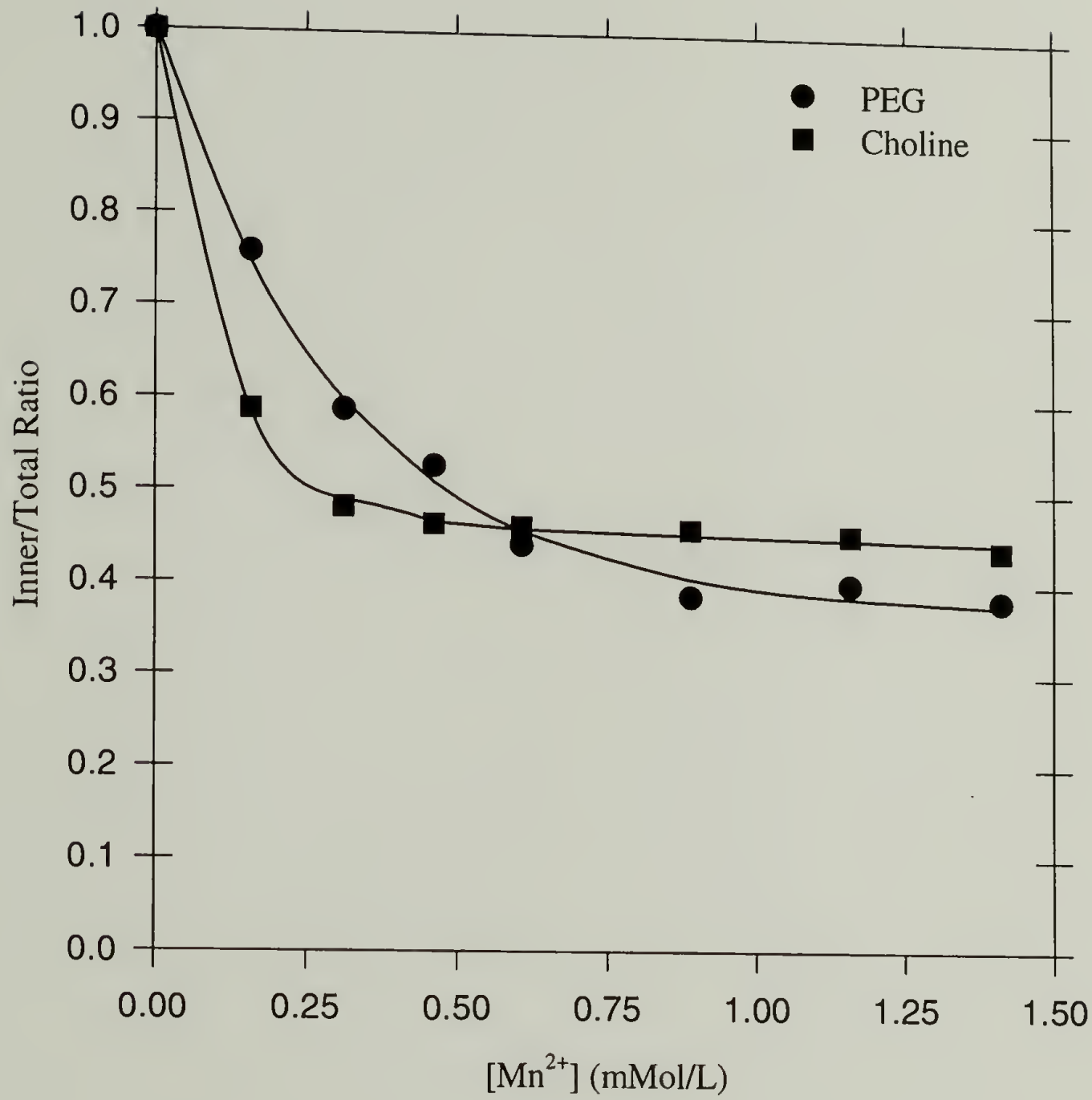


Figure 3.15 $Mn^{2+}$ titration of the ethylene oxide monomer repeats of DOPE PEG 360 MA (■) and the choline headgroup of DOPC (●) that were extruded through 100 nm pores. The average radii = 41 nm from dynamic light scattering.

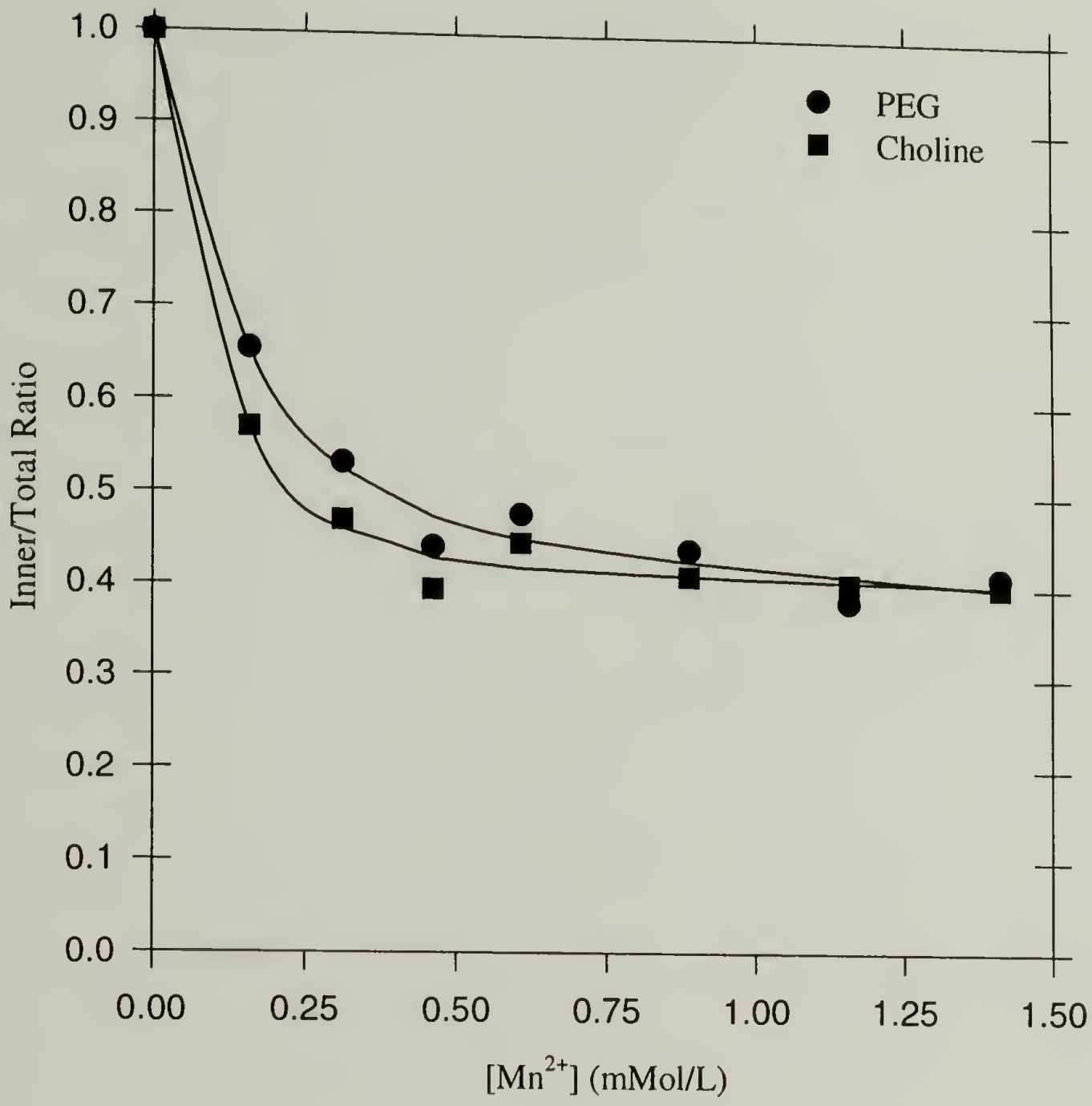


Figure 3.16 $Mn^{2+}$ titration of the ethylene oxide monomer repeats of DOPE PEG 360 MA (●) and the choline headgroup of DOPC (■) in vesicles that were extruded through 400 nm pores. The average radii = 105 nm from dynamic light scattering.

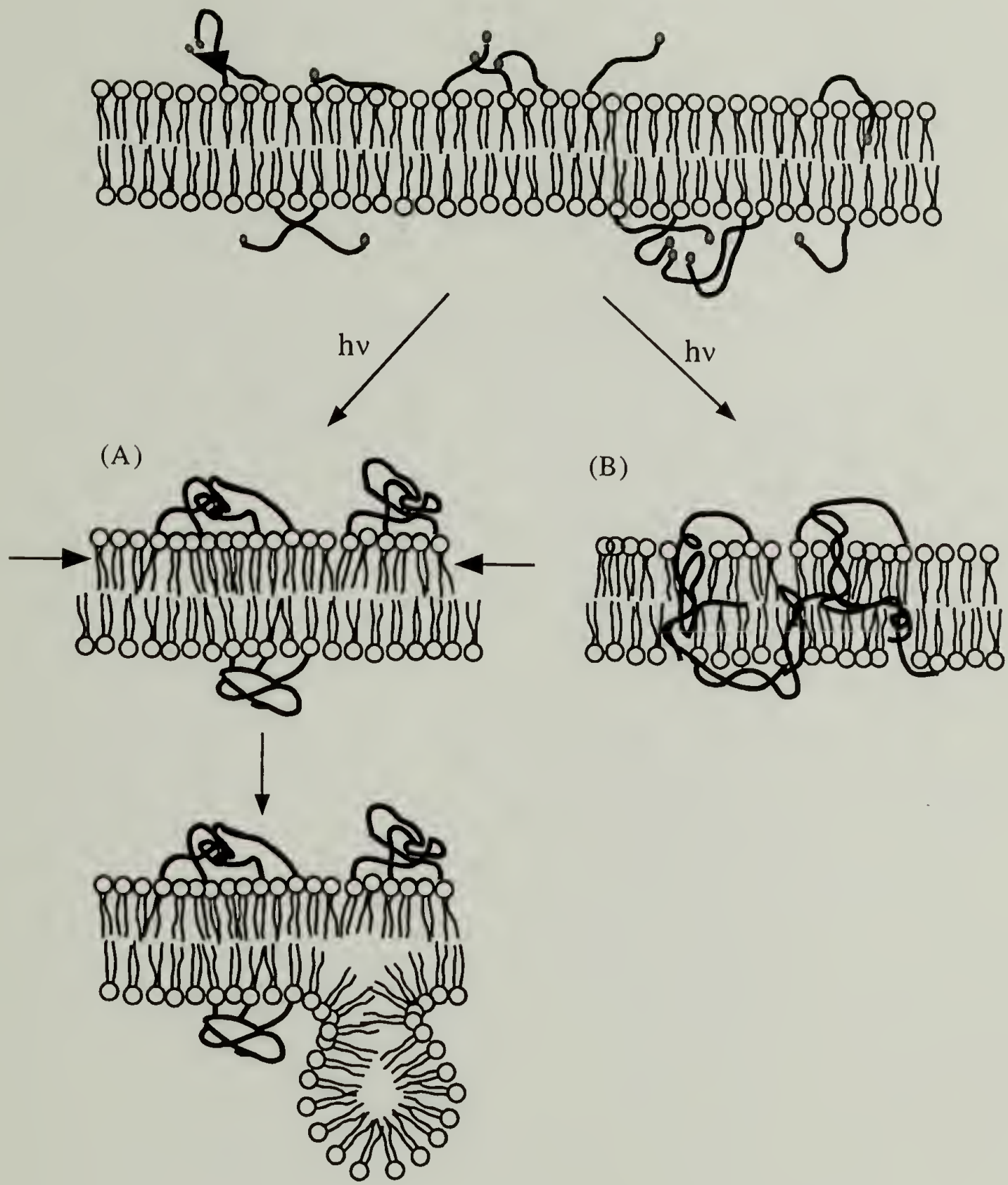


Figure 3.17 A schematic of the proposed (A) "asymmetric polymerization" and the (B) "polymeric surfactant" models for photopolymerization-induced release of vesicle contents.

Table 3.1 Summary of results of photoinduced release from mixed vesicles. All of the vesicles were passed over an osmotically balanced size exclusion column to remove non-entrapped PEGDMA (when present), Irgacure 2959 and $Ca^{2+}$ cations.

| sample no. | LIPID[a] | | | entrapped[b] monomer (mM) | percent[c, d] release |
|---|---|---|---|---|---|
| | DOPC mol % | Cholesterol mol % | DOPE PEG 360 MA mol % | | |
| 1 | 55 | 45 | 0 | 100 | 0 |
| 2 | 45 | 45 | 10 | 100 | 80 |
| 3 | 45 | 45 | 10 | 0 | 80 |

[a] The lipid was hydrated to 20 mg/ml for each experiment. [b] Concentration of entrapped poly(ethylene glycol) 1000 dimethacrylate. [c] Relative to release by addition of Triton X-100. [d] Each sample was irradiated for 30 minutes.

Table 3.2 Summary of results of contents release from different sized vesicles. The extruded vesicles were hydrated at 20 mg/ml in 50 mM HEPES, pH 7.4, 150 mM $CaCl_2$ and 4.5 mM irgacure 2959. Mean diameters and polydispersity indices were determined by dynamic light scattering at a 90 ° scattering angle using Cumulants analysis of the correlation function. The percent release of $Ca^{2+}$ is relative to the contents released upon the addition of Triton X-100.

| | Dynamic Light Scattering | | |
|---|---|---|---|
| filter pore size (nm) | Mean diameter (nm) | polydispersity index | percent release |
| 100 | 116 | 0.119 | 100 |
| 400 | 173 | 0.171 | 62 |

## References


1) Baldeschwieler, J. D.; Schmidt, P. G. "Liposomal Drugs: From Setbacks to Success," *Chem. Tech.* **1997**, 34-42.

2) Fujii, G. in *Vesicles*, Ed., Rosoff, M., Marcel Dekker, Inc.: New York, 1996, pp. 491-526.

3) Presant, C. A.; Proffitt, R. T.; Turner, A. F.; Williams, L. E.; Winson, D.; Werner, J. L.; Kennedy, P.; Weseman, C.; Gala, K.; McKenna, R. J.; Smith, J. D.; Bouzagloa, S. A.; Callahan, R. H.; Baldeschwieler, J. D.; Crossley, R. J. "Successful Imaging of Human Cancer with Indium-111-Labeled Phospholipid Vesicles, " *Cancer* **1988**, *62*, 905.

4) Lasic, D.; Martin, F., Eds. *Stealth Liposomes*, CRC Press: Boca Raton, 1995.

5) Zelphati, O.; Szoka, F. C., Jr. "Mechanism of Oligonucleotide Release from Cationic Liposomes," *Proc. Natl. Acad. Sci. USA* **1996**, *93*, 11493.

6) Nabel, G. L.; Nabel, E. G.; Yang, Z. Y.; Fox, B. A.; Plautz, G. E.; Gao, X.; Huang, L.; Shu, S.; Gordon, D.; Chang, A. E. "Direct Gene Transfer with DNA-Liposome Complexes in Melanoma: Expression, Biologic Activity, and Lack of Toxicity in Humans, " *Proc. Natl. Acad. Sci. USA* **1993**, *90*, 11307-11311.

7) Thomas, J. L.; Tirrell, D. A. "Polyelectrolyte-Sensitized Phospholipid Vesicles," *Acc. Chem. Res.* **1992**, *25*, 336-342.

8) O'Brien, D. F.; Tirrell, D. A. in *Bioorganic Photochemistry Volume 2: Biological Applications of Photochemical Switches*, Ed., Morrison, H., John Wiley & Sons, Inc.: New York, 1993, pp. 111-167.

9) Kano, K.; Tanaka, Y.; Ogawa, T.; Shimomura, M.; Kunitake, T. "Photoresponsive Artificial Membrane Permeability of Liposomal Membrane by Photoreversible Cis-Trans Isomerization of Azobenzenes," *Photochem. Photobiol.* **1981**, *34*, 323-329.

10) Sato, T.; Kijima, M.; Shiga, Y.; Yonezawa, Y. "Photochemically Controlled Ion Permeability of Liposomal Membranes Containing Amphiphilic Azobenzene," *Langmuir* **1991**, *7*, 2330-2335.

11) Fuhrhop, J. -H.; Bartsch, H.; Fritsch, D. "Colored, Unsymmetric and Light-Sensitive Vesicle Membranes," *Angew. Chem. Int. Ed. Engl.* **1981**, *20*, 804-805.

12) Fuhrhop, J.-H.; Mathieu, J. "Routes to Functional Vesicle Membranes without Proteins," *Angew. Chem. Int. Ed. Engl.* **1984**, *23*, 100-113.

13) Haubs, M.; Ringsdorf, H. "Photoreactions of N-(1-Pyridinio)amidates in Monolayers and Liposomes," *Angew. Chem. Int. Ed. Engl.* **1985**, *24*, 882-883.

14) Haubs, M.; Ringsdorf, H. "Photosensitive Monolayers, Bilayer Membranes and Polymers," *Nouv. J. Chim.* **1987**, *11*, 151-156.

15) Siegel, D. P. "Inverted Micellar Structures in Bilayer Membranes: Formation and Half-Lives," *Biophys. J.* **1984**, *45*, 399-420.

16) Ellens, H.; Bentz, J.; Szoka, F. C. "Destabilization of Phosphatidylethanolamine Liposomes at the Hexagonal Phase Transition Temperature," *Biochemistry* **1986**, *25*, 285-294.

17) Gaub, H.; Sackmann, E.; Büschl, R.; Ringsdorf, H. "Lateral Diffusion and Phase Separation in Two-Dimensional Solutions of Polymerized Butadiene Lipid in Dimyristoylphosphatidylcholine Bilayers," *Biophys. J.* **1984**, *45*, 725-731.

18) Frankel, D. A.; Lamparski, H.; Liman, U.; O'Brien, D. F. "Photoinduced Destabilization of Bilayer Vesicles," *J. Am. Chem. Soc.* **1989**, *111*.

19) Lamparski, H.; Liman, U.; Barry, J. A.; Frankel, D. A.; Ramaswami, V.; Brown, M. F.; O'Brien, D. F. "Photoinduced Destabilization of Liposomes," *Biochemistry* **1992**, *31*, 685-694.

20) Elbert, R.; Laschewsky, A.; Ringsdorf, H. "Hydrophilic Spacer Groups in Polymerizable Lipids: Formation of Biomembrane Models from Bulk Polymerized Lipids," *J. Am. Chem. Soc.* **1985**, *107*, 4134-4141.

21) Hope M. J.; Bally, M. B.; Webb, G.; Cullis, P. R. "Production of Large Unilamellar Vesicles by a Rapid Extrusion Procedure Characterization of Size Distribution, Trapped Volume and Ability to Maintain a Membrane Potential," *Biochim. Biophys. Acta* **1985**, *812*, 55-65.

22) You, H.; Tirrell, D. A. "Photoinduced, Polyelectrolyte-Driven Release of Contents of Phosphatidylcholine Bilayer Vesicles," *J. Am. Chem. Soc.* **1991**, *113*, 4022-4023.

23) Grynkiewicz, G.; Poenie, M.; Tsien, R. "A New Generation of Calcium Indicators with Greatly Improved Fluorescence Properties," *J. Biol. Chem.* **1985**, *260*, 3440-3450.

24) Odian, G. *Principles of Polymerization*, John Wiley & Sons, Inc.: New York, 1991.

25) Bystrov, V. F.; Dubrovina, N. I.; Barsukov, L. I.; Bergelson, L. D. "NMR Differentiation of the Internal and External Phospholipid Membrane Surfaces Using Paramagnetic $Mn^{2+}$ and $Eu^{3+}$ Ions," *Chem. Phys. Lipids* **1971**, *6*, 343-350.

26) de Kruijff, B.; Cullis, P. R.; Radda, G. K. "Outside-Inside Distributions and Sizes of Mixed Phosphatidylcholine-Cholesterol Vesicles," *Biochim. Biophys. Acta.* **1976**, *436*, 729-740.

27) Levine, Y. K.; Lee, A. G.; Birdsall, N. J. M.; Metcalfe, J. C.; Robinson, J. D. "The Interactions of Paramagnetic Ions and Spin Labels with Lecithin Bilayers," *Biochim. Biophys. Acta.* **1973**, *291*, 592-607.

28) Massenburg, D.; Lentz, B. R. "Poly(ethylene glycol)-Induced Fusion and Rupture of Dipalmitoylphosphatidylcholine Large, Unilamellar Extruded Vesicles," *Biochemistry* **1993**, *32*, 9172-9180.

29) Mayer, L. D.; Hope, M. J.; Cullis, P. R. "Vesicles of Variable Sizes Produced by a Rapid Extrusion Procedure," *Biochim. Biophys. Acta* **1986**, *858*, 161-168.

30) Regen, S. L.; Singh, A.; Oehme, G.; Singh, M. "Polymerized Phosphatidylcholine Vesicles. Synthesis and Characterization," *J. Am. Chem. Soc.* **1982**, *104*, 791-795.

31) Dorn, K.; Klingbiel, R. T.; Specht, D. P.; Tyminski, P. N.; Ringsdorf, H.; Obrien, D. F. "Permeability Characteristics of Polymeric Bilayer Membranes from Methacryloyl and Butadiene lipids," *J. Am. Chem. Soc.* **1984**, *106*, 1627-1633.

32) Schubert, R.; Beyer, K.; Wolburg, H.; Schmidt, K.-H. "Structural Changes in Membranes of Large Unilamellar Vesicles after Binding of Sodium Cholate," *Biochemistry* **1986**, *25*, 5263-5269.

33) Edwards, K.; Almgren, M.; Bellare, J.; Brown, W. "Effects of Triton X-100 on Sonicated Lecithin Vesicles," *Langmuir* **1989**, *5*, 473-478.

34) Nagawa, Y.; Regen, S. L. "Surfactant-Induced Release from Phosphatidylcholine Vesicles. Regulation of Rupture and Leakage Pathways by Membrane Packing," *J. Am. Chem. Soc.* **1992**, *114*, 1668-1672.

35) Liu, Y.; Regen, S. L. "Control over Vesicle Rupture and Leakage by Membrane Packing and by the Aggregation State of an Attacking Surfactant," *J. Am. Chem Soc.* **1993**, *115*, 708-713.

36) Needham, D.; Zhelev, D. V. in *Vesicles*, Ed., Rosoff, M., Marcel Dekker, Inc.: New York, 1996, pp. 373-444.

37) Zhelev, D. V.; Needham, D. "Tension-Stabilized Pores in Giant Vesicles: Determination of Pore Size and Pore Line Tension," *Biochim. Biophys. Acta* **1993**, *1147*, 89-104.

38) Hoffman, R.; Gross, L. "Modulation Contrast Microscope," *Applied Optics* **1975**, *14*, 1169-1176.

# APPENDIX A

# THE MICROMANIPULATION SYSTEM

## Introduction

The various hardware components and the microtranslation techniques implemented to manipulate single micro- and nanosized structures are described in this chapter. Much of the instrumental design and many of the experimental methods used in the nanotube project were derived from personal communications with Professor Evan Evans and Mr. Andrew Leung of the University of British Columbia. The purpose of this chapter is to describe in detail the optical components of the microscope and their function in the fabrication of nanometer-scale biomembrane templates. The chapter is divided into two sections; the first describes the microscope, and the second section describes the experimental methods used to control the movement of vesicles over distances in the submicrometer range. Some of this material has been covered in chapter 1 and is included here for the sake of convenience and completeness.

## Imaging System

In this section, the major optical components of the micromanipulation instrument in Figure A.1 are described, beginning with a brief description of the microscope and the various means used to collect and store images. The remaining portions will include a detailed description of the multi-port mercury arc lamp and the procedures used to align the brightfield and episcopic illumination pathways.

Image Collection. The optical instrument designed to isolate and manipulate micron sized vesicles is built around a Zeiss inverted Axiovert 100 H microscope. An inverted microscope is ideal because of its capacity to accommodate up to four pipette micromanipulators mounted directly on the stage. A Zeiss LD-acroplan 20X/0.4 objective modified for Hoffman modulation contrast (HMC), followed by 16X binocular eyepieces were used to observe magnified images of biomembrane templates and vesicles.

The HMC microscope produces images that appear three-dimensional, wherein a rounded vesicle appears dark on one side, bright on the other, with gray in between against a gray background. An otherwise transparent vesicle, with a refractive index gradient across the bilayer membrane, can be viewed with high contrast. Modulation contrast optics is sensitive to the direction of refractive index gradients, where images are optically shadowed in the direction of maximum gradient detection.[1]

Images of vesicles and tethers are captured by either one of the two Dage-72 CCD cameras that are mounted to the Zeiss binocular photo-TV tube (45DG/20-2 ports), and displayed on a Sony 12" video monitor and/or a computer monitor. The microscope is equipped with a binocular phototube with two ports; one port leads to a Dage CCD-72 camera for routine imaging at normal light levels, and the second port is fitted with a Geniisys image intensifier coupled with a Dage CCD-72S which is used to collect low light level images (Figure A.2). Each solid state camera has 768 X 493 active pixels, an 8.8 mm X 6.6 mm pick-up area with gain that is manually regulated by a separate remote controller connected to both camera heads. Both the intensified and the regular CCDs are

mounted to the phototube via a relay lens system (Zeiss 4X TV-tube video coupler). This setup has been designed to produce magnified images of vesicles with diameters in the range from 20-30 μm to fill most of the monitor screen, resulting in good optical resolution. Images are recorded on a Panasonic S-VHS videocassette recorder or captured digitally using an Imagraph frame grabber.

Arc Lamp. A 100 W high pressure mercury arc lamp serves as the multipurpose light source for fluorescence and brightfield illumination. It also provides the high intensity UV radiation that is necessary for initiating the free radical photopolymerizations. The high-pressure mercury arc lamp provides intense visible and UV lines (240 to 600 nm) which makes it a good light source for UV photoinitiation (e.g., Irgacure 2959 at a concentration of 1 mg/mL exhibits maximum absorption at 300 nm). The intense visible lines can be used for the excitation of fluorophores such as lissamine rhodamine B lipids excitable around 550 nm.

The mercury lamp is housed in an Oriel series Q lamp housing that is equipped with four output ports. This permits the simultaneous illumination of the brightfield and episcopic pathways as well as the sample chamber via a quartz fiber optic setup. The current mercury arc lamp is an Oriel 6281 rated at 100 W of power with an arc size of 0.25 mm X 0.25 mm. It has an expected lifetime of 200 hours at the proper current and voltage settings and is powered by an Oriel 68806 power supply with a built-in ignitor. For a typical experiment the lamp is ignited first, before switching on power to any of the other components in the micromanipulation system. This prevents damage to the other electrical circuitry during arc ignition.

Transmitted-Light Illumination. The transmitted-light pathway is illuminated by a collimated beam delivered from a 600 micron core diameter UV grade silica fiber optic (Oriel 77512). Light is collimated by a two element F/1 UV grade fused silica Oriel 60076 condenser mounted on the lamp housing and then refocused onto the fiber bundle by an F/2 focusing assembly that is coupled to the source condenser (Figure A.3). In addition to the lenses, the source condenser also houses an Oriel 59472 400 nm band pass filter and an Oriel 59060 IR blocking filter (both are 2" in diameter). Divergent light that exits from the opposite end of the fiber bundle is collimated by a single element beam probe (Oriel Corp. 77644) and properly aligned to illuminate the transmitted light carrier system.

**It is important to periodically confirm that the absorption filters housed in the lamp condensers adequately block all of the UV and IR radiation.** The UV radiation emitted by the arc lamp damages exposed skin and tissues in the eye. The microscope contains optics, e.g. condensers, objectives etc., which will degrade when exposed to constant UV and heat. The type of filters in use are typically stable and long-lived under normal conditions, but can be affected by extreme environments such as high temperature and intense UV radiation (solarization). A more efficient and possibly safer method to block UV and IR radiation is to replace the absorption filters with narrow-band interference filters. For extra safety, additional filters can be placed in the two swing-out filter holders positioned above the condenser carrier.

The following procedure is used to align the Hoffman modified contrast (HMC) microscope and arc lamp for Köhler illumination. First, remove the diffuser from the top

of the carrier for transmitted-light illuminator. Bring the microscope condenser to its proper working distance by adjusting the condenser carrier such that the condenser is 45 mm above the sample. Collimate the beam from the fiber optic assembly by adjusting the arc-lamp condenser. Next, by eye, center the beam on a sheet of paper placed at the sample stage by translating the fiber optic assembly to center the beam on the microscope mirror. Then remove the sheet and adjust the microscope condenser using the two centering screws to yield a bright, evenly illuminated field. Next, place a specimen on the microscope stage and focus sharply with the 20X objective. Remove the specimen to clear the area under observation.

Remove one of the oculars, and insert the Zeiss auxillary telescope (Model 444830) in its place and bring into focus the Hoffman modulator at the rear focal plane of the objective, see Figure A.4. Next, while focused at the modulator plane, position the special slit aperture such that the polarizer $P_2$ is aligned parallel to the gray region of the modulator, i.e., the portion of the slit covered by $P_2$ is positioned in the bright region of the modulator. Insert the second polarizer $P_1$ in the holder directly above the condenser and aperture. Use $P_1$ to adjust the contrast and spatial coherence of the image.[2]

Epiillumination. The current lamp arrangement has the episcopic port illuminated directly by the arc and its reflected image generated by an $AlMgF_2$ coated rear-reflector mirror positioned behind the arc source in the lamp housing. Light is collimated by a two-element F/1 UV grade fused silica Oriel 60076 condenser. Like the condenser used for the transmitted pathway, this condenser also contains two colored glass filters. An

Oriel 59472 400 nm long pass colored filter blocks dangerous UV, and the Oriel 59044 20 % IR blocking glass filter absorbs IR radiation.

The episcopic pathway is aligned once brightfield illumination is achieved. Highly fluorescent anthracene crystals are brought to focus in brightfield by sliding the reflector slider to free aperture. The transmitted light is shuttered, and the reflector slider position is selected that houses the Chroma wide blue set. Closing the luminous field diaphragm such that it becomes visible in the image allows the arc to be centered. After centering, the diaphragm is opened and measuring the fluorescence from a solution with a constant emission checks the uniformity of illumination. (Note: The microscope is equipped with two fluorescence filter sets: The TRITC set (exciter: HQ 535/50; dichroic mirror: Q 565/LP; emitter: HQ 610/75) and the wide blue set (exciter: D450/80X; dichroic mirror: 505DCXR; emitter: OG515/LP). Chroma Technology Corporation (Brattleboro, VT) manufactured both sets.)

## Micromanipulation Transfer Technique

The procedures and basic components that are necessary to manipulate and isolate single micron-sized vesicles are discussed in this section. Included are descriptions of the following components; the "transfer chamber" which is used to contain vesicle suspensions on the microscope stage, the hand-operated micromanipulators which allow submicron translation, and the micropipette puller and microforge which are necessary for the fabrication of micropipettes from borosilicate capillary tubes.

Suspension and Transfer Chambers

The photopolymerization of vesicles requires that a single vesicle be transferred from an aqueous suspension across an air interface into a chamber filled with monomer-free buffer. Micromanipulation of giant phospholipid vesicles at room temperature is carried out in a double microchamber that is fabricated from two thin stainless steel supports fastened by an aluminum bar. The microchamber consists of two chambers filled with two distinct aqueous solutions separated by an air gap (Figure A.5). The first chamber is referred to as the "suspension chamber", and is filled with a dilute suspension of the polymerizable vesicles. It is constructed from two 5 X 30 mm glass coverslips that are fixed to the top and bottom of the steel supports by a thin film of vacuum grease. The second chamber, the "transfer chamber", is the site for in situ photopolymerizations. It is constructed from a glass coverslip fixed to the lower support, and a 5 X 22 mm quartz slide (cut from a 1 mm thick, 22 X 50 mm quartz slide, catalog # 26010, Ted Pella Inc. Redding, CA) fixed to the top support to allow UV radiation to penetrate into the solution. The transfer chamber contains a buffer, which has a low concentration of photoinitiator and is monomer free.

Micropipette Fabrication

Micropipettes that are used to aspirate vesicles are prepared in four steps; (1) pulling the pipette from a capillary tube, (2) breaking the tip of the pipette, (3) heat polishing, and (4) backfilling the glass pipette with the appropriate solution.

Large micropipette tips of diameter 5-10 μm are pulled from Kimble borosilicate capillary tubes that have 0.7 - 1 mm outer diameters. The Narishige PC-10 vertical

pipette puller employed in a one-step pull mode is used to form large micropipettes with reproducible tip size and shape. The puller can also be used in a two-step mode to prepare pipettes with different shapes and smaller diameters. When pulling a capillary, the goal is to produce pipettes with a relatively long taper and a sealed end with a diameter in the 1 to 3 μm range. First, a capillary is centered in the platinum loop heating coil where a voltage is applied across the heating coil and the capillary separates, forming two separate pipettes. In generating a micropipette, the following parameters are used; tension is provided by all of the weights provided with the puller (233 grams) and a heater level setting between 68 and 70. Pipettes with long tapers and sealed ends with the correct dimensions are produced quite rapidly using these settings.

The objective of the second step is to break open the sealed end of the tip, leaving the end as flat and smooth as possible with the required tip size. This is accomplished by using a homemade microforge which enables the pipette tip to be observed at 64X magnification. The heat source is a 24 gauge V-shaped platinum filament with a bead of low melting point glass (Schott 8465 lead borate solder glass) in the apex. The glass bead is melted by passing a low voltage AC current from a rheostat (2-3 volts) through the wire. The tip of the micropipette is then positioned into the center of the molten glass with a micromaniplator. The pipette is advanced into the bead until the required diameter extends from the glass bead; once this is achieved the current is immediately switched off. After the glass has cooled, the pipette tip is fractured by withdrawing the pipette from the glass bead. The bead is melted once more, and the pipette tip is positioned such that it just touches the surface of the molten glass. This causes a small volume of molten glass to wick into the open tip by capillary action, with the subsequent formation of a

meniscus in the pipette tip between the air/glass interface. After the glass has cooled, the tip is fractured at the meniscus by pulling the pipette away from the bead.

The final step in micropipette fabrication is fire polishing. Quite often the tips produced by the "bead" method have tip ends which are rough and can puncture vesicles. Heat polishing removes sharp irregularities from the edge of the pipette tip, thus enabling the pipette to form a good "seal" with aspirated vesicles. This is done by simply advancing the pipette tip close to the surface of the heated glass bead without touching it. The temperature and the time of heat polishing depend upon the open tip diameter, as too much heat will cause the tip to close. Fire polishing the pipette tips results in a tip with a smooth, flat end that can form an excellent seal with a vesicle.

Micropipettes used to hold vesicles are usually not filled by simply immersing the pipettes in an aqueous solution. Extreme care must be taken to completely exclude air bubbles from the pipette when filling it with a solution. Compression of the air bubbles trapped in the pipette makes it difficult to control the aspiration pressure which is necessary to hold the vesicles at a constant membrane tension. Pipettes are filled by back filling with the appropriate buffer using a filament needle (World Precision Instruments, Inc., Sarasota, FL) and a 1 mL syringe. Quite often, back filling results in a small air gap at the micro-tip end. The air gap is removed by pushing the solution out the micro-tip end by filling the opposite end of the pipette with soft plasticine. Any trapped air is displaced from the pipette by the plasticine plug. The plug is subsequently removed by breaking off the end of the pipette using a diamond scribe.

Micromanipulators and Manometer

Micromanipulation of a single vesicle requires precise control over micropipette movement in the submicrometer range. Equally important is that the pipette be held fixed in space, free of drift in the lateral and vertical directions. This is accomplished by hand operated, hydraulically controlled micromanipulators.

The MMO-202 hydraulic manipulator (Narishige Co.) allows smooth, drift free submicron manipulation of a micropipette in the X, Y and Z directions. Each hydraulic manipulator is mounted to the microscope stage via a multi-axis XYZ Narishige MMN-1 translator. This particular translator makes possible the coarse adjustment of the micropipette position. A hand operated joystick controls the fine movement of the micropipette in the lateral and vertical directions via three separate, oil-filled tubes that transmit variable pressures to pistons housed in the MMO-202 manipulator.

Individual vesicles are picked up from the bottom of the suspension chamber with a "holding" pipette by applying a small aspiration pressure which draws the vesicle into the end of the pipette. The micropipette is mounted in a water filled injection holder (Narshige) via an air-tight seal using a silicone rubber washer and a chuck. The injection holder is connected by rubber tubing to a small, movable reservoir of water, or manometer, constructed from a sealed 30 ml syringe. An aspiration pressure is created by either lowering the syringe or by acting on the air gap above the water in the closed manometer via a mouthpiece or a second syringe.

After the vesicle is drawn into the pipette, it is moved to the transfer chamber using a buffer filled "transfer" pipette. The transfer pipette serves as an aqueous "tunnel" through the air gap between the suspension and transfer chambers. Vesicles are

transferred between the two chambers by inserting the holding pipette into the much larger transfer pipette (40-60 μm i.d.) and translating the microscope stage.

Photopolymerization

Polymerizable vesicle compositions were irradiated in the transfer chamber with a focused beam from the second fiber optic assembly shown in Figure A.3. The fiber optic assembly consists of a 200 μm UV-VIS cable (Oriel Corp. 77530, Stratford, CT) that is connected to an Oriel F/1 60076 condenser via an Oriel F/2 77800 fiber optic focusing assembly. An Oriel 77646 fused silica focusing probe is used to focus the fiber optic output on the transfer chamber. The focusing probe is a two lens system consisting of a fused silica 19 mm focal length, F/1.7 lens and an Oriel 41210 UV grade F/1.7 lens. **There are no filters in the optical path, thus the focused beam from the fiber optic is essentially the output of the high pressure mercury arc lamp. Therefore, one should always use appropriate UV safety precautions when vesicle structures are polymerized.**

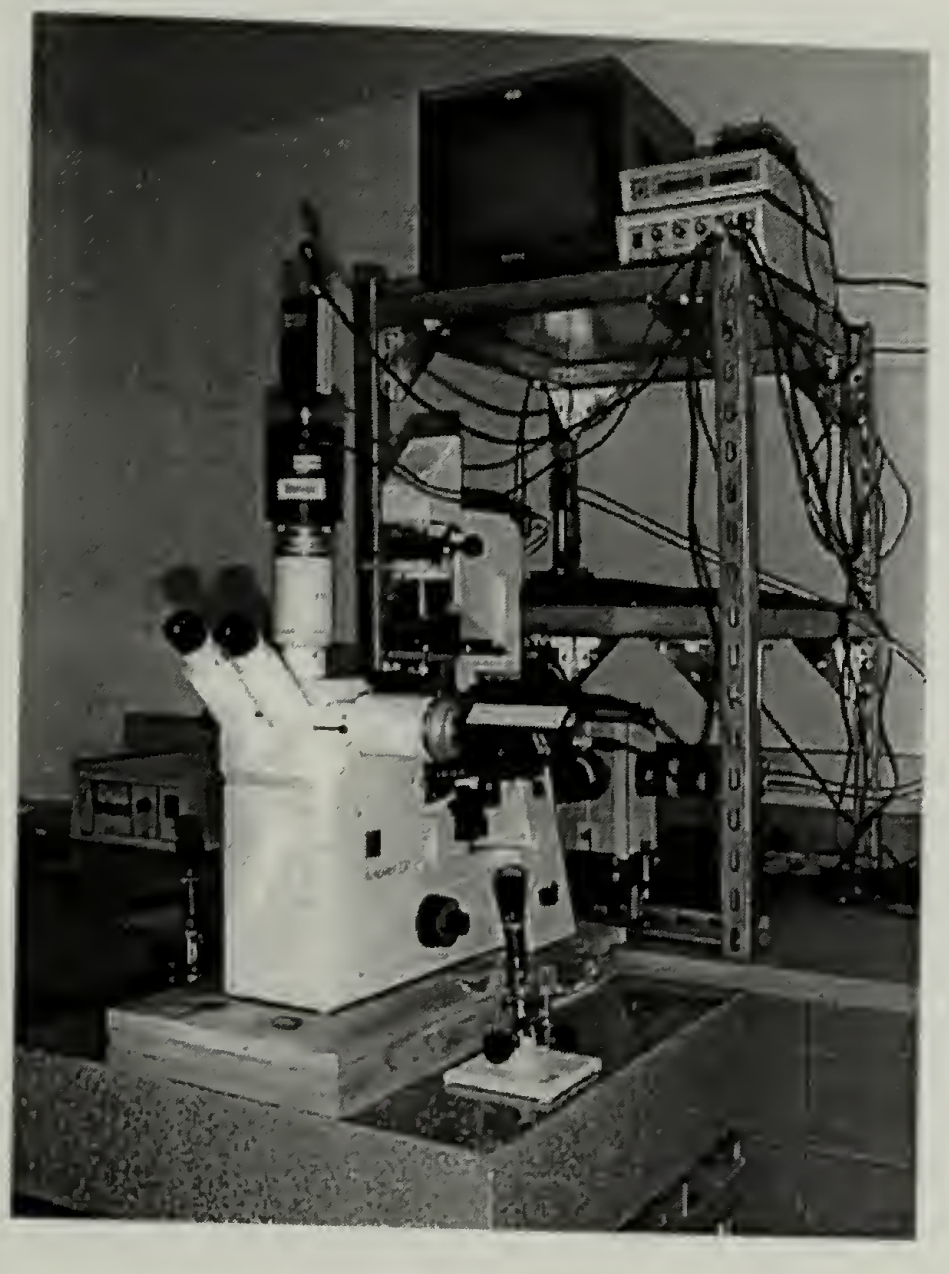

Figure A.1 The micromanipulation instrument that is built around around a Zeiss inverted microscope.

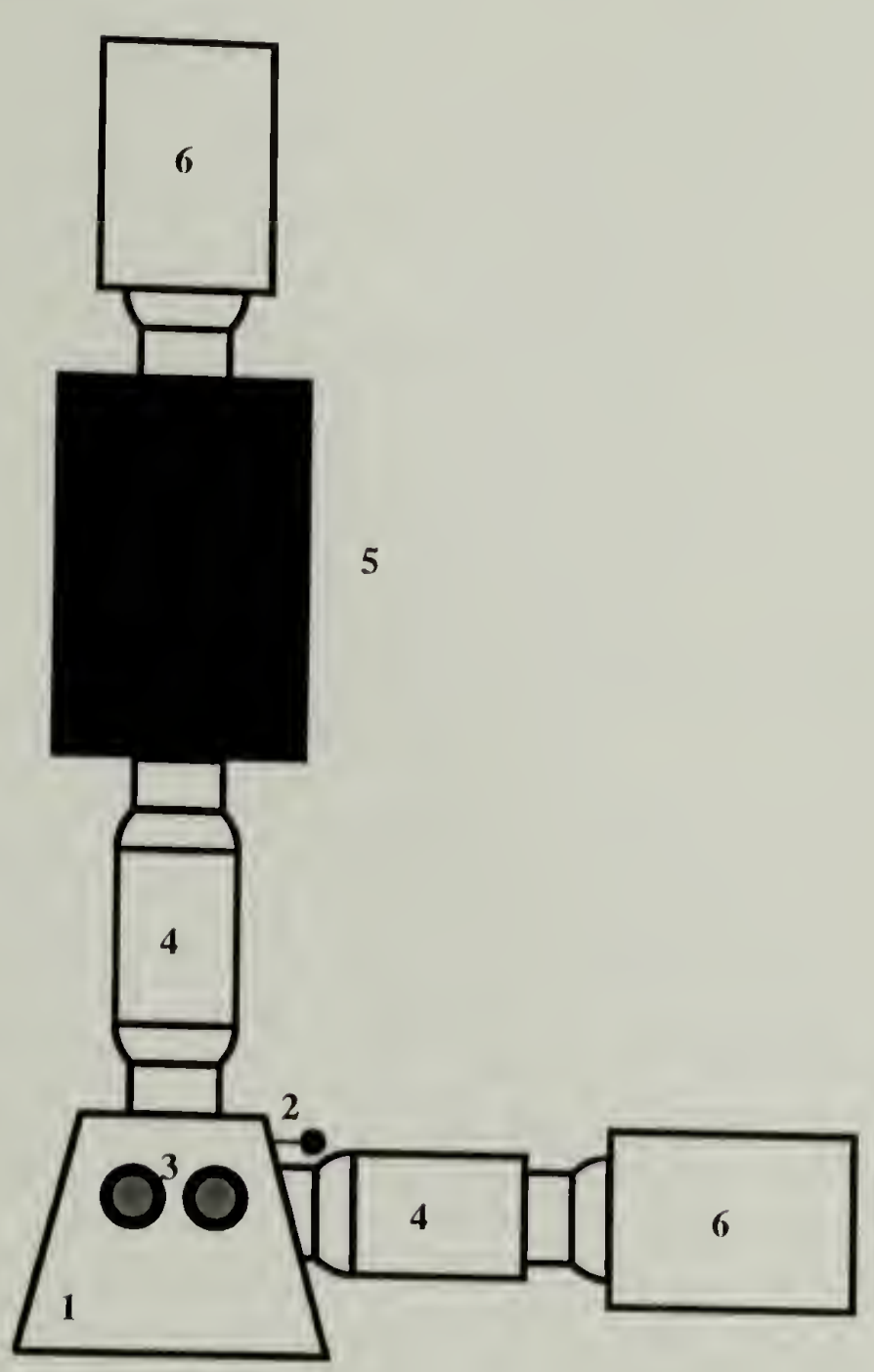


Figure A.2 A schematic diagram of the two-port binocular phototube fitted with two charge-coupled devices. Key to the numbers is as follows: 1. Binocular photo-V tube; 2. Eyepiece shutter; 3. Eyepieces; 4. 4X TV-tube; 5. Image intensifier; 6. CCD devices.

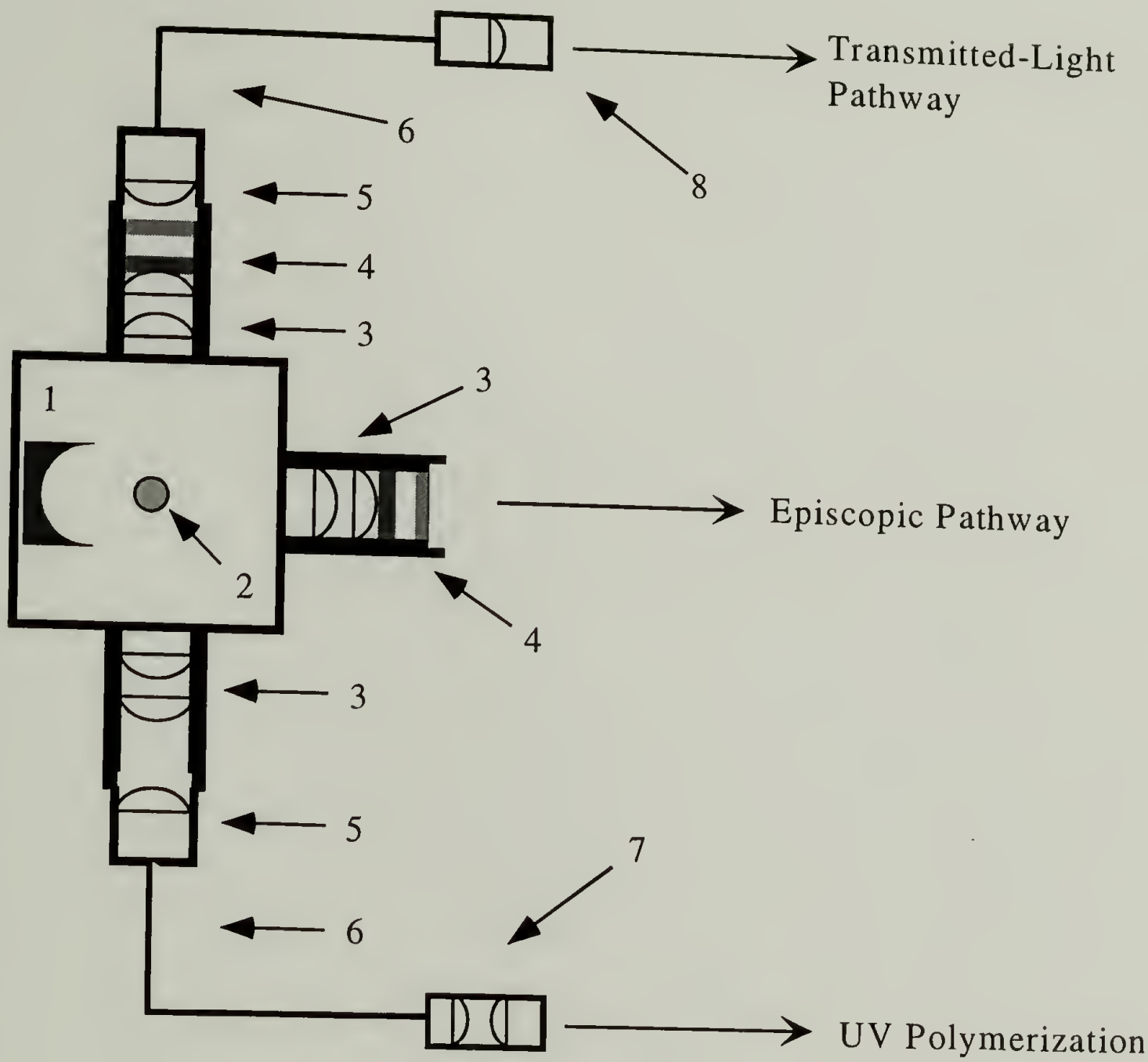


Figure A.3 A schematic diagram of the mercury-arc lamp housing fitted with UV grade condensers and fiber optics. Key to the numbers is as follows: 1. Lamp housing with rear reflector; 2. High pressure mercury-arc lamp; 3. UV grade collimating condenser; 4. UV and IR filters; 5. Fiber optic focusing assembly; 6. UV grade fiber optic cable; 7. Fiber optic focusing probe; 8. Fiber optic collimating probe.

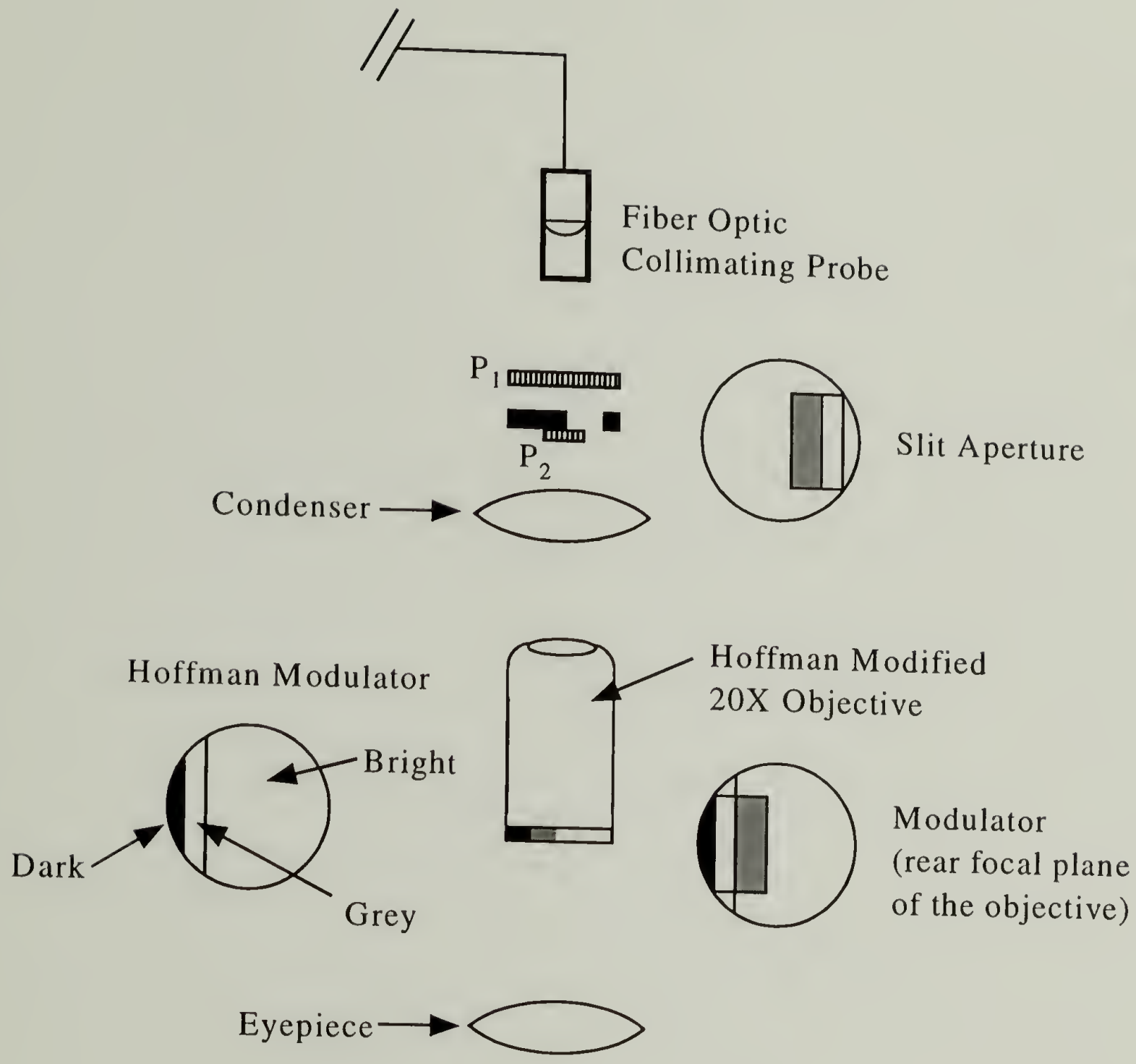


Figure A.4 A schematic drawing of the Hoffman components. The left plan view shows the modulator regions and the right plan view shows the slit and the slit image correctly registered and superimposed on the modulator. (from Hoffman[2])

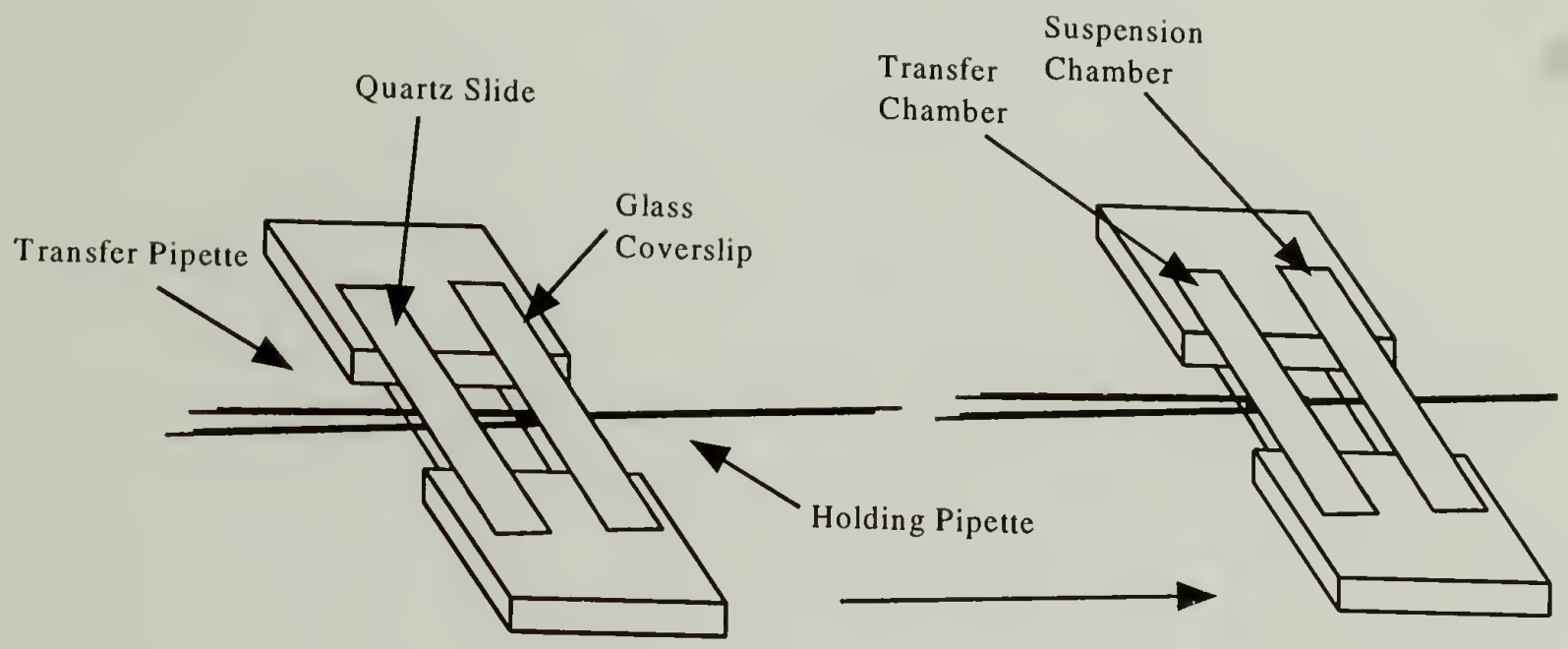


Figure A.5 A schematic diagram of the microchamber and glass micropipettes used for the micromanipulation and photopolymerization of giant vesicles. A holding pipette is used to aspirate a vesicle, and the transfer pipette serves as the aqueous tunnel that spans the air gap between the transfer and suspension chambers. A vesicle is transferred from the suspension to the transfer chamber by inserting an aspirated vesicle into the much larger transfer pipette and the stage is shifted to the right so that both pipettes are positioned in the left chamber.

## References


1) Hoffman, R.; Gross, L. "Modulation Contrast Microscope," *Applied Optics* **1975**, *14*, 1169-1176.

2) Hoffman, R. "The Modulation Contrast Microscope: Principles and Performance," *Journal of Microscopy* **1977**, *110*, 205-222.

# APPENDIX B

## THE OSMOTIC PROPERTIES OF EXTRUDED VESICLES

The osmotic release experiments reported here are representative of our earliest efforts to characterize the effects of photopolymerization on vesicles bilayer. All of the tests summarized in this appendix were carried out using the same procedures as described in the experimental section of chapter 2. Figure B.1 shows the percent release of $Ca^{2+}$ from 100 nm EPC:cholesterol (55:45 mol ratio) extruded vesicles in response to dilution into less concentrated saline buffered solutions. As in the systems previously discussed in chapter 2, the vesicles released $Ca^{2+}$ into the external medium only after the applied hypoosmotic gradient was $\geq$ 1800 mOsm/kg. Specifically, the influx of water increased as the hypoosmotic buffers became less concentrated, creating a membrane tension. Once the membrane tension reached a critical value at $\approx$ 1800 mOsm/kg due to swelling, the vesicle ruptured, releasing a fraction of the entrapped solutes and water in order to reduce the vesicle volume. UV irradiated vesicles with the same lipid composition as above were prepared in 100 mM PEGDMA, 4.5 mM Irgacure 2959 and HEPES buffer (5202 mOsm/kg) responded identically to osmotic stresses as did the control sample of non-irradiated vesicles, see Figure B.2.

We examined how incorporation of the polymerizable amphiphile DSPE PEG 400 MA in the lipid bilayer affected the permeability properties of the membrane. DSPE PEG

400 MA, like DOPE PEG 360 MA, has a reactive hydrophilic headgroup which is designed to copolymerize with monomer that was entrapped in the inner aqueous. It was during these experiments that we discovered that 10 mol percent DSPE PEG 400 MA with EPC, SOPE, DOPC could not be coextruded with even the smallest amounts of cholesterol without repeatedly clogging the pores of the polycarbonate filters used in the extruder. Because of this, we synthesized the analogous unsaturated amphiphile, DOPE PEG 360 MA, which could be coextruded with 45 mol percent cholesterol (Note: Extrusions with higher mole fractions of cholesterol were not attempted.). Nonetheless, UV irradiation of vesicles made from DOPC and DSPE PEG 400 MA (9:1 mol ratio) triggered the release of the vesicle contents (Figure B.3). The vesicles were prepared in 100 mM PEGDMA, 4.5 mM Irgacure 2959, 150 mM $CaCl_2$ and HEPES buffer (4813 mOsm/kg).

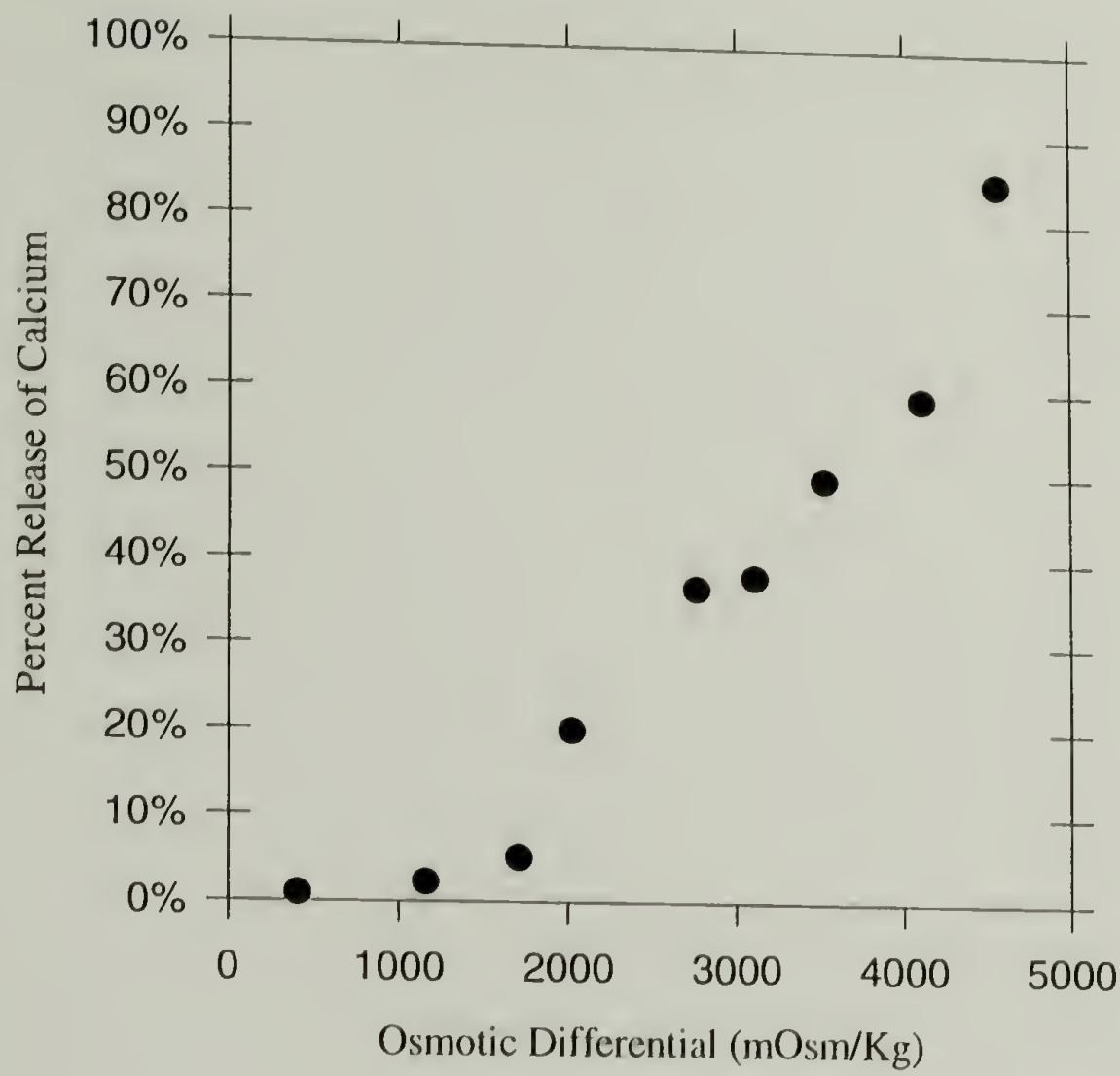


Figure B.1 Osmotic leakage of $Ca^{2+}$ from extruded EPC:cholesterol (55:45) vesicles prepared in 150 mM $CaCl_2$, 4.5 mM Irgacure 2959 and HEPES buffer 4659 mOsm/kg). $Ca^{2+}$ in the extravesicular medium was measured using the fluorescent dye, Calcium Green-5N.

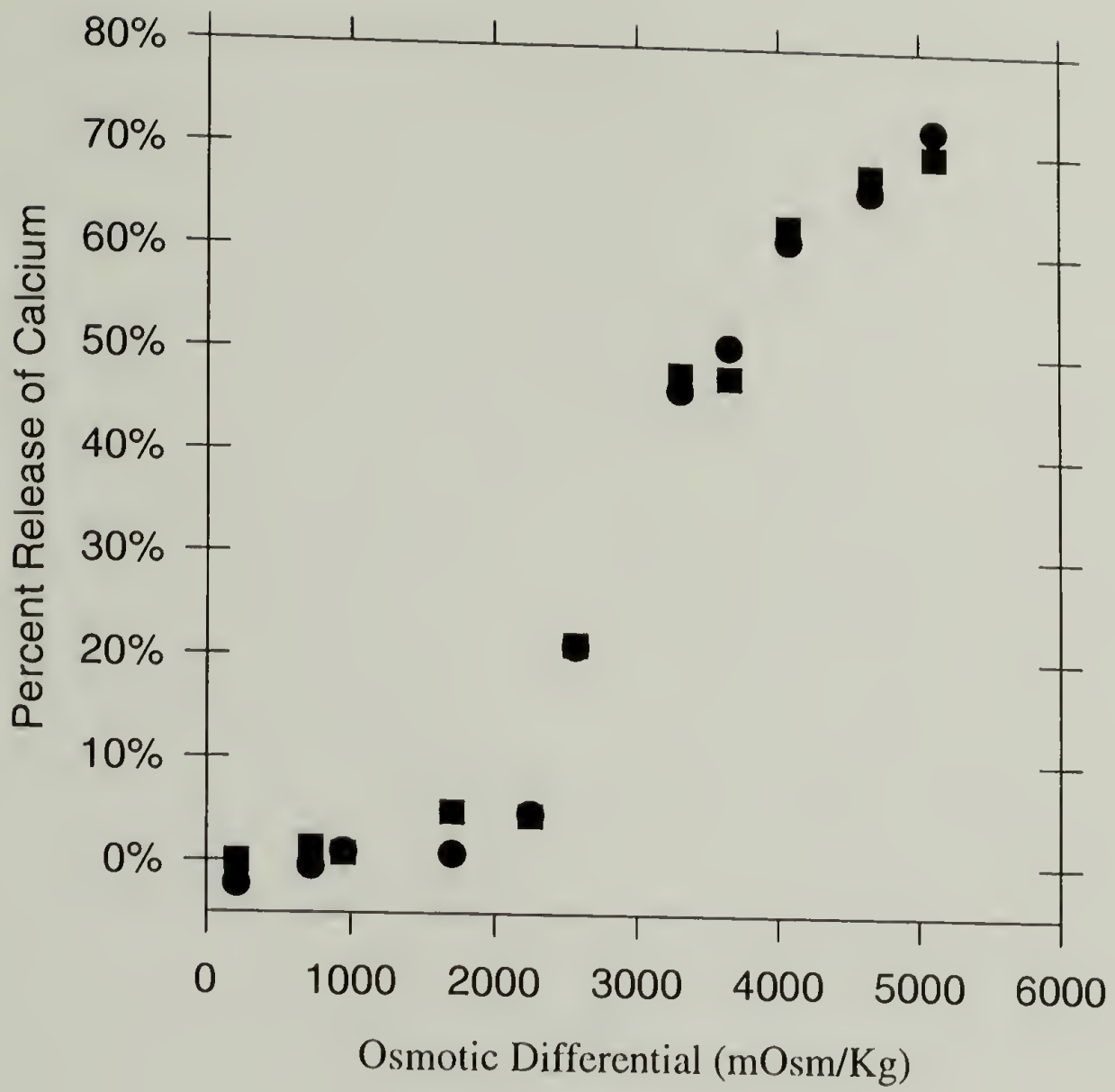


Figure B.2 Influence of UV irradiation on the osmotically induced leakage of $Ca^{2+}$ for extruded EPC:cholesterol (55:45) vesicles with entrapped monomer. The extruded vesicles were loaded with 100 mM PEGDMA, 4.5 mM Irgacure 2959,150 mM $CaCl_2$ and HEPES buffer. Vesicles were irradiated (■) for 30 minutes with a pen-ray mercury lamp, whereas (●) were not exposed to UV irradiation. $Ca^{2+}$ in the surrounding medium was measured using the fluorescent dye, Calcium Green-5N.

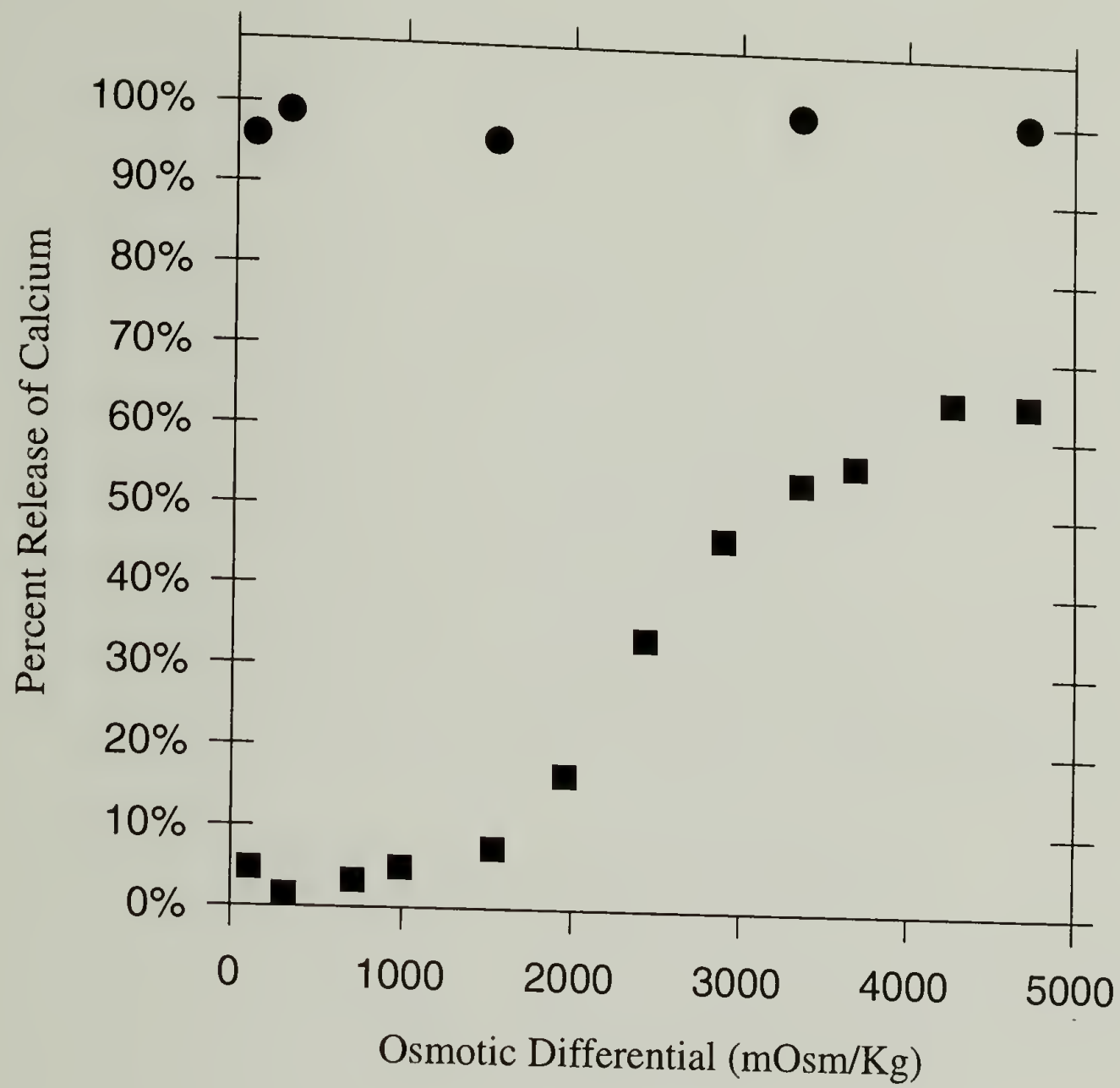


Figure B.3 Influence of UV irradiation on the osmotically induced leakage of $Ca^{2+}$ for extruded DOPC:DSPE PEG 400 MA (45:55) vesicles with entrapped monomer. Extruded vesicles were loaded with 100 mM PEGDMA, 4.5 mM Irgacure 2959, 150 mM $CaCl_2$ and HEPES buffer. Vesicles were irradiated (●) for 30 minutes with a pen-ray mercury lamp, whereas (■) were not irradiated. $Ca^{2+}$ in the extravesicular medium was measured using the fluorescent dye, Calcium Green-5N.

# APPENDIX C

## $^1$H NMR AND IR SPECTRA

This appendix includes the $^1$H NMR and IR spectra of DOPE PEG 360 MA and DSPE PEG 400 MA. The $^1$H NMR spectra were collected with a Bruker DPX-300 FT NMR at 300 MHz in chloroform-*d*. The IR spectra were collected with a Perkin Elmer 1600 FT IR using thin cast films of the lipid from chloroform on NaCl plates.

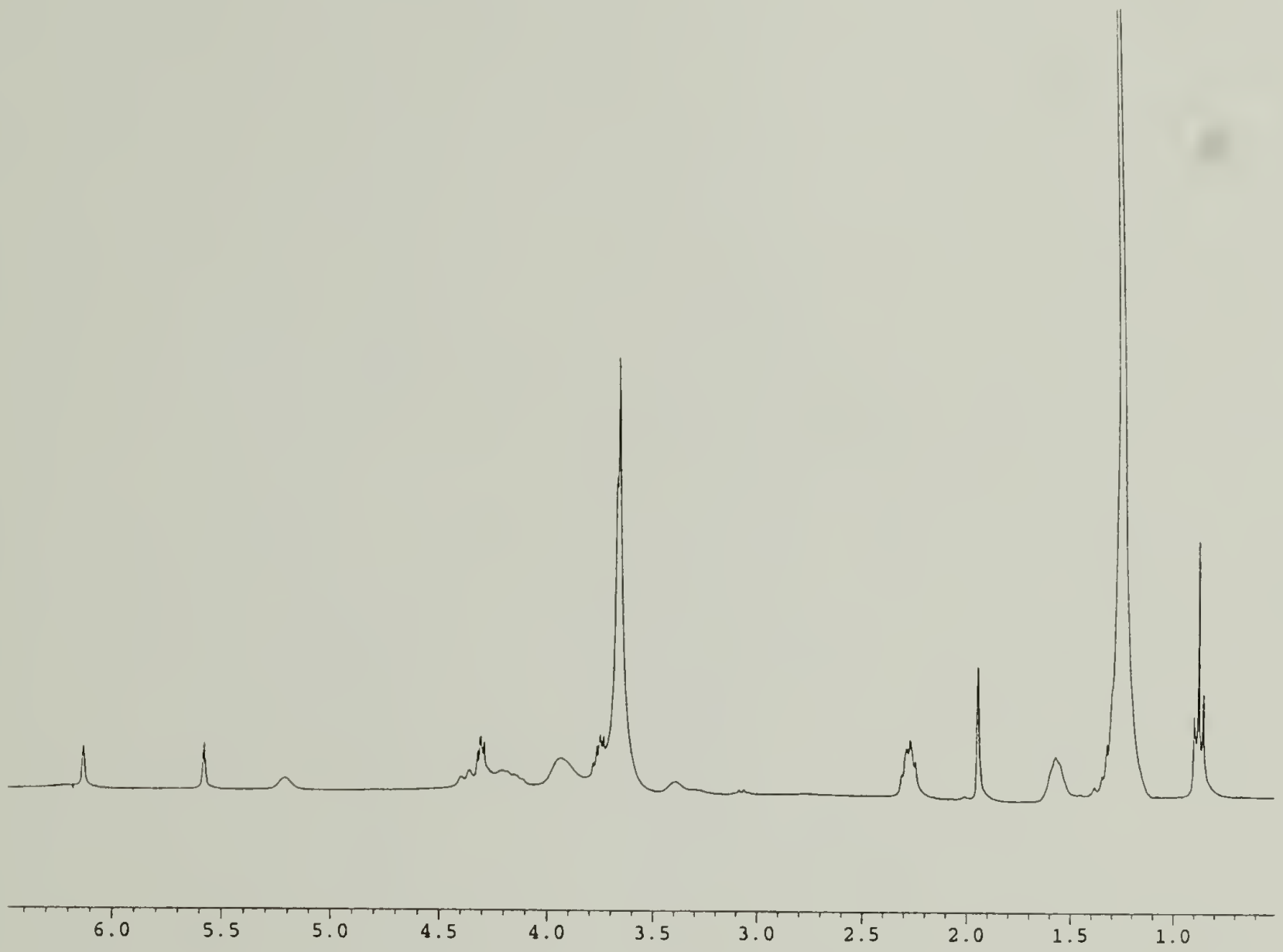


Figure C.1 $^{1}$H NMR spectrum of DSPE PEG 400 MA.

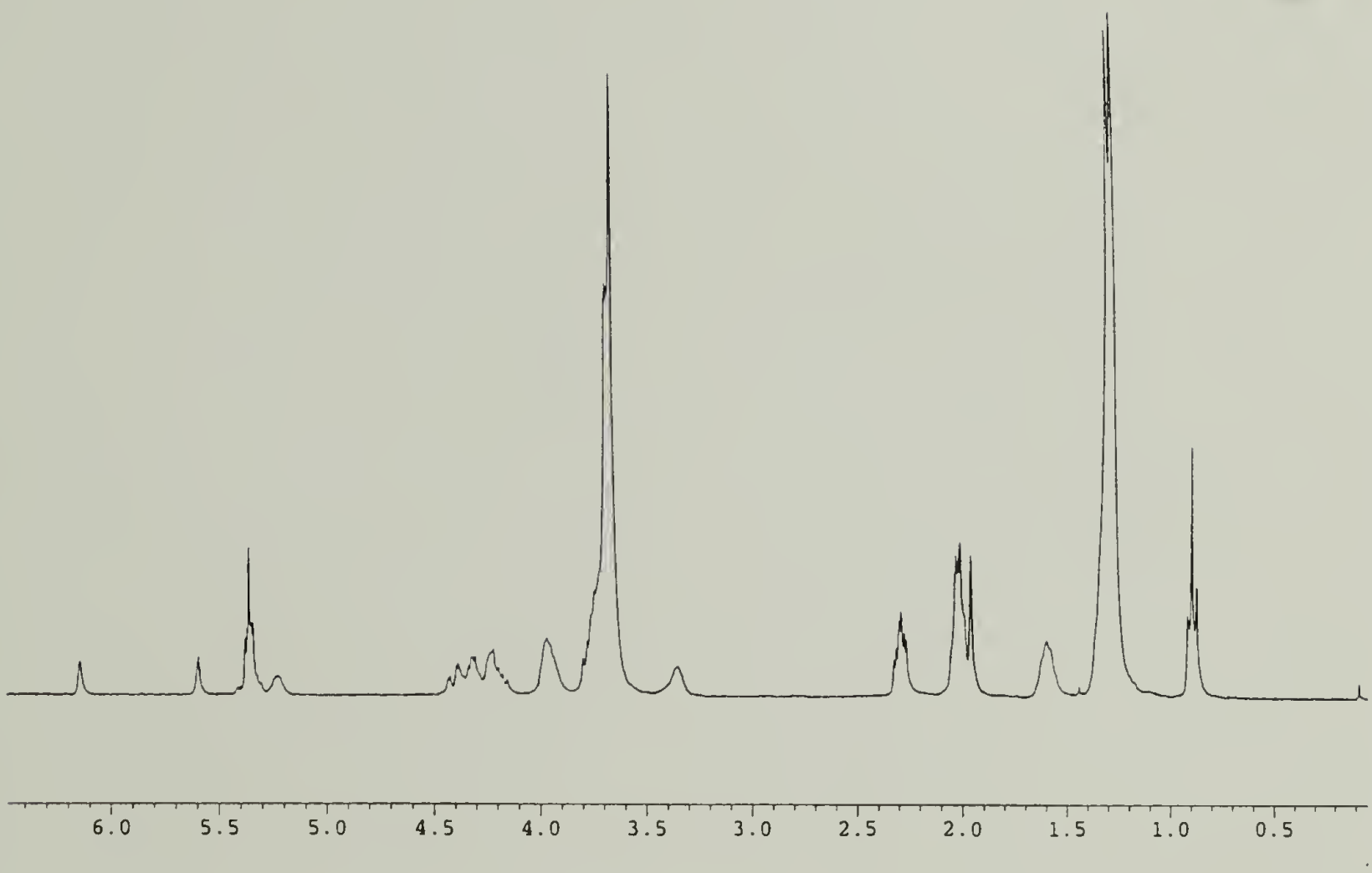


Figure C.2 $^{1}$H NMR spectrum of DOPE PEG 360 MA.

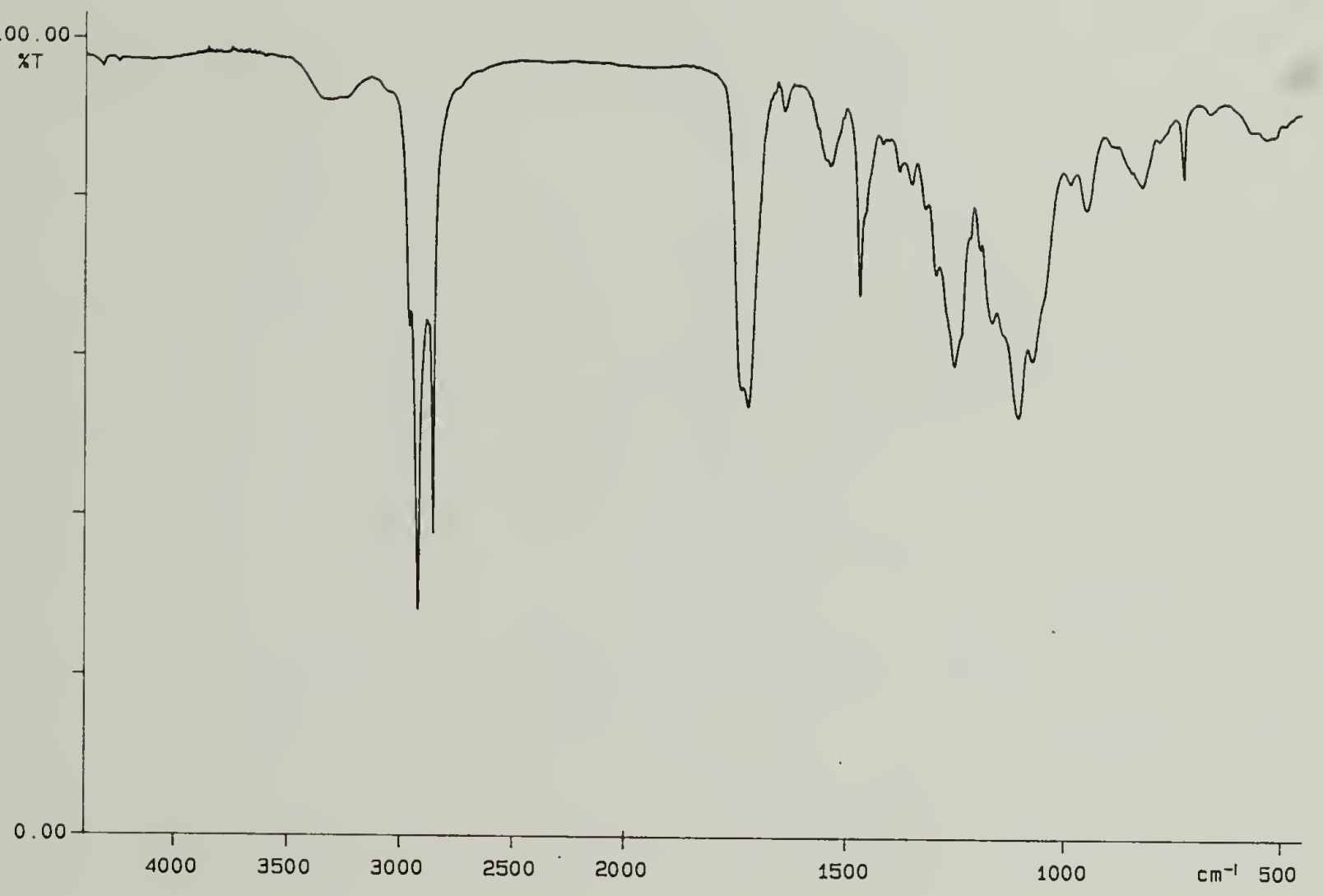


Figure C.3 IR spectrum of DSPE PEG 400 MA.

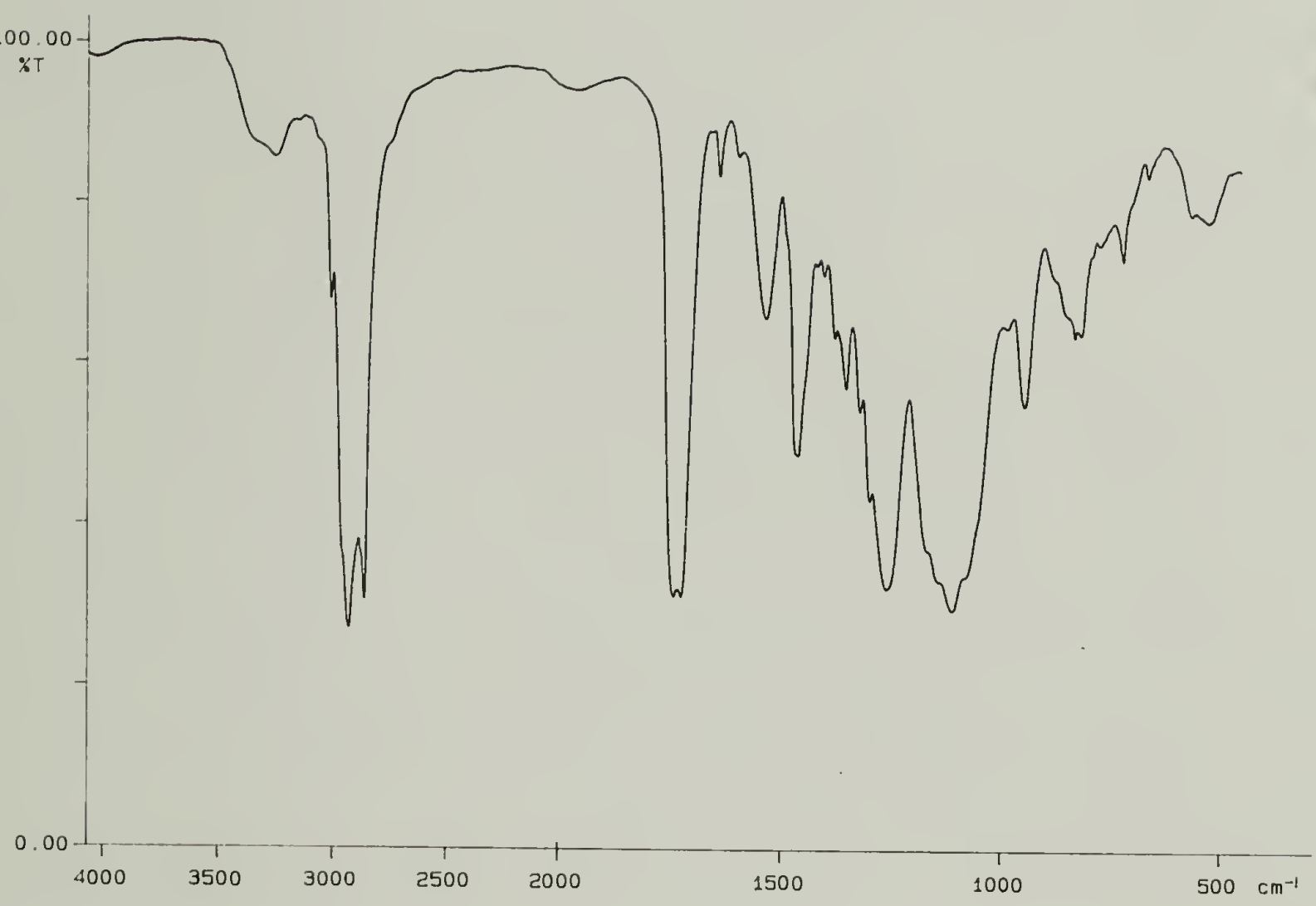


Figure C.4 IR spectrum of DOPE PEG 360 MA.

# BIBLIOGRAPHY


Allen, T. M. in *Liposome Technology Vol. 3*, Ed., Gregoriadis, G., CRC: Boca Raton, 1984, pp. 177-182.

Anseth, K. S. K., Lauren M.; Walker, Teri A.; Anderson, Karin J.; Bowman, Christopher N. "Reaction Kinetics and Volume Relaxation during Polymerizations of Multiethylene Glycol Dimethacrylates," *Macromolecules* **1995**, *28*, 2491-2499.

Archibald, D. D.; Mann, S. "Template Mineralization of Self-Assembled Anisotropic Lipid Microstructures," *Nature* **1993**, *364*, 430-433.

Bain, C. D.; Biebuyck, H. A.; Whitesides, G. M. "Comparison of Self-Assembled Monolayers on Gold: Coadsorption of Thiols and Disulfides," *Langmuir* **1989**, *5*, 723-727.

Baldeschwieler, J. D.; Schmidt, P. G. "Liposomal Drugs: From Setbacks to Success," *Chem. Tech.* **1997**, 34-42.

Baral, S.; Schoen, P. "Silica-Deposited Phospholipid Tubules as a Precursor to Hollow Submicron-Diameter Silica Cylinders," *Chem. Mater.* **1993**, *5*, 145-147.

Baum, R. "Nanotube Characterization," *Chem. Eng. News* **1998**, *76*, 6.

Blackshear, P. L. in *Biomechanics: Its Foundations and Objectives*, Eds., Fung, Y. C., Perrone, N., Anliker, M., Prentice-Hall, Inc.: Englewood Cliffs, N. J., 1972, pp. 501-528.

Bumm, L. A.; Arnold, J. J.; Cygan, M. T.; Dunbar, T. D.; Burgin, T. P.; Jones, L.; Allara, D. L.; Tour, J. M.; Weiss, P. S. "Are Single Molecular Wires Conducting?" *Science* **1996**, *271*, 1705-1707.

Bystrov, V. F.; Dubrovina, N. I.; Barsukov, L. I.; Bergelson, L. D. "NMR Differentiation of the Internal and External Phospholipid Membrane Surfaces Using Paramagnetic $Mn^{2+}$ and $Eu^{3+}$ Ions," *Chem. Phys. Lipids* **1971**, *6*, 343-350.

Cerrina, F.; Marrian, C., Eds., *Materials-Fabrication and Patterning at the Nanoscale*, Materials Research Society: Pittsburgh, 1995.

Chang, C. H.; Mar, A.; Tiefenthaler, A.; Wostratzky, D. in *Handbook of Coatings Additives: Volume 2*, Ed., Calbo, L. J., Marcel Dekker, Inc.: Monticello, 1992, pp. 1-43.

Dai, H.; Wong, E. W.; Lieber, C. M. "Probing Electrical Transport in Nanomaterials: Conductivity of Individual Carbon Nanotubes," *Science* **1996**, *272*, 523-526.

de Kruijff, B.; Cullis, P. R.; Radda, G. K. "Outside-Inside Distributions and Sizes of Mixed Phosphatidylcholine-Cholesterol Vesicles," *Biochim. Biophys. Acta.* **1976**, *436*, 729-740.

Dorn, K.; Klingbiel, R. T.; Specht, D. P.; Tyminski, P. N.; Ringsdorf, H.; Obrien, D. F. "Permeability Characteristics of Polymeric Bilayer Membranes from Methacryloyl and Butadiene lipids," *J. Am. Chem. Soc.* **1984**, *106*, 1627-1633.

Dorn, K.; Patton, E. V.; Klingbiel, R. T.; O'Brien, D. F.; Ringsdorf, H. "Molecular Weight of Polymers from Methacryloyl Lipids in Bilayer Membranes," *Makromol. Chem., Rapid Commun.* **1983**, *4*, 513-517.

Eaton, D. F. "Dye Sensitized Photopolymerization," *Adv. Photochem.* **1986**, 13, 427-487.

Edwards, K.; Almgren, M.; Bellare, J.; Brown, W. "Effects of Triton X-100 on Sonicated Lecithin Vesicles," *Langmuir* **1989**, *5*, 473-478.

Elbert, R.; Laschewsky, A.; Ringsdorf, H. "Hydrophilic Spacer Groups in Polymerizable Lipids: Formation of Biomembrane Models from Bulk Polymerized Lipids," *J. Am. Chem. Soc.* **1985**, *107*, 4134-4141.

Ellens, H.; Bentz, J.; Szoka, F. C. "Destabilization of Phosphatidylethanolamine Liposomes at the Hexagonal Phase Transition Temperature," *Biochemistry* **1986**, *25*, 285-294.

Ellingson, J. S.; Lands, W. E. M. "Phospholipid Reactivation of Plasmalogen Metabolism," *Lipids* **1968**, *3*, 111-120.

Ertel, A.; Marangoni, A. G.; Marsh, J.; Hallet, F. R.; Wood, J. M. "Mechanical Properties of Vesicles I. Coordinated Analyses of Osmotic Swelling and Lysis," *Biophys. J.* **1993**, *64*, 426-434.

Evans, E.; Rawicz, W. "Entropy-Driven Tension and Bending Elasticity in Condensed-Fluid Membranes," *Phys. Rev. Lett.* **1990**, *64*, 2094-2097.

Evans, E.; Yeung, A. "Hidden Dynamics in Rapid Changes of Bilayer Shape," *Chem. Phys. Lipids* **1994**, *73*, 39-56.

Frankel, D. A.; Lamparski, H.; Liman, U.; O'Brien, D. F. "Photoinduced Destabilization of Bilayer Vesicles," *J. Am. Chem. Soc.* **1989**, *111*.

Fuhrhop, J.-H.; Bartsch, H.; Fritsch, D. "Colored, Unsymmetric and Light-Sensitive Vesicle Membranes," *Angew. Chem. Int. Ed. Engl.* **1981**, *20*, 804-805.

Fuhrhop, J.-H.; Mathieu, J. "Routes to Functional Vesicle Membranes without Proteins," *Angew. Chem. Int. Ed. Engl.* **1984**, *23*, 100-113.

Fujii, G. in *Vesicles*, Ed., Rosoff, M., Marcel Dekker, Inc.: New York, 1996, pp. 491-526.

Gaub, H.; Sackmann, E.; Büschl, R.; Ringsdorf, H. "Lateral Diffusion and Phase Separation in Two-Dimensional Solutions of Polymerized Butadiene Lipid in Dimyristoylphosphatidylcholine Bilayers," *Biophys. J.* **1984**, *45*, 725-731.

Green, N. M. "Avidin," *Adv. Protein Chem.* **1975**, *29*, 85-133.

Gref, R.; Minamitake, Y.; Peracchia, M. T.; Trubetskoy, V.; Torchilin, V.; Langer, R. "Biodegradable Long-Circulating Polymeric Nanospheres," *Science* **1994**, *263*, 1600-1603.

Grynkiewicz, G.; Poenie, M.; Tsien, R. "A New Generation of Calcium Indicators with Greatly Improved Fluorescence Properties," *J. Biol. Chem.* **1985**, *260*, 3440-3450.

Gupta, V.; Nivarthi, S. S.; Keffer, D.; McCormick, A. V.; Davis, H. T. "Evidence of Single-File Diffusion in Zeolites," *Science* **1996**, *274*, 5285.

Hallett, F. R.; Marsh, J.; Nickel, B. G.; Wood, J. M. "Mechanical Properties of Vesicles II. A Model for Osmotic Swelling and Lysis," *Biophys. J.* **1993**, *64*, 435-442.

Haubs, M.; Ringsdorf, H. "Photoreactions of N-(1-Pyridinio)amidates in Monolayers and Liposomes," *Angew. Chem. Int. Ed. Engl.* **1985**, *24*, 882-883.

Haubs, M.; Ringsdorf, H. "Photosensitive Monolayers, Bilayer Membranes and Polymers," *Nouv. J. Chim.* **1987**, *11*, 151-156.

Hershfield, M. S.; Buckley, R. H.; Greenberg, M. L.; Melton, A. L.; Schiff, R.; Hatem, C.; Kurtzberg, J.; Markert, M. L.; Kobayashi, R. H.; Kobayshi, A. L.; Abuchowski, A. "Treatment of Adenosine Deaminase Deficiency with Polyethylene Glycol-Modified Adenosine Deaminase," *N. Engl. J. Med.* **1987**, *316*, 589-596.

Hochmuth, R. M.; Evans, E. A. "Extensional Flow of Erythrocyte Membrane from Cell Body to Elastic Tether I. Analysis," *Biophys J.* **1982**, *39*, 71-81.

Hochmuth, R. M.; Evans, E. A.; Wiles, H. C.; McCown, J. T. "Mechanical Measurement of Red Cell Membrane Thickness," *Science* **1983**, *220*, 101-102.

Hochmuth, R. M.; Mohandas, N.; Blackshear, P. L. "Measurement of the Elastic Modulus for Red Cell Membrane Using Fluid Mechanical Technique," *Biophys. J.* **1973**, *13*, 747-762.

Hochmuth, R. M.; Mohandas, N.; Spaeth, E. E.; Williamson, J. R.; Blackshear, P. L. "Surface Adhesion, Deformation and Detachment at Low Shear or Red Cells and White Cells," *Trans. Am. Soc. Artif. Intern. Organs* **1972**, *18*, 420.

Hochmuth, R. M.; Shao, J. Y.; Dai, J.; Sheetz, M. P. "Deformation and Flow of Membrane into Tethers Extracted from Neuronal Growth Cones," *Biophys. J.* **1996**, *70*, 358-369.

Hochmuth, R. M.; Wiles, H. C.; Evans, E. A.; McCown, J. T. "Extensional Flow of Erythrocyte Membrane from Cell Body to Elastic Tether," *Biophys. J.* **1982**, *39*, 83-89.

Hoffman, R. "The Modulation Contrast Microscope: Principles and Performance," *Journal of Microscopy* **1977**, *110*, 205-222.

Hoffman, R.; Gross, L. "Modulation Contrast Microscope," *Applied Optics* **1975**, *14*, 1169-1176.

Hope, M. J.; Bally, M. B.; Webb, G.; Cullis, P. R. "Production of Large Unilamellar Vesicles by a Rapid Extrusion Procedure. Characterization of Size Distribution, Trapped Volume and Ability to Maintain a Membrane Potential," *Biochim. Biophys. Acta* **1985**, *812*, 55-65.

Iijima, S. "Helical Microtubules of Graphitic Carbon," *Science* **1991**, *354*, 56-58.

Jain, M. K.; Wagner, R. C. *Introduction to Biological Membranes*, John Wiley & Sons: New York, 1980.

Kano, K.; Tanaka, Y.; Ogawa, T.; Shimomura, M.; Kunitake, T. "Photoresponsive Artificial Membrane Permeability of Liposomal Membrane by Photoreversible Cis-Trans Isomerization of Azobenzenes," *Photochem. Photobiol.* **1981**, *34*, 323-329.

Koppel, D. E. "Analysis of Macromolecular Polydispersity in Intensity Correlation Spectroscopy: The Method of Cumulants," *J. Chem. Phys.* **1972**, *57*, 4814-4820.

Kulkarni, V. S.; Anderson, W. H.; Brown, R. "Bilayer Nanotubes and Helical Ribbons Formed by Hydrated Galactosylceramides: Acyl Chain Headgroup Effects," *Biophys. J.* **1995**, *69*, 1976-1986.

Lago, R. M.; Tsang, S. C.; Lu, K. L.; Chen, Y. K.; Green, M. L. H. "Filling Carbon Nanotubes with Small Palladium Metal Crystallites: The Effect of Surface Acid Groups," *J. Chem. Soc., Chem. Commun.* **1995**, no. 13, 1355-1356.

Lamparski, H.; Liman, U.; Barry, J. A.; Frankel, D. A.; Ramaswami, V.; Brown, M. F.; O'Brien, D. F. "Photoinduced Destabilization of Liposomes," *Biochemistry* **1992**, *31*, 685-694.

Lamparski, H.; O'Brien, D. F. "Two-Dimensional Polymerization of Lipid Bilayers: Degree of Polymerization of Sorbyl Lipids," *Macromolecules* **1995**, *28*, 1786-1794.

Lasic, D.; Martin, F., Eds. *Stealth Liposomes*, CRC Press: Boca Raton, 1995.

Lee, Y. -S.; Yang, J. -Z.; Sisson, T. M.; Frankel, D. A.; Gleeson, J. T.; Aksay, E.; Keller, S. L.; Gruner, S. M.; O'Brien, D. F. "Polymerization of Nonlamellar Lipid Assemblies," *J. Am. Chem. Soc.* **1995**, *117*, 5573-5578.

Lehn, J. -M. "Perspectives in Supramolecular Chemistry- From Molecular Recognition Towards Molecular Information Processing and Self-Organization," *Angew. Chem. Int. Ed. Engl.* **1990**, *29*, 1304-1319.

Levine, Y. K.; Lee, A. G.; Birdsall, N. J. M.; Metcalfe, J. C.; Robinson, J. D. "The Interactions of Paramagnetic Ions and Spin Labels with Lecithin Bilayers," *Biochim. Biophys. Acta.* **1973**, *291*, 592-607.

Liu, Y.; Regen, S. L. "Control over Vesicle Rupture and Leakage by Membrane Packing and by the Aggregation State of an Attacking Surfactant," *J. Am. Chem Soc.* **1993**, *115*, 708-713.

Martin, C. R. "Nanomaterials: A Membrane-Based Synthetic Approach," *Science* **1994**, *266*, 1961-1966.

Martin, C. R. "Template Synthesis of Electronically Conductive Polymer Nanostructures," *Acc. Chem. Res.* **1995**, *28*, 61-68.

Massenburg, D.; Lentz, B. R. "Poly (ethylene glycol)-Induced Fusion and Rupture of Dipalmitoylphosphatidylcholine Large, Unilamellar Extruded Vesicles," *Biochemistry* **1993**, *32*, 9172-9180.

Mayer, L. D.; Hope, M. J.; Cullis, P. R. "Vesicles of Variable Sizes Produced by a Rapid Extrusion Procedure," *Biochim. Biophys. Acta* **1986**, *858*, 161-168.

Mirkin, C. A.; Ratner, M. A. "Molecular Electronics," *Annu. Rev. Phys. Chem.*, **1992**, 43, 719-754.

Mui, B. L. S.; Cullis, P. R.; Evans, E. A.; Madden, T. D. "Osmotic Properties of Large Unilamellar Vesicles Prepared by Extrusion," *Biophys. J.* **1993**, *64*, 443-453.

Nabel, G. L.; Nabel, E. G.; Yang, Z. Y.; Fox, B. A.; Plautz, G. E.; Gao, X.; Huang, L.; Shu, S.; Gordon, D.; Chang, A. E. "Direct Gene Transfer with DNA-Liposome Complexes in Melanoma: Expression, Biologic Activity, and Lack of Toxicity in Humans," *Proc. Natl. Acad. Sci. USA* **1993**, *90*, 11307-11311.

Nagawa, Y.; Regen, S. L. "Surfactant-Induced Release from Phosphatidylcholine Vesicles. Regulation of Rupture and Leakage Pathways by Membrane Packing," *J. Am. Chem. Soc.* **1992**, *114*, 1668-1672.

Needham, D.; Nunn, R. S. "Elastic Deformation and Failure of Lipid Bilayer Membranes Containing Cholesterol," *Biophys. J.* **1990**, *58*, 997-1009.

Needham, D.; Zhelev, D. V. in *Vesicles*, Ed., Rosoff, M., Marcel Dekker, Inc.: New York, 1996, pp. 373-444.

Nivarthi, S. S.; McCormick, A. V.; Davis, H. T. "Evidence for Single File Diffusion of Ethane in the Molecular Sieve $AlPO_4$-5," *Chem. Phys. Lett.* **1994**, *247*, 596.

Nostrum, C. F. v.; Picken, S. J.; Schouten, A.-J.; Nolte, R. J. M. "Synthesis and Supramolecular Chemistry of Novel Liquid Crystalline Crown Ether-Substituted Phthalocyanines: Toward Molecular Wires and Molecular Ionoelectronics," *J. Am. Chem. Soc.* **1995**, *117*, 9957-9965.

O'Brien, D. F. in *Encyclopedia of Polymer Science and Engineering*, Eds., Mark, H. F.; Bikales, N. M.; Overberger, C. G.; Menges, G. J., John Wiley & Sons: New York, 1989, pp. 108-135.

O'Brien, D. F.; Tirrell, D. A. in *Bioorganic Photochemistry Volume 2: Biological Applications of Photochemical Switches*, Ed., Morrison, H., John Wiley & Sons, Inc.: New York, 1993, pp. 111-167.

Odian, G. *Principles of Polymerization,* John Wiley & Sons, Inc.: New York, 1991.

Okahata, Y.; Kunitake, T. "Formation of Stable Monolayer Membranes and Related Structures in Dilute Aqueous Solution from Two-Headed Ammonium Amphiphiles," *J. Am. Chem. Soc.* **1979**, *101*, 5231-5234.

Parthasarathy, R.; Martin, C. R. "Synthesis of Polymeric Microcapsule Arrays and Their Use for Enzyme Immobilization," *Nature* **1994**, *369*, 298.

Porter, M. D.; Bright, T. B.; Allara, D. L.; Chidsey, C. E. D. "Spontaneously Organized Molecular Assemblies. 4. Structural Characterization of n-Alkyl Thiol Monolayers on Gold by Optical Ellipsometry, Infrared Spectroscopy, and Electrochemistry," *J. Am. Chem. Soc.* **1987**, *109*, 3559-3568.

Presant, C. A.; Proffitt, R. T.; Turner, A. F.; Williams, L. E.; Winson, D.; Werner, J. L.; Kennedy, P.; Weseman, C.; Gala, K.; McKenna, R. J.; Smith, J. D.; Bouzagloa, S. A.; Callahan, R. H.; Baldeschwieler, J. D.; Crossley, R. J. "Successful Imaging of Human Cancer with Indium-111-Labeled Phospholipid Vesicles, " *Cancer* **1988**, *62*, 905.

Regen, S. L.; Singh, A.; Oehme, G.; Singh, M. "Polymerized Phosphatidylcholine Vesicles. Synthesis and Characterization," *J. Am. Chem. Soc.* **1982**, *104*, 791-795.

Regen, S. L. C., Bronislaw; Singh, A. "Polymerized Vesicles," *J. Am. Chem. Soc.* **1980**, *102*, 6638-6640.

Reiser, A. *Photoreactive Polymers: The Science and Technology of Resists*, John Wiley & Sons: New York, 1989.

Ringsdorf, H.; Schlarb, B.; Venzmer, J. "Molecular Architecture and Function of Polymeric Oriented Systems: Models for the study of Organization, Surface Recognition, and Dynamics of Biomembranes," *Angew. Chem. Int. Ed. Engl.* **1988**, *27*, 113-158.

Rutkowski, C. A.; Williams, L. M.; Haines, T. H.; Cummins, H. Z. "The Elasticity of Synthetic Phospholipid Vesicles Obtained by Photon Correlation Spectroscopy," *Biochemistry* **1991**, *30*, 5688-5696.

Sato, T.; Kijima, M.; Shiga, Y.; Yonezawa, Y. "Photochemically Controlled Ion Permeability of Liposomal Membranes Containing Amphiphilic Azobenzene," *Langmuir* **1991**, *7*, 2330-2335.

Schnur, J. M. "Lipid Tubules: A Paradigm for Molecularly Engineered Structures," *Science* **1993**, *262*, 1669-1676.

Schubert, R.; Beyer, K.; Wolburg, H.; Schmidt, K.-H. "Structural Changes in Membranes of Large Unilamellar Vesicles after Binding of Sodium Cholate," *Biochemistry* **1986**, *25*, 5263-5269.

Siegel, D. P. "Inverted Micellar Structures in Bilayer Membranes: Formation and Half-Lives," *Biophys. J.* **1984**, *45*, 399-420.

Smith, R. C.; Fischer, W. M.; Gin, D. L. "Ordered Poly (*p*-phenylenevinylene) Matrix Nanocomposites via Lyotropic Liquid-Crystalline Monomers," *J. Am. Chem. Soc.* **1997**, *119*, 4092-4093.

Snow, E. S.; Campbell, P. M. "AFM Fabrication of Sub-10-Nanometer Metal-Oxide Devices with in Situ Control of Electrical Properties," *Science* **1995**, *270*, 1639-1641.

Thomas, J. L.; Tirrell, D. A. "Polyelectrolyte-Sensitized Phospholipid Vesicles," *Acc. Chem. Res.* **1992**, *25*, 336-342.

Tolles, W. M. in *Nanotechnology: Molecularly Designed Materials*, Eds., Chow, G. -M. and Gonsalves, K. E., American Chemical Society: Washington, D. C., 1996, pp. 1-18.

Tonucci, R. J.; Justus, B. L.; Campillo, A. J.; Ford, C. E. "Nanochannel Array Glass," *Science* **1992**, *258*, 783-785.

Torchilin, V. P.; Klibanov, A. L.; Ivanov, N. N.; Ringsdorf, H.; Schlarb, B. "Polymerization of Liposome-Encapsulated Hydrophilic Monomers," *Makromol. Chem., Rapid Commun.* **1987**, *8*, 457-460.

Tsang, S. C.; K., C. Y.; Harris, P. J. F.; Green, M. L. H. "A Simple Chemical Method of Opening and Filling Carbon Nanotubes," *Nature* **1994**, *372*, 159-162.

Wallraff, G. M.; Allen, R. D.; Hinsberg, W. D.; Simpson, L. L.; Kunz, R. R. "Designing Tomorrow's Photoresists," *Chemtech* **1993**, *23*, 22-30.

Waugh, R. E. "Surface Viscosity Measurements from Large Bilayer Vesicle Tether Formation," *Biophys. J.* **1982**, *38*, 29-37.

Waugh, R. E.; Hochmuth, R. M. "Mechanical Equilibrium of Thick, Hollow, Liquid Membrane Cylinders," *Biophys. J.* **1987**, *52*, 391-400.

Whitesides, G. W.; Mathias, J. P.; Seto, C. T. "Molecular Self-Assembly and Nanochemistry: A Chemical Strategy for the Synthesis of Nanostructures," *Science* **1991**, *254*, 1312-1319.

Williams, L. M.; Evans, S. D.; Flynn, T. M.; Marsh, A.; Knowles, P. F.; Bushby, R. J.; Boden, N. "Kinetics of the Unrolling of Small Unilamellar Phospholipid Vesicles onto Self-Assembled Monolayers," *Langmuir* **1997**, *13*, 751-757.

You, H.; Tirrell, D. A. "Photoinduced, Polyelectrolyte-Driven Release of Contents of Phosphatidylcholine Bilayer Vesicles," *J. Am. Chem. Soc.* **1991**, *113*, 4022-4023.

Zalipsky, S. "Functionalized Poly (ethylene glycol) for Preparation of Biologically Relevent Conjugates," *Bioconjugate Chem.* **1995**, *6*, 150-165.

Zelphati, O.; Szoka, F. C., Jr. "Mechanism of Oligonucleotide Release from Cationic Liposomes," *Proc. Natl. Acad. Sci. USA* **1996**, *93*, 11493.

Zhelev, D. V.; Needham, D. "Tension-Stabilized Pores in Giant Vesicles: Determination of Pore Size and Pore Line Tension," *Biochim. Biophys. Acta* **1993**, *1147*, 89-104.